

1-1-2004

## Matrix free fiber reinforced polymeric composites via high-temperature high-pressure sintering.

Tao Xu  
*University of Massachusetts Amherst*

Follow this and additional works at: [https://scholarworks.umass.edu/dissertations\\_1](https://scholarworks.umass.edu/dissertations_1)

---

### Recommended Citation

Xu, Tao, "Matrix free fiber reinforced polymeric composites via high-temperature high-pressure sintering." (2004). *Doctoral Dissertations 1896 - February 2014*. 1058.  
<https://doi.org/10.7275/v7z9-bg22> [https://scholarworks.umass.edu/dissertations\\_1/1058](https://scholarworks.umass.edu/dissertations_1/1058)

This Open Access Dissertation is brought to you for free and open access by ScholarWorks@UMass Amherst. It has been accepted for inclusion in Doctoral Dissertations 1896 - February 2014 by an authorized administrator of ScholarWorks@UMass Amherst. For more information, please contact [scholarworks@library.umass.edu](mailto:scholarworks@library.umass.edu).



★ UMass/AMHERST ★



312066 0288 9967 5



**MATRIX FREE FIBER REINFORCED POLYMERIC COMPOSITES  
VIA HIGH-TEMPERATURE HIGH-PRESSURE SINTERING**

A Dissertation Presented

by

TAO XU

Submitted to the Graduate School of the  
University of Massachusetts Amherst in partial fulfillment  
of the requirements for the degree of

DOCTOR OF PHILOSOPHY

May 2004

Polymer Science and Engineering

© Copyright by Tao Xu 2004

All Rights Reserved



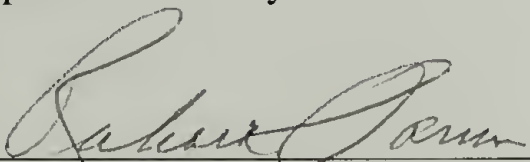
**MATRIX FREE FIBER REINFORCED POLYMERIC COMPOSITES**  
**VIA HIGH-TEMPERATURE HIGH-PRESSURE SINTERING**


A Dissertation Presented

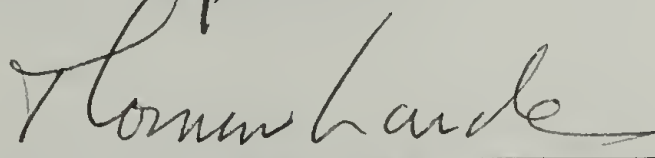
by

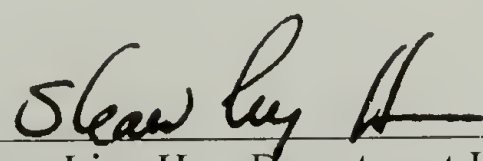
TAO XU

Approved as to style and content by:

  
Richard J. Farris, Chair

  
Alan J. Lesser, Member

  
Thomas J. Lardner, Member

  
Shaw Ling Hsu, Department Head  
Polymer Science and Engineering

## DEDICATION

To my loving parents and uncle .

## ACKNOWLEDGMENTS

I would like express my sincere gratitude to my advisor Richard J. Farris for his continuous, patient guidance and support throughout my graduate study. His direction and encouragement has been invaluable to me and will be forever appreciated. I would also like to thank the members of my committee Alan J. Lesser and Thomas J. Lardner for their thoughtful comments and useful suggestions.

I want to extend my appreciation to the past and current members of the Farris and Lesser research groups for their help, discussions and suggestions. My Ph.D study in the Polymer Science and Engineering Department was a pleasant and rewarding journey. We have a wonderful group of faculty, staff, and students. Thanks to Eileen Besse, Lou Raboin, Alan Waddon, and John Domian for their expertise and patience in helping me.

I want to thank the US Army Natick Center for funding this research. The generous help from Philip Cunniff, Janet Ward and Heidi Schreuder-Gibson is greatly appreciated. Thanks to Honeywell Corporation for providing research materials. The discussions with Ashok Bhatnagar and Lori Wagner were very helpful.

Finally, I would like to thank my parents and uncle for the support and encouragement that they have provided me throughout my academic studies. My special thanks go to Maohua Cao, for her love and support that constantly motivates me to achieve excellence.



## ABSTRACT

### MATRIX FREE FIBER REINFORCED POLYMERIC COMPOSITES VIA HIGH-TEMPERATURE HIGH-PRESSURE SINTERING

MAY 2004

TAO XU, B.S., FUDAN UNIVERSITY

Ph.D., UNIVERSITY OF MASSACHUSETTS AMHERST

Directed by: Professor Richard J. Farris

A novel manufacturing process called high-temperature high-pressure sintering was studied and explored. Solid fiber reinforced composites are produced by consolidating and compacting layers of polymeric fabrics near their melting temperature under high pressure. There is no need to use an additional matrix as a bonding material. Partial melting and recrystallization of the fibers effectively fuse the material together. The product is called a “matrix free” fiber reinforced composite and essentially a one-polymer composite in which the fiber and the matrix have the same chemical composition. Since the matrix is eliminated in the process, it is possible to achieve a high fiber volume fraction and light weight composite. Interfacial adhesion between fibers and matrix is very good due to the molecular continuity throughout the system and the material is thermally shapeable. Plain woven Spectra<sup>®</sup> cloth made of Spectra<sup>®</sup> fiber<sup>1</sup> was used to comprehensively study the process. The intrinsic properties of the material demonstrate that matrix free Spectra<sup>®</sup> fiber reinforced composites have the potential to make ballistic shields such as body armor and helmets.

The properties and structure of the original fiber and the cloth were carefully examined. Optimization of the processing conditions started with the probing of sintering temperatures by Differential Scanning Calorimetry. Coupled with the information from structural, morphological and mechanical investigations on the samples sintered at different processing conditions, the optimal processing windows were determined to ensure that the outstanding original properties of the fibers translate into high ballistic performance of the composites. Matrix free Spectra<sup>®</sup> composites exhibit excellent ballistic resistance in the  $V_{50}$  tests conducted by the US Army. In the research, process-structure-property relationship is established and correlations between various properties and structures are understood. Thorough knowledge is obtained for this creative process regarding the procedures, outcomes, advantages and capabilities. Two other ultra high molecular weight polyethylene fiber containing materials, Dyneema Fraglight<sup>®</sup> nonwoven felt<sup>2,3</sup> and Spectra Shield<sup>®</sup> Plus PCR<sup>4</sup> prepreg, were also carefully studied using the process of high-temperature high-pressure sintering. Their structures, morphologies and thermo-mechanical properties were compared with consolidated Spectra<sup>®</sup> cloth. The results clearly demonstrate that Spectra<sup>®</sup> cloth is the best candidate for making ballistic protective shields.

# TABLE OF CONTENTS

	Page
ACKNOWLEDGMENTS .....	v
ABSTRACT.....	vi
LIST OF TABLES .....	xii
LIST OF FIGURES .....	xiv
CHAPTER	
1. BACKGROUND AND INTRODUCTION .....	1
1.1 Fiber Reinforced Composites .....	1
1.2 Ultra High Molecular Weight Polyethylene (UHMWPE) Fibers.....	6
1.3 Spectra <sup>®</sup> Fiber Reinforced Composites .....	13
1.4 One-polymer Composites .....	17
1.5 Project Overview .....	19
2. THERMO-MECHANICAL PROPERTIES, STRUCTURE AND MORPHOLOGY OF SPECTRA <sup>®</sup> FIBER, YARN, AND CLOTH.....	22
2.1 Introduction.....	22
2.2 Experimental .....	24
2.2.1 Materials .....	24
2.2.2 Testing methods and instruments.....	24
2.2.2.1 Tensile properties.....	24
2.2.2.2 Thermal analysis .....	25
2.2.2.3 Structure and morphology.....	26
2.3 Results and Discussion .....	27
2.3.1 Tensile properties of single fibers and yarns at ambient and elevated temperatures.....	27
2.3.2 Thermal shrinkage of single filaments.....	34
2.3.3 Thermal mechanical analysis of a single filament.....	35
2.3.4 Differential scanning calorimetry of the unconstrained and constrained filaments and the as-received Spectra <sup>®</sup> cloth .....	37
2.3.5 Scanning electron microscopy images of Spectra <sup>®</sup> fiber 900 and Spectra <sup>®</sup> cloth 903.....	40



2.3.6	Wide angle X-ray diffraction of unidirectionally aligned Spectra <sup>®</sup> fiber and the as-received Spectra <sup>®</sup> cloth.....	42
2.4	Conclusion .....	44
3.	OPTIMIZATION OF THE HIGH-TEMPERATURE HIGH-PRESSURE SINTERING PROCESS FOR CONSOLIDATING SPECTRA <sup>®</sup> CLOTH..	46
3.1	Introduction.....	46
3.2	Experimental .....	47
3.2.1	Materials .....	47
3.2.2	Processing procedures.....	47
3.2.3	Measurement of crystallinity changes by DSC.....	48
3.2.4	Measurement of orientation changes by WAXD.....	48
3.2.5	Measurement of impact properties by puncture test.....	49
3.3	Results and Discussion .....	49
3.3.1	Overall and original crystallinity .....	49
3.3.2	WAXD patterns and Hermans orientation function.....	55
3.3.3	Correlation between crystallinity and orientation.....	58
3.3.4	Normalized to thickness total energy of impact .....	61
3.4	Conclusion .....	66
4.	EVALUATION OF CONSOLIDATED STRUCTURES: PROCESS-STRUCTURE-PROPERTY RELATIONSHIP.....	67
4.1	Introduction.....	67
4.2	Experimental .....	68
4.2.1	Materials .....	68
4.2.2	Density measurement.....	68
4.2.3	T-peel test.....	69
4.2.4	Three-point bend test .....	70
4.2.5	Ballistic test.....	70
4.2.6	SEM and sample preparation .....	70
4.2.7	WAXD of multilayer consolidated Spectra <sup>®</sup> cloth.....	71
4.2.8	Studies on the surface and center layers .....	72
4.3	Results and Discussion .....	72
4.3.1	Density of the multilayer consolidated structure .....	72
4.3.2	Interlayer adhesion.....	73
4.3.3	Flexural properties .....	77

4.3.4	Ballistic performance .....	79
4.3.5	Morphology and sintering mechanism.....	82
4.3.6	Molecular orientation.....	85
4.3.7	Comparison of the surface and center layers .....	87
4.4	Conclusion .....	92
5.	THERMOFORMING OF SPECTRA® CLOTH AND THE PROPERTIES OF HEMISPHERICAL DOME STRUCTURES .....	94
5.1	Introduction.....	94
5.2	Experimental .....	94
5.2.1	Materials .....	94
5.2.2	Mold design .....	95
5.2.3	Molding schemes .....	96
5.2.4	Typical procedures.....	97
5.2.5	Property measurements.....	99
5.3	Results and Discussion .....	99
5.3.1	Thermoformability .....	99
5.3.2	Dome dimensions and thermal dimensional stability .....	100
5.3.3	Compressive properties.....	102
5.3.4	DSC studies of dome top and edge.....	103
5.4	Conclusion .....	105
6.	STUDIES ON DYNEEMA FRAGLIGHT® NONWOVEN FELT AND SPECTRA SHIELD® PLUS PCR PREPREG.....	106
6.1	Introduction.....	106
6.2	Experimental .....	106
6.2.1	Materials .....	106
6.2.2	Material processing and property measurements.....	107
6.2.2.1	Processing procedure .....	107
6.2.2.2	Measurement of crystallinity changes by DSC.....	108
6.2.2.3	Measurement of orientation changes by WAXD.....	108
6.2.2.4	Measurement of impact properties by puncture test.....	108
6.2.2.5	Measurement of interlayer adhesion by T-peel test.....	109
6.2.2.6	Measurement of flexural properties by three-point bend test.....	109

6.2.3 Thermoforming of Dyneema Fraglight <sup>®</sup> and Spectra Shield <sup>®</sup> Plus PCR.....	109
6.3 Results and Discussion .....	110
6.3.1 Dyneema Fraglight <sup>®</sup> nonwoven felt .....	110
6.3.1.1 Crystallinity change .....	111
6.3.1.2 Impact properties .....	114
6.3.1.3 Interlayer adhesion.....	115
6.3.1.4 Flexural properties .....	116
6.3.1.5 Thermoformability .....	117
6.3.2 Spectra Shield <sup>®</sup> Plus PCR prepreg.....	118
6.3.2.1 Crystallinity change .....	118
6.3.2.2 Orientation change .....	122
6.3.2.2 Impact properties .....	123
6.3.2.3 Interlayer adhesion.....	125
6.3.2.4 Flexural properties .....	126
6.3.2.5 Thermoformability .....	127
6.3.3 Comparison of consolidated Spectra <sup>®</sup> cloth, Dyneema Fraglight <sup>®</sup> and Spectra Shield <sup>®</sup> Plus PCR.....	128
6.3.3.1 Crystallinity.....	128
6.3.3.2 Molecular orientation.....	130
6.3.3.3 Impact properties .....	132
6.3.2.3 Interlayer adhesion.....	134
6.3.2.4 Flexural properties .....	137
6.4 Conclusion .....	138
7. CONCLUSIONS AND FUTURE WORK .....	140
7.1 Matrix free Spectra <sup>®</sup> fiber reinforced composites .....	140
7.2 Potential Applications.....	144
7.3 Processable Polymers.....	145
BIBLIOGRAPHY .....	146



## LIST OF TABLES

Table	Page
1.1 Properties of common high performance fibers.....	12
1.2 Comparison of Spectra <sup>®</sup> fiber and Kevlar <sup>®</sup> fiber unidirectional composites .....	15
2.1 Tensile properties of Spectra <sup>®</sup> fiber 900 at ambient temperature .....	28
2.2 Tensile properties of Spectra <sup>®</sup> 900 filament at ambient and elevated temperatures.....	30
2.3 Tensile properties of Spectra <sup>®</sup> 900 yarn at ambient and elevated temperatures.....	31
2.4 Tensile properties of Spectra <sup>®</sup> 900 filament annealed at elevated temperatures.....	34
2.5 Thermal shrinkage of Spectra <sup>®</sup> 900 single filaments at elevated temperatures.....	35
2.6 Hermans orientation function of unidirectionally aligned Spectra <sup>®</sup> fiber 900 and the as-received Spectra <sup>®</sup> cloth 903.....	44
3.1 Overall crystallinity of the as-received and consolidated Spectra <sup>®</sup> cloth 903 sintered under 7.6MPa for 30 minutes at different sintering temperatures.....	52
3.2 Changes in crystallinity corresponding to the original crystals for single layer Spectra <sup>®</sup> cloth 903 sintered under 7.6MPa for 30 minutes at different sintering temperatures.....	54
3.3 Hermans orientation function for unidirectional fibers, as-received Spectra <sup>®</sup> cloth, and Spectra <sup>®</sup> cloth consolidated under 7.6MPa for 30 minutes at different processing temperatures .....	57
3.4 Degree of crystallinity and Hermans orientation function of the as-received Spectra <sup>®</sup> cloth and Spectra <sup>®</sup> cloth consolidated under 7.6MPa for 30 minutes at different processing temperatures .....	59
3.5 NTT total impact energy (KJ/m) and failure mode of Spectra <sup>®</sup> cloth consolidated under different processing conditions, as-received Spectra <sup>®</sup> cloth, and unoriented UHMWPE sheet.....	63
4.1 T-peel strength of two layers of Spectra <sup>®</sup> cloth 903 bonded under 7.6MPa for 30 minutes at different temperatures.....	75
4.2 Flexural modulus (GPa) of twelve layers of Spectra <sup>®</sup> cloth 903 sintered at different processing conditions and unoriented UHMWPE panel.....	77

4.3	V <sub>50</sub> ballistic limits of matrix free Spectra <sup>®</sup> composite, Spectra <sup>®</sup> fiber/vinyl ester matrix composites, and Spectra <sup>®</sup> cloth against different sized projectiles.....	80
4.4	Overall crystallinity for the surface and center layers from twelve-layer Spectra <sup>®</sup> cloth panels sintered under 17.2MPa for 30 minutes at different processing temperatures.....	90
4.5	Hermans orientation function for the surface and center layers from twelve-layer Spectra <sup>®</sup> cloth panels sintered under 17.2MPa for 30 minutes at different processing temperatures.....	91
6.1	Overall crystallinity of single layer as-received and consolidated Dyneema <sup>®</sup> felt sintered under 7.6MPa for 30 minutes at different processing temperatures ...	113
6.2	Changes in crystallinity corresponding to the original crystals for single layer consolidated Dyneema <sup>®</sup> felt sintered under 7.6MPa for 30 minutes at different processing temperatures.....	113
6.3	Overall crystallinity and retained original crystallinity for the as-received Spectra Shield <sup>®</sup> Plus PCR and single layer Spectra Shield <sup>®</sup> Plus PCR consolidated under 7.6MPa for 30 minutes at different temperatures .....	121
6.4	Overall crystallinity of the as-received and consolidated single layer Spectra <sup>®</sup> cloth, Dyneema Fraglight <sup>®</sup> , and Spectra Shield <sup>®</sup> Plus PCR sintered under 7.6MPa for 30 minutes at different processing temperatures .....	129
6.5	Hermans orientation function of the as-received and consolidated single layer Spectra <sup>®</sup> cloth and Spectra Shield <sup>®</sup> Plus PCR sintered under 7.6MPa for 30 minutes at different processing temperatures .....	131
6.6	NTT total impact energy (KJ/m) of the as-received and consolidated single layer Spectra <sup>®</sup> cloth, Dyneema Fraglight <sup>®</sup> , and Spectra Shield <sup>®</sup> Plus PCR sintered under 7.6MPa for 30 minutes at different processing temperatures .....	133
6.7	T-peel strength (N/cm) of bilayer Spectra <sup>®</sup> cloth, Dyneema Fraglight <sup>®</sup> , and Spectra Shield <sup>®</sup> Plus PCR bonded under 7.6MPa for 30 minutes at different temperatures .....	135
6.8	T-peel strength (N/cm) of Spectra <sup>®</sup> cloth bilayer, Dyneema Fraglight <sup>®</sup> , bilayer and Spectra <sup>®</sup> cloth- Dyneema Fraglight <sup>®</sup> bilayer bonded under 7.6MPa for 30 minutes at different temperatures.....	136

## LIST OF FIGURES

Figure	Page
1.1 Morphology of PE fibers: (i) extended chain PE fiber, (ii) conventional melt-spun PE fiber.....	7
1.2 Model of microfibrils in Spectra <sup>®</sup> fibers.....	9
1.3 Generalized models for fibrous materials .....	10
1.4 Comparison of ballistic properties against 2 caliber projectiles: Spectra <sup>®</sup> fiber 900 composites vs. aramid fiber composites .....	17
1.5 Schematic of high-temperature high-pressure sintering coupled with thermoforming process .....	21
2.1 Typical stress-strain curve of a single filament at ambient temperature .....	29
2.2 Typical stress-strain curve of a yarn at ambient temperature .....	29
2.3 Young's modulus of the filament and yarn at ambient and elevated temperatures .....	32
2.4 Breaking strength of the filament and yarn at ambient and elevated temperatures .....	32
2.5 Strain at break of the filament and yarn at ambient and elevated temperatures .....	33
2.6 Thermal shrinkage of Spectra <sup>®</sup> 900 single filaments at elevated temperatures.....	35
2.7 The observed shrinkage force of a Spectra <sup>®</sup> 900 single filament with increasing temperature .....	36
2.8 DSC traces of Spectra <sup>®</sup> fiber 900 in unconstrained and constrained states.....	38
2.9 The first run DSC trace of Spectra <sup>®</sup> cloth 903.....	39
2.10 The second run DSC trace of Spectra <sup>®</sup> cloth 903 after quenching.....	40
2.11 SEM image of a bundle of Spectra <sup>®</sup> fibers in the cloth .....	41
2.12 SEM image of Spectra <sup>®</sup> cloth 903 .....	42
2.13 WAXD pattern of unidirectionally aligned Spectra <sup>®</sup> 900 fiber.....	43
2.14 WAXD pattern of the as-received Spectra <sup>®</sup> cloth 903 .....	43



2.15 Hermans orientation function .....	44
3.1 DSC trace overlay for single layer Spectra <sup>®</sup> cloth 903 sintered under 7.6MPa for 30 minutes at different temperatures .....	50
3.2 Overall crystallinity of the as-received and consolidated Spectra <sup>®</sup> cloth 903 sintered under 7.6MPa for 30 minutes at different sintering temperatures.....	52
3.3 Picture of single layer Spectra <sup>®</sup> cloth 903 sintered under 7.6MPa for 30 minutes at different sintering temperatures.....	53
3.4 Changes in crystallinity corresponding to the original crystals for consolidated Spectra <sup>®</sup> cloth 903 sintered under 7.6MPa for 30 minutes at different sintering temperatures .....	54
3.5 WAXD patterns for the as-received Spectra <sup>®</sup> cloth and Spectra <sup>®</sup> cloth consolidated under 7.6MPa for 30 minutes at different processing temperatures .....	56
3.6 Degree of orientation calculated using Hermans orientation function for unidirectional fibers, as-received Spectra <sup>®</sup> cloth, and Spectra <sup>®</sup> cloth consolidated under 7.6MPa for 30 minutes at different processing temperatures .....	58
3.7 Schematic of Spectra <sup>®</sup> fiber microfibrils .....	59
3.8 Linear correlation between the degree of crystallinity and Hermans orientation function .....	60
3.9 Typical Load vs. Deflection curve from an impact test of single layer of consolidated Spectra <sup>®</sup> cloth .....	62
3.10 NTT total impact energy vs. temperature and time for single layer of consolidated Spectra <sup>®</sup> cloth 903 under 7.6MPa.....	64
3.11 NTT total impact energy of single layer of consolidated Spectra <sup>®</sup> cloth 903 at 150°C for 30 minutes under various pressures .....	65
4.1 Density of multilayer Spectra <sup>®</sup> cloth panels sintered under 17.2MPa for 30 minutes at various processing temperatures .....	73
4.2 Typical load vs. detachment curve in a T-peel test.....	74
4.3 SEM images of peeled surfaces for specimens sintered under 7.6MPa for 30 minutes at different processing temperatures .....	76

4.4 Flexural modulus of twelve layers of Spectra <sup>®</sup> cloth 903 sintered at different processing conditions (sintering pressure = 17.2MPa) and unoriented UHMWPE panel .....	78
4.5 Ballistic performance of the multilayer consolidated Spectra <sup>®</sup> cloth compared with other composites (from the US Army) .....	82
4.6 Low magnification SEM images showing the cross sections of multilayer Spectra <sup>®</sup> cloth sintered under 17.2MPa for 30 minutes at different processing temperatures .....	83
4.7 High magnification SEM images showing the cross sections of multilayer Spectra <sup>®</sup> cloth sintered under 17.2MPa for 30 minutes at different processing temperatures .....	84
4.8 SEM images of the boundary between two orthogonal yarns in a multilayer consolidated Spectra <sup>®</sup> cloth and schematic of consolidation mechanism .....	85
4.9 Hermans orientation function for single and six layer Spectra <sup>®</sup> cloth sintered under 7.6MPa for 30 minutes at different processing temperatures .....	87
4.10 DSC trace overlay for the surface layers from twelve-layer Spectra <sup>®</sup> cloth panels sintered under 17.2MPa for 30 minutes at different processing temperatures .....	88
4.11 DSC trace overlay for the center layers from twelve-layer Spectra <sup>®</sup> cloth panels sintered under 17.2MPa for 30 minutes at different processing temperatures .....	89
4.12 Hermans orientation function for the surface and center layers from twelve-layer Spectra <sup>®</sup> cloth panels sintered under 17.2MPa for 30 minutes at different processing temperatures .....	91
5.1 The design of the hemispherical mold .....	95
5.2 Typical molding procedures using a twenty-five layer consolidated Spectra <sup>®</sup> cloth flat panel .....	98
5.3 Dimension and thickness of the dome .....	101
5.4 Compressive properties of the dome .....	103
5.5 DSC trace overlay for samples taken from the top and edge regions of the dome .....	104
6.1 DSC trace overlay for single layer as-received and consolidated Dyneema <sup>®</sup> felt sintered under 7.6MPa for 30 minutes at different processing temperatures ...	112



6.2 Changes in overall crystallinity and crystallinity from the original crystals for single layer as-received and consolidated Dyneema <sup>®</sup> felt sintered under 7.6MPa for 30 minutes at different processing temperatures .....	114
6.3 NTT total impact energy (KJ/m) of the as-received Dyneema <sup>®</sup> felt and single layer consolidated Dyneema <sup>®</sup> felt sintered under 7.6MPa for 30 minutes at different processing temperatures .....	115
6.4 T-peel strength for Dyneema <sup>®</sup> -Dyneema <sup>®</sup> bilayers sintered under 7.6MPa for 30 minutes at different temperatures.....	116
6.5 Flexural modulus of 14 layers Dyneema <sup>®</sup> felt panels consolidated under 17.2MPa for 30 minutes at different temperatures .....	117
6.6 DSC trace overlay of the as-received Spectra Shield <sup>®</sup> Plus PCR and single layer Spectra Shield <sup>®</sup> Plus PCR consolidated under 7.6MPa for 30 minutes at different processing temperatures .....	119
6.7 Overall and original crystallinity of the as-received Spectra Shield <sup>®</sup> Plus PCR and single layer Spectra Shield <sup>®</sup> Plus PCR consolidated under 7.6MPa for 30 minutes at different processing temperatures .....	121
6.8 Hermans orientation function of the as-received Spectra Shield <sup>®</sup> Plus PCR and single layer Spectra Shield <sup>®</sup> Plus PCR consolidated under 7.6MPa for 30 minutes at different processing temperatures .....	123
6.9 NTT total impact energy (KJ/m) of the as-received Spectra Shield <sup>®</sup> Plus PCR and single layer Spectra Shield <sup>®</sup> Plus PCR consolidated under 7.6MPa for 30 minutes at different processing temperatures .....	124
6.10 T-peel strength for Spectra Shield <sup>®</sup> Plus PCR bilayers sintered under 7.6MPa for 30 minutes at different processing temperatures.....	125
6.11 Flexural properties of 32 layers Spectra Shield <sup>®</sup> Plus PCR panels consolidated under 17.2MPa for 30 minutes at different processing temperatures .....	127
6.12 Overall crystallinity of the as-received and consolidated single layer Spectra <sup>®</sup> cloth, Dyneema Fraglight <sup>®</sup> , and Spectra Shield <sup>®</sup> Plus PCR sintered under 7.6MPa for 30 minutes at different processing temperatures .....	130
6.13 Hermans orientation function of the as-received and consolidated single layer Spectra <sup>®</sup> cloth and Spectra Shield <sup>®</sup> Plus PCR sintered under 7.6MPa for 30 minutes at different processing temperatures .....	132
6.14 NTT total impact energy (KJ/m) of the as-received and consolidated single layer Spectra <sup>®</sup> cloth, Dyneema Fraglight <sup>®</sup> , and Spectra Shield <sup>®</sup> Plus PCR sintered under 7.6MPa for 30 minutes at different processing temperatures .....	134

6.15 T-peel strength of bilayer Spectra<sup>®</sup> cloth, Dyncema Fraglight<sup>®</sup>, and Spectra Shield<sup>®</sup> Plus PCR bonded under 7.6MPa for 30 minutes at different temperatures ..... 135

6.16 T-peel strength of Spectra<sup>®</sup> cloth bilayer, Dyncema Fraglight<sup>®</sup> bilayer, and Spectra<sup>®</sup> cloth- Dyncema Fraglight<sup>®</sup> bilayer bonded under 7.6MPa for 30 minutes at different temperatures..... 137

6.17 Flexural modulus of multilayer consolidated Spectra<sup>®</sup> cloth, Dyncema Fraglight<sup>®</sup>, Spectra Shield<sup>®</sup> Plus PCR, and UHMWPE panels sintered under 17.2MPa for 30 minutes at different processing temperatures ..... 138



## CHAPTER 1

### BACKGROUND AND INTRODUCTION

#### 1.1 Fiber Reinforced Composites

Webster's dictionary shows that the word "composite" came from the Latin term *compositus*. Originally the word was used as an adjective that meant "made up of distinct parts", but later, it was used as a noun. A composite is a solid material which is composed of two or more substances having different physical characteristics and in which each substance retains its identity while contributing desirable properties to the whole.

Traditionally, a composite material is a combination of two or more chemically different materials with a distinct interface between them.<sup>5</sup> Composites consist of two phases; one is continuous and is called a matrix, and the other is discontinuous and is in form of fibers or particulates. The discontinuous phase is well dispersed in the matrix and acts as a reinforcement or modifier, to improve and alter the matrix properties.

Matrix materials used in composites are typically ceramics, metals, or polymers. Fibers are the common reinforcements due to their effectiveness, although particulates of various geometries are also used. Polymer matrix composites, with fiber reinforcement, are the most commonly used high performance composites and are widely used in many applications because of their unique properties and characteristics. Fiber reinforced polymeric composites consist of high strength and modulus fibers embedded in or bonded to a polymer matrix with distinct interfaces between them.<sup>6</sup> Fiber reinforced polymeric composites have many distinctive advantages over traditional materials; the most significant one being their light weight. Low density leads to high specific strength and

specific stiffness. Polymer matrices and reinforcing fibers have densities between 0.9 - 1.5g/cm<sup>3</sup> and 1.0 - 2.7g/cm<sup>3</sup>, respectively, and the resulting composites have densities between 0.9 - 2g/cm<sup>3</sup>. Compared to steel and aluminum alloys with a density of 7.9 g/cm<sup>3</sup> and 2.7 g/cm<sup>3</sup>, respectively, polymer composites offer a large advantage in weight-sensitive applications such as those in aerospace and military.

Another benefit of polymer composites is their design flexibility and freedom. By varying the fiber type, the fiber direction and volume fraction, and adopting different manufacturing processes, the composites' properties and characteristics can be easily controlled and adjusted. Anisotropic materials with direction dependent properties, rather than isotropic materials, may be produced. Materials with hybrid properties can be prepared by using two or more different types of fibers. Since some fibers have negative coefficients of thermal expansion, materials with zero coefficients of thermal expansion can be made by combining these reinforcements with appropriate matrices.

Fiber reinforced polymers have many advantages over conventional composite materials, which make them very attractive for various applications. Polymeric composites do not exhibit catastrophic failure mechanically, as opposed to ceramics or metals, instead they damage and fail progressively. They have good corrosion and electrical resistance and have high damping factors against noise and vibrations. Also, polymeric composites have low coefficients of thermal expansion and thus have good dimensional stability.

Matrices used in fiber reinforced polymeric composites are either thermosets or thermoplastics. They play several important roles in the composites:<sup>5</sup>

- Hold the fibers in place
- Transfer stress between fibers
- Protect fibers from adverse environment or mechanical abrasion

The matrix contributes little in tensile load-carrying capacity, although it affects the interlaminar shear and in-plane shear properties of the composites. The matrix provides support for the fibers under compression, thus influencing the compressive properties of the composites. In unidirectional fiber composites, transverse tensile modulus and strength are largely determined by the properties of the matrix.

Traditionally the matrices of fiber reinforced polymers are thermosets, such as epoxies, vinyl esters and phenolics, as they are usually low viscosity prepolymers and their wettability to fibers is generally good. In addition, thermosets have high  $T_g$ , good thermal stability and chemical resistance, and exhibit low creep and stress relaxation behavior. However, thermosets have long fabrication time due to the slow crosslinking and solidifying processes. Also, thermoset matrices can be brittle and fail at low strain and as a result, resistance to microcracks and impact can be poor.

The most important benefit of thermoplastic matrices is their high fracture resistance and impact strength, due to their high strain to failure; these are desirable properties in certain applications like ballistic shields. Thermoplastics have short fabrication times, are thermoformable and can be easily repaired by welding or solvent bonding. Since thermoplastic matrices are not crosslinked polymers, they are easily



recycled and reused. However, their wettability to fibers is relatively poor because of their high viscosities and there is no direct chemical bonding between matrix and fiber.

Fibers are the major component that occupies the largest volume fraction in fiber reinforced polymer composites. They are the principal load-bearing constituents that dominate the characteristics and properties of the composites. It is important to select the proper fibers in order to meet the requirements for the final product. The following factors are usually considered when designing a composite with fiber reinforcement:

- Density
- Tensile modulus and strength
- Compressive strength
- Fatigue strength and mechanism
- Resistance to fracture and impact
- Chemical resistance
- Electrical and thermal conductivity
- Adhesion to the selected matrix
- Chemical compatibility with the selected matrix

There are a large variety of commercially available fibers with different properties that can be used as reinforcements: glass fibers, carbon/graphite fibers, aramid fibers, polyethylene fibers, boron fibers, silicon carbide (SiC), aluminum oxide ( $\text{Al}_2\text{O}_3$ ) and metal fibers. Glass fibers are the most common reinforcement due to their low cost, high tensile strength, high chemical resistance and excellent insulating properties. The disadvantages of glass fibers are their low tensile modulus, high density, low resistance to abrasion and fatigue, and high hardness.<sup>6</sup> They are mostly used in automotives, durable



goods and consumer goods. Carbon fibers have the advantage of high specific tensile modulus and strength, high fatigue performance and low coefficient of thermal expansion. The disadvantages include low impact resistance and high electrical conductivity. Their main application is limited in the field of aerospace because of their high cost. Aramid fibers, such as Kevlar<sup>®</sup> family<sup>7</sup>, have higher specific tensile strength and strain to failure than carbon fibers, which offers them good damage tolerance against impact. Kevlar<sup>®</sup> fibers have good chemical and thermal stability, and poor compressive properties. They are widely used in aerospace, marine and military applications.

The fibers used in composites can adopt many forms; they can be used as continuous filaments or yarns, as well as discontinuous chopped fibers. Two- and three-dimensional fabrics can be made from continuous fibers using textile processes such as weaving, knitting, braiding and needle-punching. Fabrics are easy to handle and provide good control over the fiber orientation and placement. The alignment of fibers in composites can be unidirectional, bidirectional, multidirectional or random. Unidirectional fiber composites use fibers most effectively if the loading direction coincides with fiber direction; the strength and modulus is poor in other directions, especially in the transversal direction. Two dimensional fabrics create somewhat equal properties in the longitudinal and transversal directions. The multi-dimensional arrangement gives them quasi-isotropic materials in the fiber plane. Isotropic properties can only be achieved by incorporating randomly oriented fibers in the composites and overall mechanical properties are lower.

Fiber volume fraction  $V_f$  is an important parameter that dictates the composites' properties. Fiber volume fraction should be as high as possible to maximize the strength

of the composites. Theoretically, the highest achievable fiber volume fraction is 90.7% if the fibers are uniform in diameters and hexagonally close-packed. The actual volume fraction can be calculated from the fiber weight fraction according to Equation 1.1.

$$V_f = \frac{w_f / \rho_f}{w_f / \rho_f + w_m / \rho_m} \quad (1.1)$$

where  $w_f$  = fiber weight fraction       $\rho_f$  = fiber density

$w_m$  = matrix weight fraction       $\rho_m$  = matrix density

Another important aspect of fiber reinforced composites is the interfacial adhesion between fibers and matrices; good bonding strength is needed for fibers to achieve good reinforcement. The influence of interfacial adhesion on composites properties is profound; compression strength, flexural strength, transverse tensile strength, in-plane shear strength, interlaminar shear strength, mode I fracture toughness and impact damage resistance increase with the level of adhesion. Tensile strength is either independent of or decreases with increasing bonding strength and elastic constants, such as Young's modulus, are unaffected by adhesion. Interestingly, ballistic resistance decreases with increase in bonding strength. Relatively poor adhesion makes interfiber and interlaminar debonding easier, thus ballistic energy is efficiently dissipated laterally, and resistance to penetration is enhanced.<sup>5</sup>

## 1.2 Ultra High Molecular Weight Polyethylene (UHMWPE) Fibers

Historically, polyethylene (PE) is known as a low strength, low stiffness material. Conventional methods to make polyethylene fibers, such as melt-spinning, yield only

“folded chain” molecular structure. Theory predicts that if PE chains could be fully extended and “frozen” in a highly dense packing state, the resulting fibers would be extraordinarily strong because of the intrinsic high strength of the carbon-carbon covalent bond. The schematic illustration of the morphology of extended chain PE fibers and conventional melt-spun PE fibers is compared in Figure 1.1.<sup>8</sup>

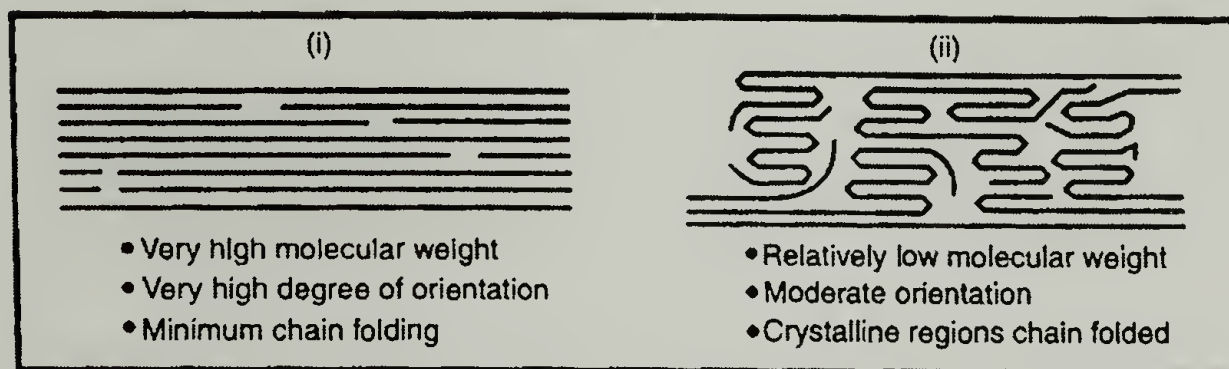


Figure 1.1 Morphology of PE fibers: (i) extended chain PE fiber, (ii) conventional melt-spun PE fiber

The high strength and modulus of the extended chain PE fibers are attributed to their high molecular weight, degree of orientation, and crystallinity. After years of research in several leading universities and prompt recognition by industry, extended chain polyethylene fibers were commercialized in 1985 as ultra high strength, high modulus, and high performance fibers.

Polyethylene fibers can be obtained by three methods: solid-state extrusion, special drawing technique, and solution/gel spinning. Solid-state extrusion was developed by Porter et al. at University of Massachusetts. It involves extrusion of PE polymer through a conical die at a temperature below its melting point. Due to flow-



induced orientation and pressure effects, the extruded material has a high modulus and strength.<sup>9</sup>

The special drawing technique utilizes a melting spinning method combined with a unique drawing process at a temperature close to the polymer melting point to yield a high modulus fiber. This technique was developed by Ward at University of Leeds and is currently licensed to Cclanese in the United States and Snia BVP in Europe.<sup>10</sup>

The principles for solution/gel spinning of ultra high molecular weight polyethylene were developed by Pennings and his students Smith, Lemstra and Kalb at University of Groeningen<sup>11</sup> and the practical processes were refined by many other researchers such as Kavesh and Prevorsek. In solution spinning, typically 2-5 wt% solution of UHMWPE (MW 1-5 million) in decalin is extruded at 130-150°C into a cold water bath. The fiber forms a gel and contains as much as 98% solvent and is therefore referred to as “gel spinning”. The solvent is evaporated from the fiber under the vacuum and the fiber is ultra-drawn between 100-135°C. Typical draw ratios are between 30× ~ 100× and the strength and modulus of the fiber is determined by the draw.<sup>5</sup> Currently, ultra high molecular weight extended chain polyethylene fibers on the market are all made by solution/gel spinning technology and are represented by Honeywell’s Spectra<sup>®</sup> fibers, DSM-Toyobo’s Dyneema<sup>®</sup> fibers and Mitsui’s Tekmilon<sup>®</sup> fibers.<sup>12</sup>

Since all three brands of UHMWPE gel-spun fibers resemble each other, Spectra<sup>®</sup> fibers are chosen as the example to illustrate their common characteristics and properties in this thesis. The microscopic structure of Spectra<sup>®</sup> fibers is typical of all organic fibrous materials. The microfibrils are about 5nm in diameter and have finite length, and the aggregated macrofibrils are about 50nm in diameter. Schaper<sup>13</sup> showed that the



longitudinal dimension of the microfibrils is about 1000-2000nm and they have an aspect ratio of 250-500. Grubb<sup>14</sup> reported from SAXS analysis, that the microfibrils exhibit a long period of ~200nm, which suggests that the microfibrils have non-uniform density and that the low density domains contain mainly crystal defects. Based on these investigations, Kavesh and Prevorsek<sup>15</sup> proposed a model for the microfibril structure shown in Figure 1.2. In this model the disordered domains appear to be 4-5nm and they are “amorphous” regions formed by chain ends. The “amorphous” domains are covalently bonded to the adjacent nearly perfect, needle-like crystalline domains whose aspect ratio is 40.

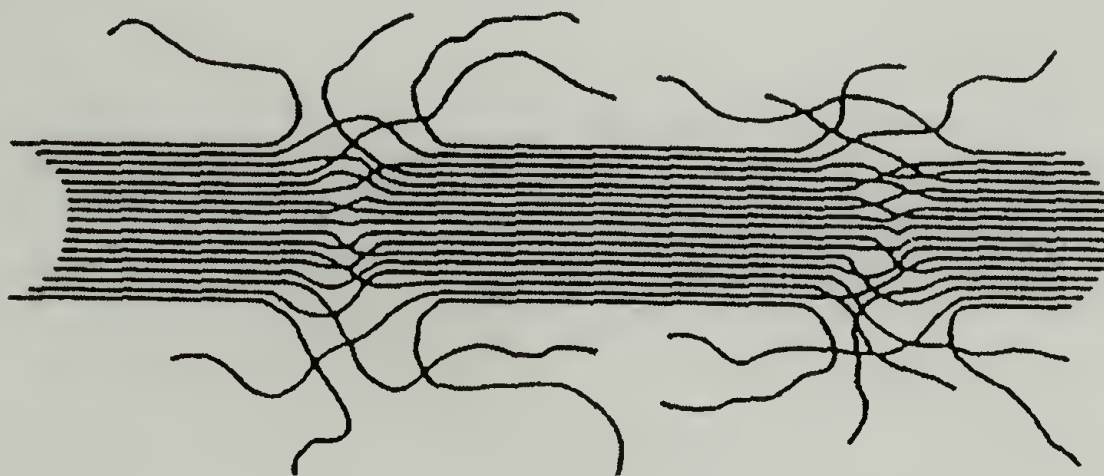


Figure 1.2 Model of microfibrils in Spectra<sup>®</sup> fibers

The fundamental difference between Spectra<sup>®</sup> fibers and other high strength organic fibers, such as aramid fibers, lies in their longitudinal characteristics. Nearly perfect crystals and fewer folded chains and localized defects make Spectra<sup>®</sup> fibers superior to most other high performance fibers. A generalized schematic illustration for fibrous materials is shown in Figure 1.3.<sup>15</sup>

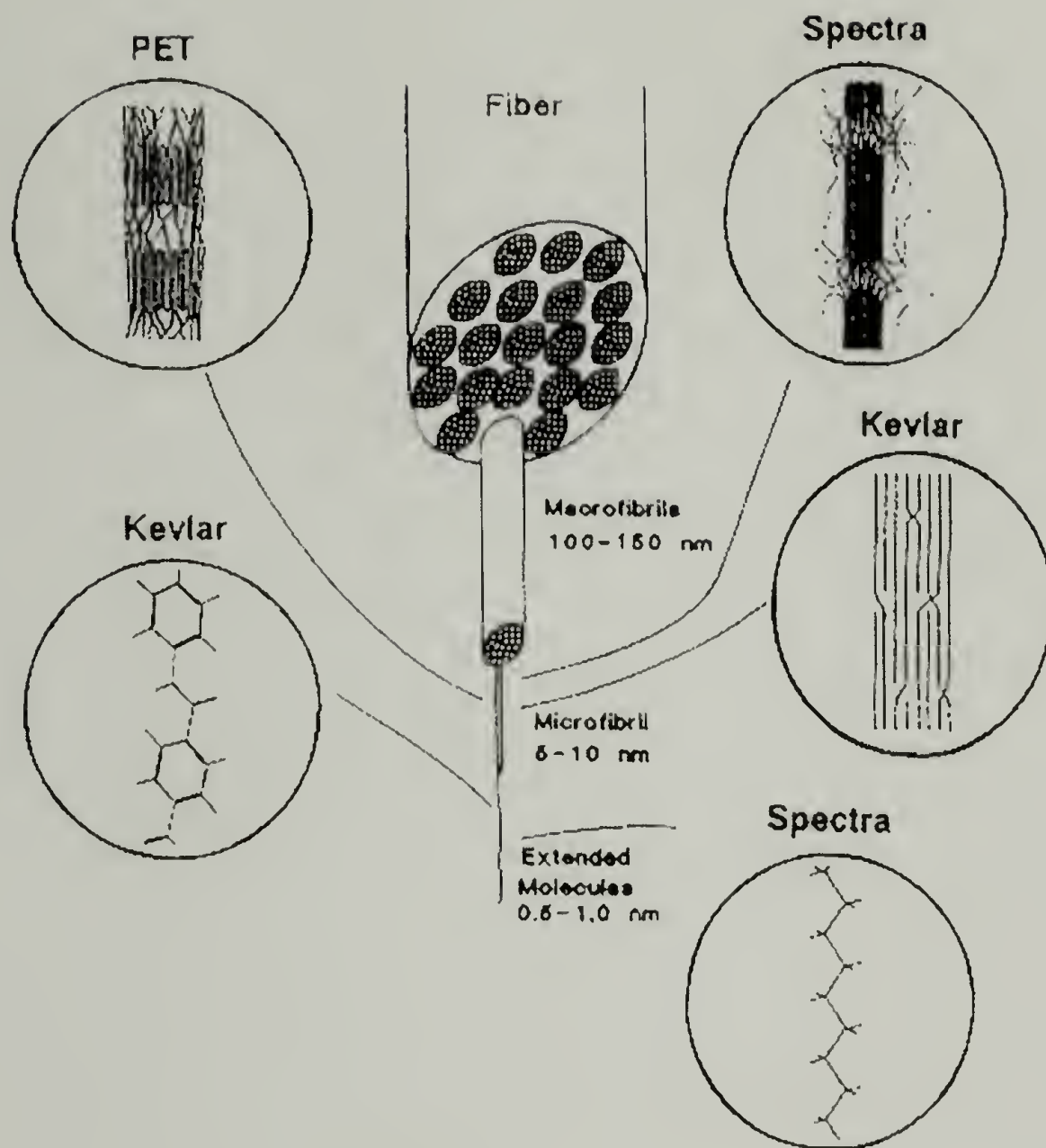


Figure 1.3 Generalized models for fibrous materials

Fu<sup>16</sup> et al. examined the morphology of Spectra<sup>®</sup> fibers by means of full pattern X-ray diffraction, powder X-ray diffraction, SAXS, solid state <sup>13</sup>CNMR and DSC and they concluded that there are three different phases in the fiber structure: a crystalline phase, an amorphous phase and an intermediate phase. The crystalline phase consists of orthorhombic and monoclinic crystals, which makes up ~75% and ~10% of the total fiber, respectively. About 5% of the fiber is composed of the amorphous phase and the final ~10% is the so-called intermediate phase. The intermediate phase is made of polyethylene chains that adopt a trans conformation and preferentially orient parallel to

the fiber axis. The axial distance between layers of neighboring carbon atoms is similar to that of the crystalline domain. However, the lateral packing is not as perfect and ordered as it is within the crystals. The mobility of the chains in the intermediate phase is one order of magnitude higher than that of the crystalline phase and one order of magnitude lower than that of the amorphous phase. Based on the three-phase model, the initial modulus is governed by the crystalline phase. The crystalline phase consists of predominately fully extended chains and has low strains at break, therefore the intermediate phase becomes the primary load-carrying component at increased strains and determines the ultimate strength of the fibers.

Spectra<sup>®</sup> fibers possess extraordinary physical and mechanical properties, such as low specific gravity, high modulus and strength, high impact resistance, high abrasion tolerance, excellent chemical resistance, low dielectric constant, good UV resistance, low moisture absorption, etc. Spectra<sup>®</sup> fibers have the lowest density of all the fibers. The density of Spectra<sup>®</sup> fibers is  $0.97 \text{ g/cm}^3$ , approximately 2/3 of that of aramid fibers and 1/2 of that of carbon fibers. The low density of Spectra<sup>®</sup> fibers gives them the highest specific tensile strength and the second highest specific tensile modulus (only below carbon fibers) among all high performance fibers. The cross section of Spectra<sup>®</sup> fibers is non-circular and irregular. The overall crystallinity of Spectra<sup>®</sup> fibers is between 80% and 95% depending on the manufacturing condition and the measuring methods, and the degree of crystalline orientation is as high as 95% - 99%. The melting point of Spectra<sup>®</sup> fibers is about 150°C; almost 15 degrees higher than that of unoriented polyethylene. This superheating phenomenon is due to different crystal sizes in the unoriented and



highly oriented polyethylene, as well as, high orientation and close packing that impose constraints on the crystals and reduce their mobility.

Some of the mechanical properties of Spectra<sup>®</sup> fiber 900 and other high performance fibers, such as aramid fiber, glass fiber, carbon fiber and melt-spun PE fiber Snia<sup>®18</sup>, are listed in Table 1.1.<sup>8,17</sup>

Table 1.1 Properties of common high performance fibers

Fiber Types	Spectra <sup>®</sup> 900	Snia <sup>®</sup>	Kevlar <sup>®</sup>	S- Glass	Carbon HM
Tensile strength (GPa)	2.6	1.2	2.8	4.6	2.2
Specific tensile strength ( $10^6$ N·m/Kg)	0.27	0.13	0.20	0.19	0.13
Tensile modulus (GPa)	117	58	124	90	393
Specific tensile modulus ( $10^6$ N·m/Kg)	12.6	6.1	9.3	3.6	22.4
Elongation (%)	3.5	3.0	2.5	5.4	0.6
Tenacity (gf/den)	30	13	22	21	14

Based on numerous experimental and theoretical studies, it is widely accepted that the crystalline modulus of Spectra<sup>®</sup> fibers is estimated to be  $300 \pm 20$  GPa. The actual fibers contain approximately 20% volume fraction of non-crystalline components and nano-scale defects, so the maximum measured modulus is only  $\sim 120$  GPa. In addition, the fiber modulus is temperature and strain rate dependent. At low temperatures and/or high strain rates, the modulus of Spectra<sup>®</sup> fibers becomes fairly close to the theoretical value of the crystalline modulus. As for theoretical strength, there is less agreement among various researchers and the reported values range from 20 GPa to 50 GPa. The



actual achieved strength of Spectra<sup>®</sup> fiber is about 3-4GPa at ambient temperature and normal strain rate.

Apart from the outstanding tensile properties of Spectra<sup>®</sup> fibers, they also have excellent abrasion and cut resistance. Ropes made of Spectra<sup>®</sup> fibers are eight times better than aramid ropes in accelerated sheave and wear tests.<sup>17</sup> Spectra<sup>®</sup> fibers exhibit higher chemical resistance than aramid fibers in various corrosive solvents. They have excellent vibration damping capability, flex fatigue properties, self-lubricating properties and a low coefficient of friction. Low dielectric constant makes them virtually transparent to radar. Despite the impressive list of properties, Spectra<sup>®</sup> fibers also have their limitations; low  $T_g$  and relatively low melting point prevent them from being used at high temperatures. Due to their chemical inertness and lack of functional groups, Spectra<sup>®</sup> fibers are difficult to bond to most materials, which makes it difficult to make Spectra<sup>®</sup> fiber reinforced polymer composites. Their compressive properties are among the lowest of all high performance fibers and they are weak in wear and tension fatigue.

### 1.3 Spectra<sup>®</sup> Fiber Reinforced Composites

Since Spectra<sup>®</sup> fibers were introduced to the market, there have been tremendous efforts put to make Spectra<sup>®</sup> fiber reinforced composites. The fiber yarns can be impregnated unidirectionally in composites by conventional prepreg routes. Fibers can be cross-ply, angle-ply and quasi-isotropically arranged using the wet/dry lay-up process. Fabrics in the form of woven cloth or nonwoven felt can also be used in composites. Both thermoset and thermoplastic matrices have been adopted, e.g., epoxy resin, polyester and urethane, for use with Spectra<sup>®</sup> fibers and fabrics.

In order to translate the outstanding properties of Spectra<sup>®</sup> fibers into the composites, good interfacial adhesion between fibers and matrices is required. However, because Spectra<sup>®</sup> fibers are nonpolar and have no reactive surface chemical groups, they stick to virtually no common matrices. The way to overcome this obstacle is by means of various fiber pre-treatments. Spectra<sup>®</sup> fibers can be chemically etched by chromic acid<sup>19</sup> or oxidized by polypyrrole<sup>20</sup> to increase the surface roughness. Plasma and corona treatments in O<sub>2</sub> or CO<sub>2</sub> introduce chemical groups onto the fiber surface through chain scission and substitution, and etch and roughen the fiber surface.<sup>21,22</sup> Cohen et al.<sup>23,24</sup> developed a novel method to make Spectra<sup>®</sup> fiber based composites using UHMWPE as matrix. They treated Spectra<sup>®</sup> fibers with a hot UHMWPE solution. Surface swelling of the fibers and consequent physical entanglement with the UHMWPE molecules in the solution formed a “brush” layer around the individual fibers and upon cooling the “brush” layer crystallized. The treated fibers were aligned unidirectionally and subjected to heat and pressure. The product was essentially a prepreg with UHMWPE as matrix. The final composite can be fabricated by compression molding or calendaring into any desired shape. All the fiber pre-treatments mentioned previously are proven to significantly improve the bonding of Spectra<sup>®</sup> fibers to matrices but generally degrade the fiber properties.

The mechanical properties of Spectra<sup>®</sup> fiber reinforced composites have been investigated by many researchers; unidirectional laminated epoxy matrix composites reinforced by Spectra<sup>®</sup> fibers and Kevlar<sup>®</sup> fibers are compared in Table 1.2.<sup>6</sup> In terms of longitudinal tensile strength, Spectra<sup>®</sup> fiber composites are almost as good as Kevlar<sup>®</sup> fiber composites. However, Kevlar<sup>®</sup> fiber composites out-perform Spectra<sup>®</sup> fiber

composites in both transverse tensile strength and shear strength, mainly because of better interfacial adhesion.

Table 1.2 Comparison of Spectra<sup>®</sup> fiber and Kevlar<sup>®</sup> fiber unidirectional composites

Unidirectional composites	Spectra <sup>®</sup> fiber epoxy matrix composites	Kevlar <sup>®</sup> fiber epoxy matrix composites
Shear strength (MPa)	9-15	50-60
Longitudinal tensile strength (GPa)	1.0-1.3	1.3-1.4
Transversal tensile strength (MPa)	9-11	20-25

One of the major interests in Spectra<sup>®</sup> fiber reinforced composites is their potential as ballistic protective materials. Today's state-of-the-art products use Kevlar<sup>®</sup> fiber reinforcement. Kevlar<sup>®</sup> fibers are covalently bonded in only one direction and the amide linkages promote hydrogen bonds between chains to form a three-dimensional network. Spectra<sup>®</sup> fibers have no active chemical groups and are essentially a one-dimensional structure<sup>25</sup> and polymer chains can slide past each other under load. As a result, Spectra<sup>®</sup> fibers have a high ductility and energy absorption capability. Unlike carbon fibers, Spectra<sup>®</sup> fibers do not show abrupt brittle failure at high stress and thus they are highly suitable for applications that require energy absorption, overload protection, and ductile non-catastrophic failure.

Although Spectra<sup>®</sup> fibers are somewhat viscoelastic at standard strain rates, they behave in a linear elastic manner at high strain rates such as happens in ballistic impact. The fiber strength and modulus increase with increasing strain rate. In ballistic conditions, their strength and modulus are estimated to be 5GPa and 280GPa, respectively.<sup>15</sup> It has been shown that the penetration of soft body armor and military



helmets happens primarily by breaking in tension, cutting and lateral displacement of the filaments.<sup>15</sup> Spectra<sup>®</sup> fibers have substantially higher cut resistance than Kevlar<sup>®</sup>. The velocity of the strain wave propagating through a material is in proportion to the square root of the Young's modulus to density ratio ( $\sqrt{E/\rho}$ ). The wave speed determines how fast the impact energy can be transported away from the impact site. In a laminated structure, like a helmet, the wave propagation speed is slower through thickness direction compared to the laminate plane. Increased wave velocity in the plane rapidly spreads out the impact energy laterally and results in a high volume of material involved in energy absorption in a short time. Due to Spectra<sup>®</sup> fibers' high modulus and low density, the value of  $\sqrt{E/\rho}$  is higher than for other fibers (e.g. 17.8 km/s for Spectra<sup>®</sup> vs. 12.3 km/s for aramid).<sup>26</sup> Spectra<sup>®</sup> fibers have excellent damage tolerance. Repetitive impact tests show increased rigidity of the samples.<sup>15</sup> Contrary to the expectation of weakening, Spectra<sup>®</sup> fiber composites actually enhance their properties after impact. The lack of adhesive bond between Spectra<sup>®</sup> fiber and matrix, a drawback in other applications, is actually desirable in ballistic applications. The extensive delamination and debonding in the composites when subject to ballistic impact provides excellent channels to dissipate high energy.

Another huge advantage of Spectra<sup>®</sup> fiber based armor is its light weight without sacrificing the high level of protection. As shown in Figure 1.4,<sup>15</sup> Spectra<sup>®</sup> fiber 900 based composites have better ballistic properties compared to aramid fiber composites for the same areal density. Composite armor produced from Spectra<sup>®</sup> fibers weighs 30%-50% less than for the same performance level aramid composite armor. Lower weight

armor, especially helmets, can significantly reduce wearer fatigue and allows for more sophisticated combat equipment to be mounted on the helmets. The standard aramid military helmet currently made from Kevlar<sup>®</sup> 29 weighs three pounds and in comparison a helmet made from Spectra<sup>®</sup> fibers weighs only slightly over two pounds.<sup>27</sup>

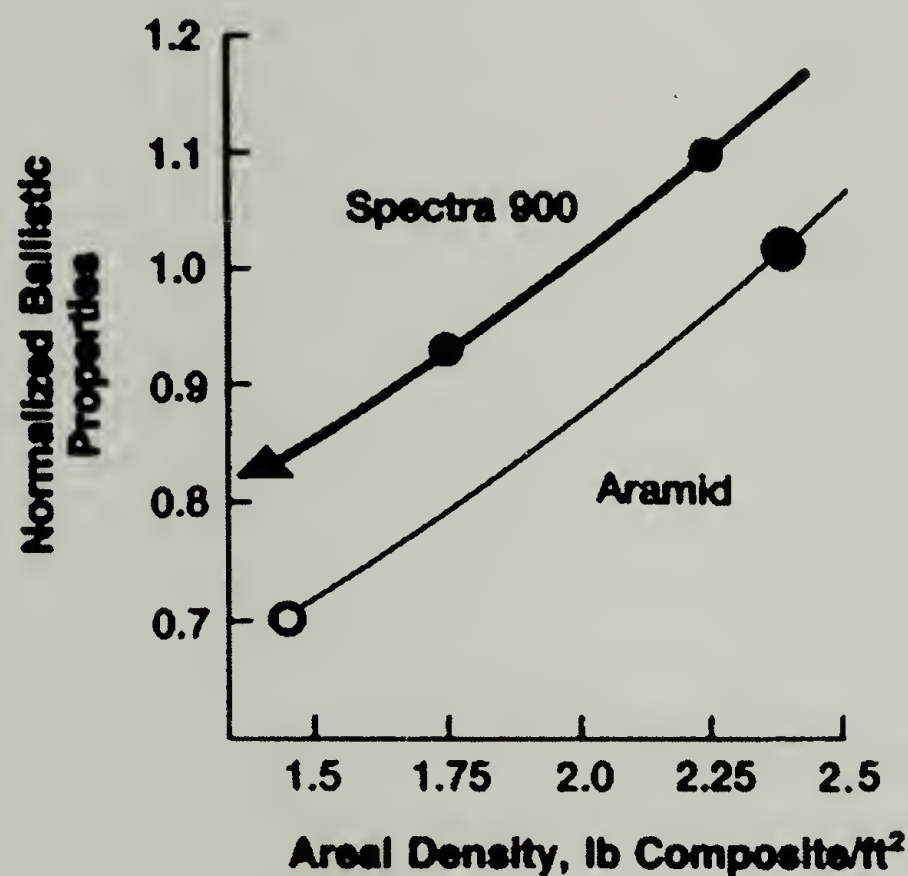


Figure 1.4 Comparison of ballistic properties against 2 caliber projectiles: Spectra<sup>®</sup> fiber 900 composites vs. aramid fiber composites

#### 1.4 One-polymer Composites

There has been growing interest in producing fiber reinforced composites in which the oriented phase and the continuous phase have similar chemical compositions. Usually these kinds of composites have good interfacial adhesion between the fibers and matrices. In the first example, presented by Capiati and Porter,<sup>28</sup> a high modulus PE filament with a high melting temperature was embedded in a block of HDPE with a low

melting temperature and they called it a “one-polymer composite”. The interfacial shear strength was fairly high due to the epitaxial transcrystallinity developed in the interphase region of the fiber and matrix. Later, other researchers extended this technique and developed the film stacking method.<sup>29,30</sup> Other approaches to make one-polymer composites have included powder impregnation<sup>31</sup> and solvent impregnation.<sup>32</sup> Most recently, Cohen et al. invented a unique method to produce UHMWPE fiber/UHMWPE matrix composites, as mentioned in the previous section.

In the above cases a secondary polymer, besides the polymeric fibers, is used as a binder or matrix to form the continuous phase. Ward at the University of Leeds has developed a new process called “hot compaction” which utilizes only one starting component (a highly oriented fiber or tape) and applies sufficient heat and pressure so that the surface of the oriented phase melts partially and recrystallizes on cooling to form the matrix phase. Since only a small portion of the oriented phase is melted to fill the interstice and serve as a binder, the majority of the original properties of the oriented phase are preserved. There is strong adhesion bonding between the two phases because of the molecular continuity throughout the composites. The challenge is to find the proper processing window in terms of time, temperature, and pressure. Since the lateral adhesion and strength are developed at the cost of the longitudinal strength, it is critical to strictly control the processing conditions so as to achieve a balanced overall mechanical integrity. Melt-spun polyethylene fiber was the first system studied by Ward, where the compaction scheme adopted is a two-stage process. First the fibers are pressed under a relatively low contact pressure at the “compaction temperature”. The “soaking time” is several minutes in order to allow for the selective melting of the fiber surface. Then a



substantially higher pressure is applied for a short period to consolidate the structure and upon cooling a stiff, strong sheet with one chemical composition is formed.

Subsequently, similar research was carried out using other materials, such as PET, PP, Spectra<sup>®</sup>, and Vectran<sup>®</sup> LCP fibers.<sup>33-42</sup>

Meanwhile, a parallel study conducted by Farris et al. at the University of Massachusetts introduced a similar process. The initial motivation was to make a protective coating for optics on military airplanes that could sustain the supersonic impact of rain and dust and be transparent to IR. Spectra<sup>®</sup> plain woven cloth was chosen as the starting material because of its desired properties. The process involves constraint of the cloth under lateral pressure to prevent shrinking and then increase of temperature near or slightly above the melting point of the Spectra<sup>®</sup> fiber. Upon cooling, while pressure is maintained, the cloth fuses together and forms a strong sheet. This research has led to several patents regarding the making of high strength, high modulus polymeric materials for impact resistant application.<sup>43-47</sup>

## 1.5 Project Overview

High strength, high impact resistant polymeric composites are very useful materials. They have numerous applications in the fields of aerospace, automotive, marine, military, industry, and sporting goods, etc. Usually they are made of a high performance fiber and an appropriate resin matrix. The objective of this research is to explore a novel method to make “matrix free” polymeric composites.<sup>48</sup> The approach involves the consolidation of fabrics using only heat and pressure without the addition of resin matrices or bonding agents. The surface melting of the fibers and subsequent

recrystallization upon cooling serves as the bonding mechanism. By eliminating the matrices, the composite achieves a high fiber volume fraction, which leads to better properties. Also the overall weight of the composites is significantly reduced, which is an enormous advantage for applications such as airplane structures and ballistic shields.

The motivation for the work is to make ballistic armor and helmets using fabrics made of ultra high molecular weight polyethylene (UHMWPE) fibers (trade name: Spectra<sup>®</sup>). It is well known that at elevated temperatures polyethylene is “rubbery” and can be subjected to considerable stretching. If layers of cloth are properly confined to prevent shrinkage, exposed to an appropriate heating and stretching sequence, consolidated and allowed to cool, it is feasible to produce a thick, rigid ballistic shield with curvatures and shapes. The schematic of this method is illustrated in Figure 1.5. Currently, ballistic hard armors are made of multiple layers of tightly woven cloth of high performance fibers and an adhesive matrix. When complex shapes involving double curvature are required, such as helmets or body armor, specially cut patterns are needed for lay-up to create the complex geometries since the materials used are not extensible. The proposed method does not involve the cutting of complex patterns or the use of any adhesive matrices, therefore simplifies the manufacturing process. A detailed method of fabrication, such as heating and stretching sequence, was developed and the optimal processing conditions, in terms of molding time, temperature and pressure, were established for Spectra<sup>®</sup> cloth. Thermo-mechanical properties, microstructures and morphologies, and ballistic performance of the products were investigated and evaluated. The results were correlated and reflected in the process-structure-property relationship. Two other commercial products that consist of the extended chain UHMWPE fibers,

Dynecma Fraglight<sup>®</sup> and Spectra Shield<sup>®</sup> Plus PCR, were also studied using this process as a comparison.

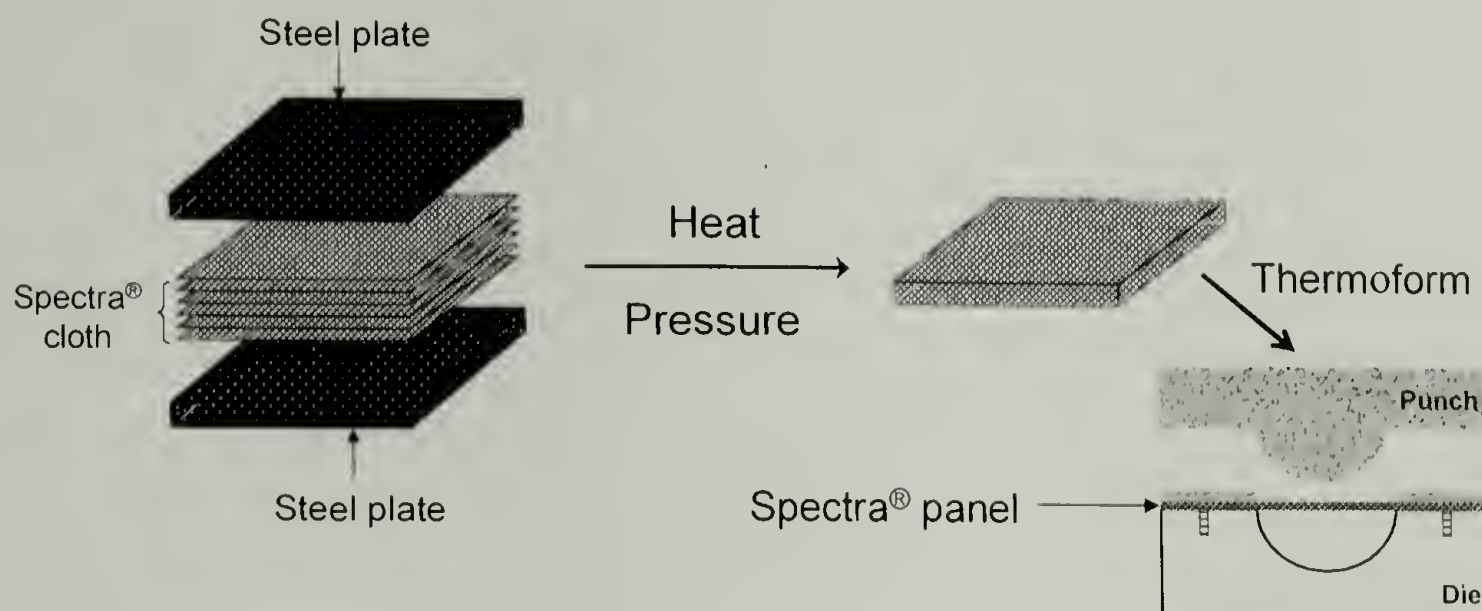


Figure 1.5 Schematic of high-temperature high-pressure sintering coupled with thermoforming process

Matrix free Spectra<sup>®</sup> fiber reinforced composites are made from one thermoplastic polymeric fiber. A distinctive feature is that they are thermoformable and therefore can be further processed in many ways such as compression molding or calendaring. As a unique concept, this methodology can be applied to other polymers, such as polypropylene, PET, Nylon, Vectran<sup>®</sup>, Lycra<sup>®</sup> and Nomex<sup>®</sup>, in forms of either fibers or woven and nonwoven fabrics. Many useful products and applications are foreseeable, such as tear resistant protective coatings, pressure vessels, high strength tubes, automobile bumpers, radomes, sporting goods and orthopedic implants, etc.



## CHAPTER 2

# THERMO-MECHANICAL PROPERTIES, STRUCTURE AND MORPHOLOGY OF SPECTRA<sup>®</sup> FIBER, YARN, AND CLOTH

### 2.1 Introduction

Since the commercialization of ultra high molecular weight polyethylene fibers in the mid 1980s, their structures and properties have been the subject of numerous researchers.<sup>16,49-56</sup> Their common properties as high performance fibers were briefly described in the previous chapter. Honeywell produces Spectra<sup>®</sup> fiber in several grades with different properties due to different manufacturing processes. In order to investigate property evolution during the high-temperature high-pressure sintering process, it is crucial to thoroughly study the properties of the virgin materials, including the single filament, yarn and woven cloth. The structure and morphology are important factors in determining the final properties of the material and also need to be carefully examined.

This chapter describes the measurement of various thermo-mechanical properties and studies of the structure and morphology of Spectra<sup>®</sup> single fiber, yarn and woven cloth. Property and structural information are necessary in order to understand, apply, and optimize the sintering process. Tensile modulus and strength are among the most important mechanical properties associated with the fibers, since they indicate the load carrying capacity of the fibers. As a thermoplastic material, the tensile properties of Spectra<sup>®</sup> fiber are expected to have a strong dependence on temperature. Experiments were conducted to measure the tensile properties of Spectra<sup>®</sup> single fibers and yarns at both ambient and elevated temperatures. The tensile properties of annealed Spectra<sup>®</sup>

fibers were measured at ambient temperature to determine the influence of thermal histories on the mechanical properties. Spectra<sup>®</sup> fiber is “ultra-drawn” during manufacturing (the draw ratio can be over 100×) and the result is highly oriented polymer molecules in an extended chain conformation. At elevated temperatures the extended chains tend to relax towards the entropically favorable random coil conformation; macroscopically the fiber shrinks and if constrained a shrinking force develops within the fiber. Thermal shrinkage was determined by soaking filaments in a hot bath at various temperatures and measuring the change in length. The shrinkage force developed with increasing temperature for the single filament under iso-strain condition was monitored using a Thermal Mechanical Analyzer (TMA) until the filament broke. Polyethylene is a semicrystalline polymer and its melting behavior can be monitored by Differential Scanning Calorimetry (DSC). The peak melting temperatures were identified, the crystalline melting enthalpy was measured, and the degree of crystallinity was calculated for Spectra<sup>®</sup> fiber and cloth. The fibers are under lateral pressure and constrained during the sintering process. Efforts were made to simulate the constrained state of the fibers and study the constraining effect on the fiber melting by DSC. Spectra<sup>®</sup> fiber is highly oriented polyethylene and the extended chains are parallel to each other. The molecular orientation of unidirectionally aligned fibers and the as-received cloth was investigated using Wide Angle X-ray Diffraction (WAXD) and the Hermans orientation function values were calculated. The microscopic features of Spectra<sup>®</sup> fiber and the weaving patterns of the cloth were examined by Scanning Electron Microscopy (SEM).

## 2.2 Experimental

### 2.2.1 Materials

Spectra<sup>®</sup> fiber was obtained from Honeywell and designated as Spectra<sup>®</sup> 900.<sup>57</sup> The yarn contains 120 filaments per tow and has a linear density of 1200 denier. The density of the fiber is 0.97g/cm<sup>3</sup>. Spectra<sup>®</sup> cloth was also provided by Honeywell and designated as Spectra<sup>®</sup> cloth 903. It is a plain woven cloth with an average thickness of 0.5mm and an areal density of 0.024g/cm<sup>2</sup>. Both materials were sampled and tested in the as-received state without any further treatments. Spectra<sup>®</sup> cloth 903 is the material of choice for ballistic protective hard armor.

### 2.2.2 Testing methods and instruments

#### 2.2.2.1 Tensile properties

The tensile properties of the single filament and yarn were tested on an Instron<sup>®</sup> 5564 equipped with an environmental chamber according to ASTM standard D2256. The specimen gauge length was 150mm and the strain rate was 10% per minute. Spectra<sup>®</sup> fiber tends to slip from the grips, so a set of special homemade grips were used. The grips consist of an aluminum rod and two aluminum gripping pieces with matching faces. The fiber was wrapped tightly around the aluminum rod and then sandwiched between the two gripping pieces using four screws to fasten. The novel grips provide a locking mechanism that prevents fiber slippage during tensile deformation. The specimens were tested at ambient and elevated temperatures. An environmental chamber, which encloses both the upper and lower grip, enabled specimens to be tested at 100°C, 130°C, 135°C, 140°C, and 145°C. A fiber specimen was mounted in grips and



the environmental chamber was heated. A thermal controller was used to monitor the temperature of the chamber. A thermal couple was placed into the chamber near the middle of the specimen to monitor the temperature experienced by the specimen. Once the specimen reached the final temperature, the test was begun and run until the specimen broke. Annealing of the specimen was achieved by heating the mounted fiber in the environmental chamber and then holding the fiber at set temperatures for two minutes. The specimen was rapidly cooled to room temperature in air. The tensile test was performed on the annealed specimens at ambient temperature. The fiber diameter was measured by optical microscopy and calculated from the linear density of the fiber. The tensile modulus, breaking strength and strain at break were determined.

#### 2.2.2.2 Thermal analysis

##### *Thermal shrinkage*

Free shrinkage of the filament at 130°C, 135°C, 140°C, 142°Cs, and 145°C was determined. The filament was immersed into a preheated oil bath for a period of time, removed, and the final filament length was measured. The free shrinkage is calculated from the change in length relative to the initial filament length. The initial filament length was 300 mm and a soak time of 10 minutes was used at 130°C, 135°C, 140°C and 142°C, and 5 seconds at 145°C.

##### *Thermal mechanical analysis*

A TA Instrument TMA 2940 was used to monitor the shrinkage force developed during heating of a constrained fiber. A specimen gauge length was 12.5mm and an

initial load of 0.008N was used. The specimen was heated at 10°C/min. under an iso-strain condition in nitrogen (35 ml/min.) and the change in load with temperature was recorded.

#### *Differential scanning calorimetry*

A TA Instrument DSC 2910 was used to observe the melting behavior of chopped Spectra<sup>®</sup> fiber and Spectra<sup>®</sup> cloth and to study the influence of constraint on fiber melting. ~10 mg of the samples in hermetically sealed pans were heated at 10°C/min. from room temperature to 200°C under nitrogen (50 ml/min.). Two methods of constraining were used: winding and knotting. The fiber was wound tightly around a small piece of aluminum and the ends were fastened, or the fiber was tied into a series of tight knots.

#### 2.2.2.3 Structure and morphology

##### *Scanning Electron Microscopy*

Spectra<sup>®</sup> cloth was mounted onto a SEM plate, sputter-coated with gold, and examined using a Field Emission Scanning Electron Microscope (FESEM JEOL JSM-6320FXV).

##### *Wide Angle X-ray Diffraction*

Wide Angle X-ray Diffraction (WAXD) patterns were collected using pin hole collimated, monochromatic Cu K $\alpha$  radiation and a Bruker<sup>®</sup> “High Star” two dimensional detector. Unidirectionally aligned fiber samples were prepared by winding fiber around a

metal frame which had two aligned notches. The unidirectionally aligned fiber was oriented perpendicular to the X-ray beam and the diffraction pattern was collected. The diffraction pattern from the as-received Spectra<sup>®</sup> cloth 903 was also collected. The cloth was oriented “flat-on” so that the incident X-ray beam was perpendicular to the cloth and the weft or warp yarn was aligned parallel to the horizon. A radiation time of 300 seconds was used and diffraction patterns were captured digitally. The integration of the intensity was preformed using GADDS commercial software.

## 2.3 Results and Discussion

### 2.3.1 Tensile properties of single fibers and yarns at ambient and elevated temperatures

Spectra<sup>®</sup> 900 is a high performance fiber with a high modulus and strength. Yet, it is hard to believe that polyethylene, a material typically found in items such as “milk jug” plastics, possesses such outstanding tensile properties. Made by the gel-spinning process, Spectra<sup>®</sup> fiber has extremely high molecular orientation and crystallinity resulting from its extended chain conformation which provides its unique properties. The crystalline orientation is also very high and needle-like crystals align parallel to the fiber axis.<sup>15</sup>

#### *Testing at ambient temperature*

Single filaments measured at ambient temperature have better tensile properties than those of yarns measured under similar conditions. The measured Young’s modulus, breaking strength, and strain at break for the single filaments are close to the values reported by other researchers, suggesting that our homemade grips effectively prevented



fiber slippage and quality data were collected. A yarn consists of bundles of fibers which have had a few twists applied during the manufacturing to ease handling. During tensile testing, each fiber within a yarn is not as perfectly aligned as a single fiber would be when it is mounted in the grips and there is greater possibility of slippage for the yarn. Both the single filaments and yarns have very high Young's modulus and breaking strength (Table 2.1). Strains at break are relatively low which is characteristic of high modulus fibers. Typical stress-strain curves for the filaments and yarns are shown in Figure 2.1 and 2.2, respectively. The filament specimen shows an almost linear elastic response until break and the yarn shows an initially linear elastic behavior to a yielding point, followed by gradual decrease in stress. Individual filaments in the yarn break gradually upon stretching, not all at the same strain level, resulting in the gradual decrease of the load.

Table 2.1 Tensile properties of Spectra<sup>®</sup> fiber 900 at ambient temperature

Specimen Type	Filament	Yarn
Young's Modulus (GPa)	69.8	55.5
Breaking Strength (GPa)	1.97	1.34
Strain at Break (%)	4.50	3.01

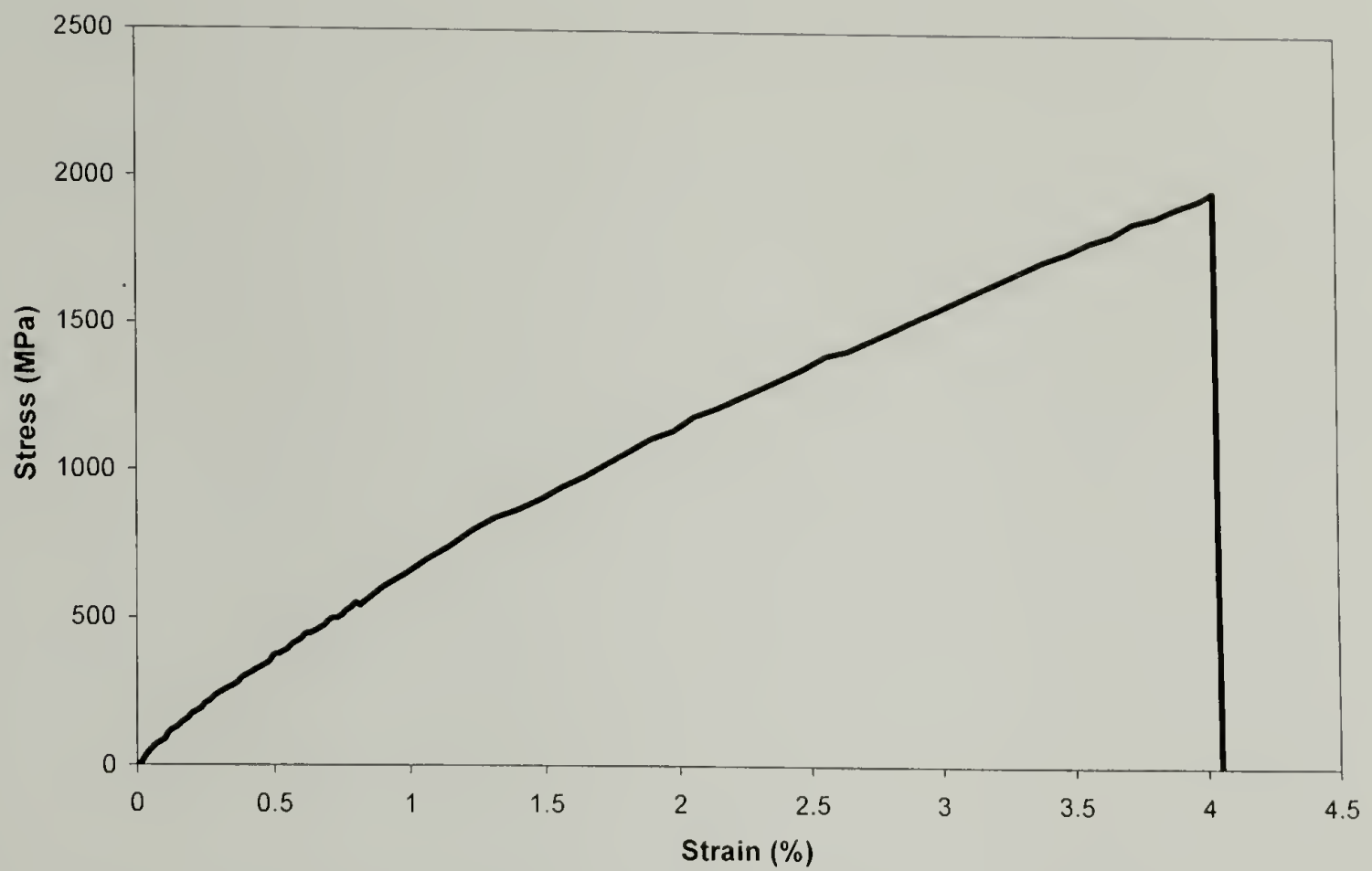


Figure 2.1 Typical stress-strain curve of a single filament at ambient temperature

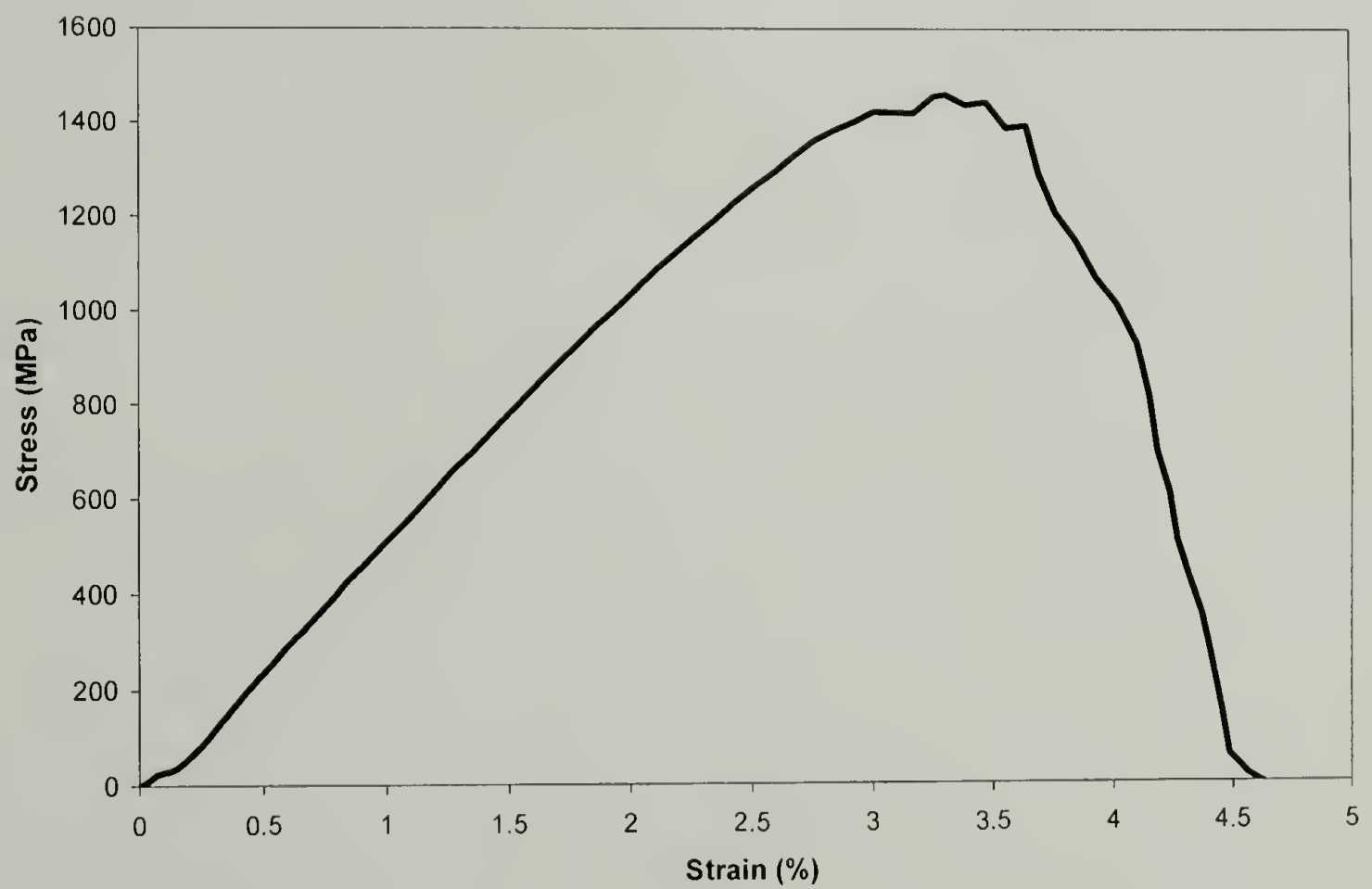


Figure 2.2 Typical stress-strain curve of a yarn at ambient temperature

### *Testing at elevated temperatures*

Polyethylene is thermoplastic. At elevated temperatures, polymer chain mobility increases and viscosity decreases. Polymer crystal melting temperature depends on its lamellae size; smaller crystals melt at lower temperatures relative to larger crystals in a non-uniformed crystalline system.<sup>59</sup> In a mechanical test, these factors manifest themselves by a dramatic decrease of Young's modulus and breaking strength with increasing test temperature.

The mechanical properties measured at elevated temperatures and at ambient temperature for filaments and yarns are compared in Table 2.2 and 2.3, respectively. Filament modulus and strength decrease rapidly with increasing test temperature; at 145°C the Young's modulus is only 9.5% of its original value and breaking strength is only 3.6% of its original value. Strain at break increases initially with test temperature, reaches 168% of its original value at 140°C and then drops to 3.18% at 145°C. The fiber becomes compliant and stretchy at elevated temperatures. As the temperature is increased near to the melting temperature (145°C),  $T_m$  of the fiber, much of the crystallinity within the fiber is lost with its mechanical integrity.

Table 2.2 Tensile properties of Spectra<sup>®</sup> 900 filament at ambient and elevated temperatures

Test Temperature	ambient	100°C	130°C	140°C	145°C
Young's Modulus (GPa)	69.8	43.9	28.4	12.8	6.66
Breaking Strength (GPa)	1.97	1.19	0.57	0.16	0.07
Strain at Break (%)	4.50	5.08	6.46	7.58	3.18



Table 2.3 Tensile properties of Spectra<sup>®</sup> 900 yarn at ambient and elevated temperatures

Test Temperature	ambient	100°C	130°C	140°C	145°C
Young's Modulus (GPa)	55.5	16.5	10.5	7.10	3.55
Breaking Strength (GPa)	1.34	0.47	0.11	0.06	0.04
Strain at Break (%)	3.01	7.93	5.85	4.32	3.50

The yarn modulus and strength decrease quickly with increasing test temperature compared to that of the filament. At 145°C the Young's modulus is 6.4% of its original value and strength 3%. The strain at break at 100°C is more than double the original value, but decreases with increasing temperature due to crystal melting. The Young's modulus, breaking strength, and strain at break for the filament and yarn at ambient and elevated temperatures are compared in Figure 2.3, 2.4 and 2.5, respectively.

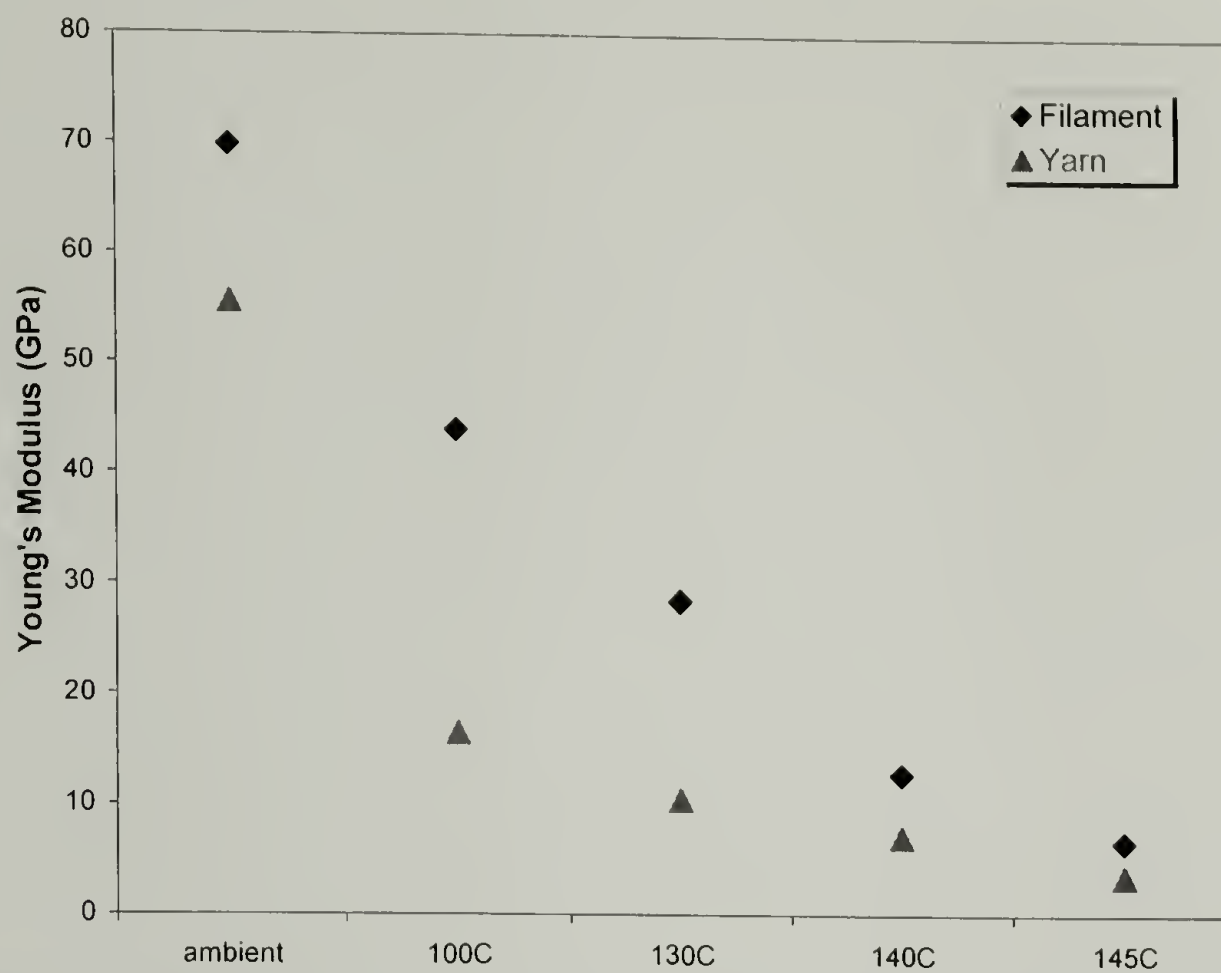


Figure 2.3 Young's modulus of the filament and yarn at ambient and elevated temperatures

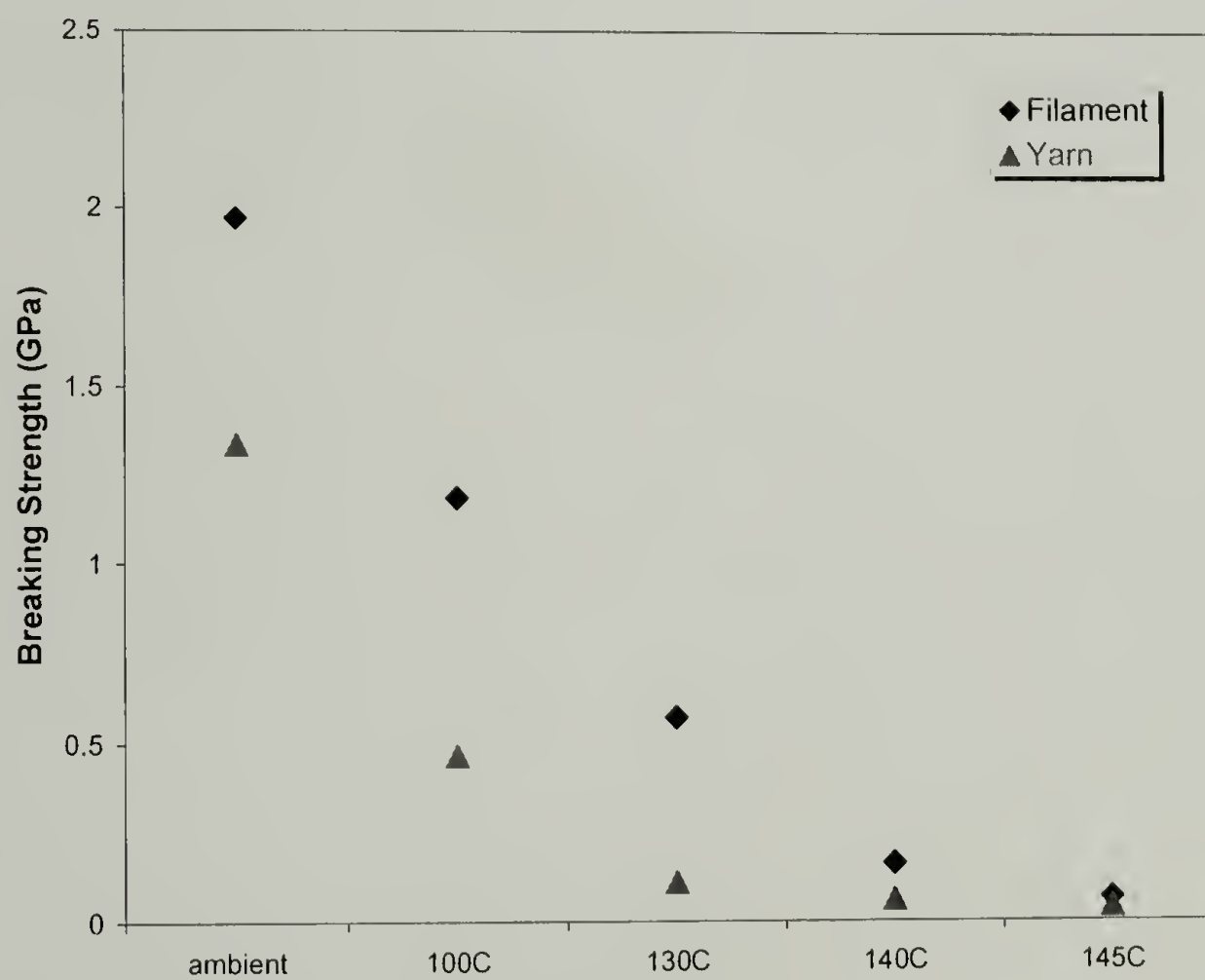


Figure 2.4 Breaking strength of the filament and yarn at ambient and elevated temperatures

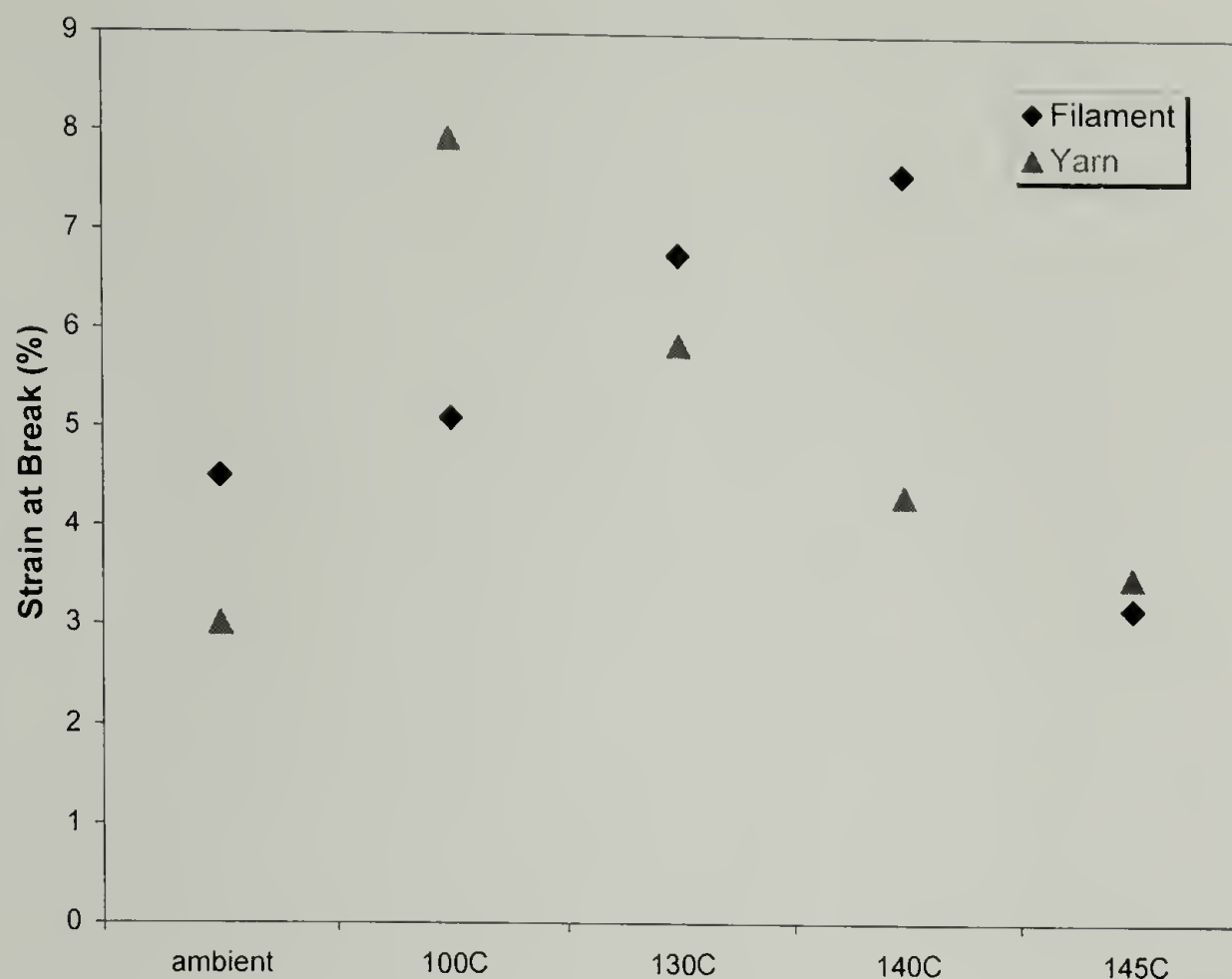


Figure 2.5 Strain at break of the filament and yarn at ambient and elevated temperatures

#### *Testing at ambient temperature after annealing at elevated temperatures*

During fiber annealing, a single filament was clamped between grips and a small initial force was applied to the fiber prior to heating. As the temperature was increased, the specimen was allowed slack due to the thermal expansion of the aluminum grips and connecting rod. After annealing for two minutes, the specimen was rapidly cooled, it returned to its original taut position in the grips and the tensile test was begun. The filament was capable of shrinkage during the annealing process which was detrimental the tensile properties of the filament (Table 2.4). Due to experimental difficulties the fibers could not be constrained during annealing. If the filament had been held under constraint tension during annealing the tensile properties would have been preserved. Constraint of the fibers can raise the melting temperature of the fibers, as will be discussed later in the chapter (Section 2.3.4). The highest annealing temperature at which



the specimen will not break prematurely is 145°C. The Young's modulus and breaking strength of the filament is significantly maintained after annealing; at 145°C the modulus of the single filament is 75% and strength is 82% of its original values, while the strain at break remains relatively unchanged. Annealing increases the breaking strength of the filament, in comparison to the as-received virgin material, possibly due to the recoil of the chains during shrinkage.

Table 2.4 Tensile properties of Spectra<sup>®</sup> 900 filament annealed at elevated temperatures

Annealing Temperature	ambient	135°C	140°C	145°C
Young's Modulus (GPa)	69.8	66.4	65.1	52.4
Breaking Strength (GPa)	1.97	1.79	1.84	1.61
Strain at Break (%)	4.50	5.19	5.25	5.06

### 2.3.2 Thermal shrinkage of single filaments

Shrinkage of the filament was measured at temperatures between 130°C and 145°C; an upper limiting temperature of 145°C was chosen as the melting onset temperature of the fiber is ~ 140°C and huge shrinkage resulting in the destruction of the sample would be expected at temperatures greater than that. Spectra<sup>®</sup> fiber shrinks dramatically at above 142°C in a short period of time. Shrinkage is reported as a percentage with respect to the original length in Table 2.5 and Figure 2.6. Shrinkage is an entropy-driven transformation of chain conformations, from the extended state to the random coil state. Shrinkage results in the loss of molecular orientation and hence diminishes the longitudinal strength and stiffness of the fiber. A sufficient constraint is

required to prevent shrinkage when subjecting Spectra<sup>®</sup> fiber to high temperatures in order to preserve its original strength.

Table 2.5 Thermal shrinkage of Spectra<sup>®</sup> 900 single filaments at elevated temperatures

Soaking Temperature	130°C	135°C	140°C	142°C	145°C
Length (mm)	291	289	283	278	118
Shrinkage (%)	3.11%	3.67%	5.67%	7.28%	60.8%

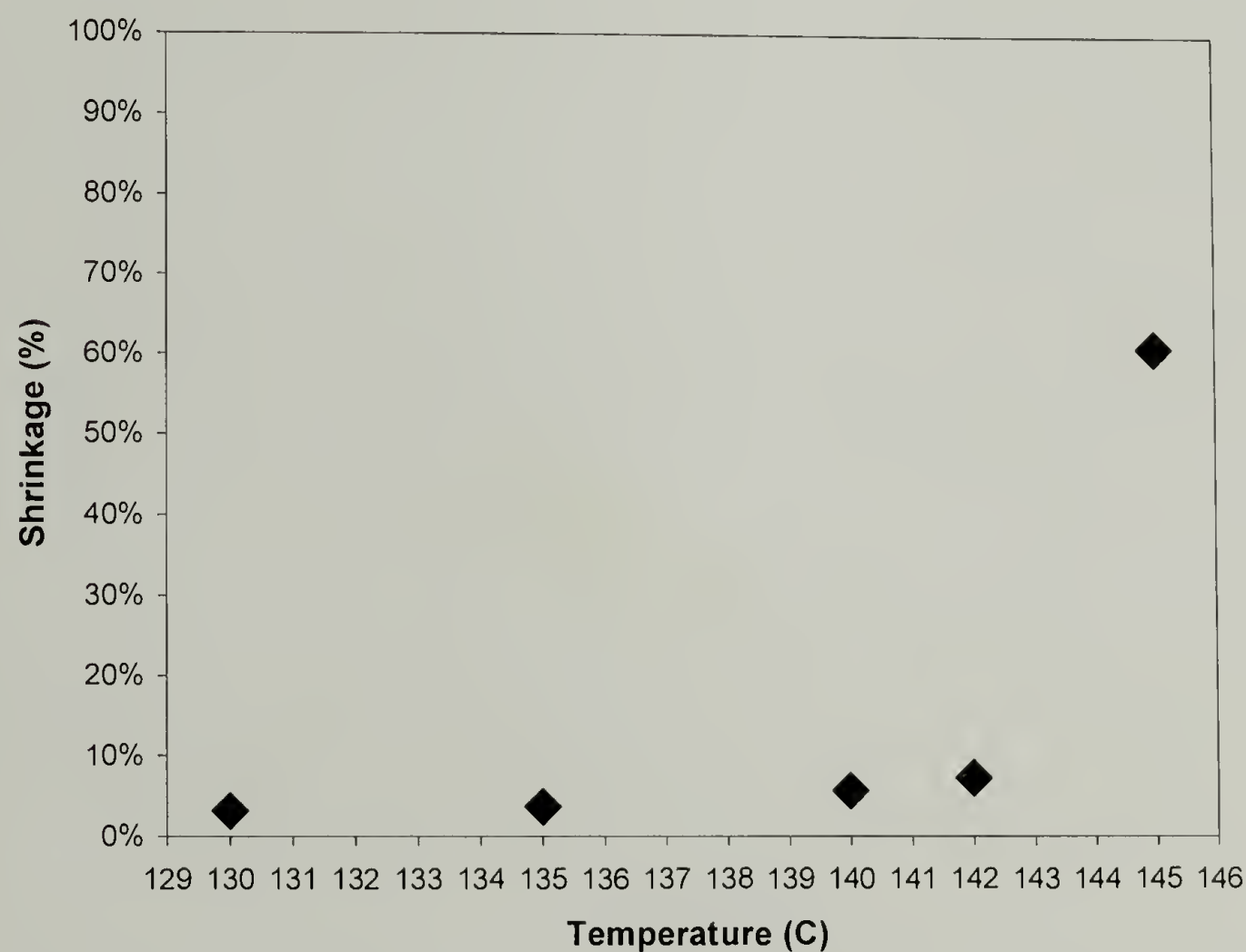


Figure 2.6 Thermal shrinkage of Spectra<sup>®</sup> 900 single filaments at elevated temperatures

### 2.3.3 Thermal mechanical analysis of a single filament

According to the shrinkage measurement Spectra<sup>®</sup> fiber has a negative coefficient of thermal expansion; a large shrinkage force is developed within the fiber when it is

heated under an iso-strain condition. Thermal mechanical analysis (TMA) was used to monitor the shrinkage force within the fiber as a function of temperature. The shrinkage force is shown to increase with temperature (Figure 2.7) and at 142°C a maximum force of 0.0363N is measured (approximately 4.5 times the initial force applied to hold the specimen taut). The stress at break is calculated to be 0.03GPa and comparable to the breaking strength of the single filament at 145°C (0.07GPa) as shown in the previous section (Table 2.2). A sufficient constraint is required to prevent the fiber from shrinking during the consolidation and a large force is needed to stretch the fiber during the shaping and molding process in order to overcome the thermal shrinkage.

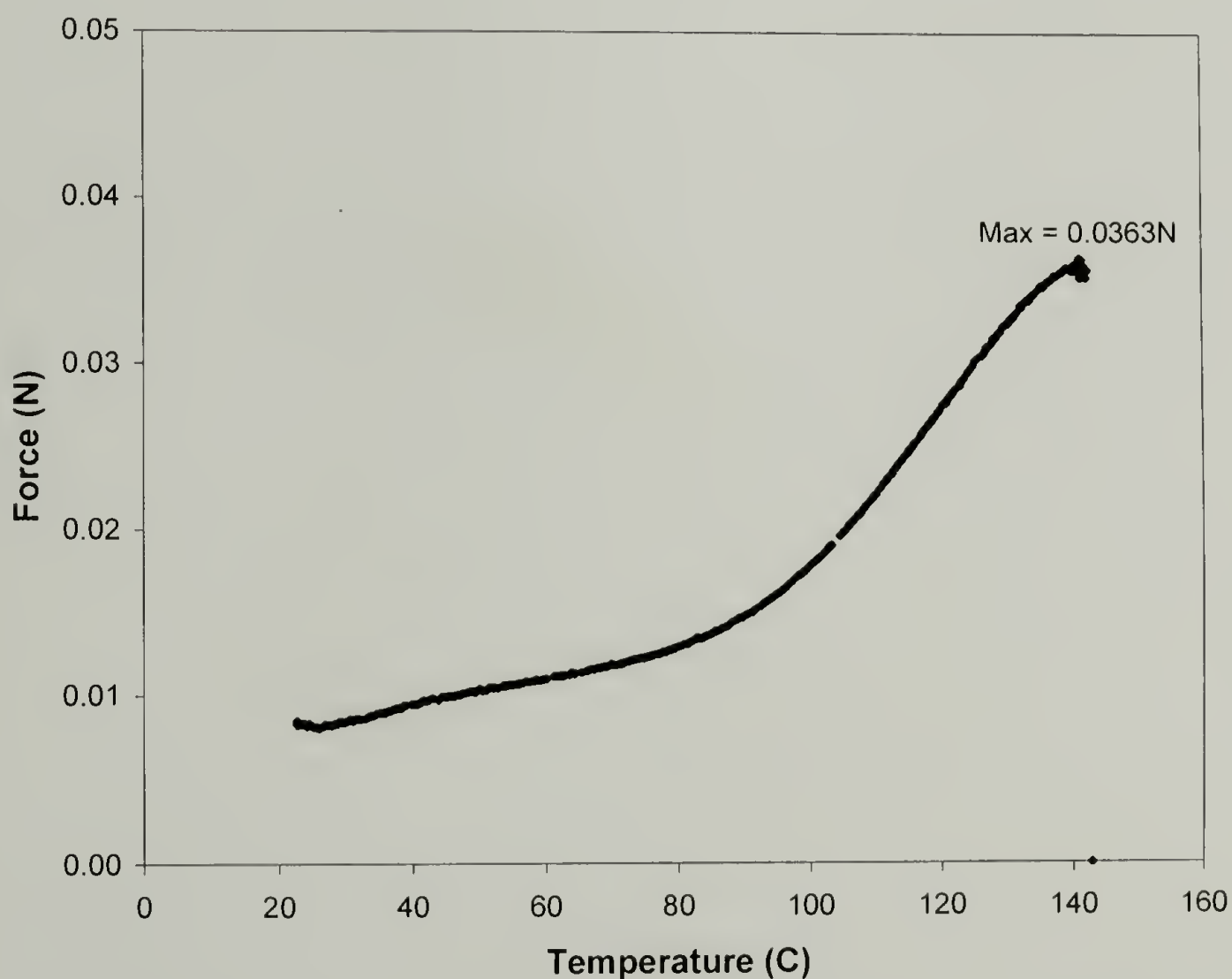


Figure 2.7 The observed shrinkage force of a Spectra® 900 single filament with increasing temperature



#### 2.3.4 Differential scanning calorimetry of the unconstrained and constrained filaments and the as-received Spectra<sup>®</sup> cloth

The Differential scanning calorimetry (DSC) trace for each of the unconstrained and two types of constrained wound and knotted fibers shows a single melting endotherm (Figure 2.8). The melting peak for the unconstrained Spectra<sup>®</sup> fiber 900 is at approximately 150°C. Constraining the fiber either by winding tightly or making tight knots one on another has raised the melting peak temperature by nearly 10°C.

“Superheating” phenomenon<sup>58</sup> is well known to researchers, and its occurrence is related to the constraint limiting the molecular relaxation and motion, thus deferring the onset of the melting. The retarded stress release within the specimen leads to additional superheating that is lost during melting.<sup>50</sup> This phenomenon is the basis of the high-temperature high-pressure sintering technique. The enormous lateral pressure exerted on the fibers during processing effectively constrains them. The fibers may then be heated to their normal melting temperature without excessive melting except for the amount required to weld the fibers together. The high crystallinity of the fiber would be preserved, as it is crucial to the high strength of the fiber. The crystalline melting enthalpy for two types of constrained fibers is smaller than that of the unconstrained fiber, although this is not to suggest that the constrained fiber has a lower degree of crystallinity. When the fiber is constrained, either by winding or knotting, strain energy stored in the material can not be transformed into work. The internal energy of the material is raised so less thermal energy is needed to melt the crystals. The heat measured by DSC corresponds to the thermal energy added to the material to cause melting.

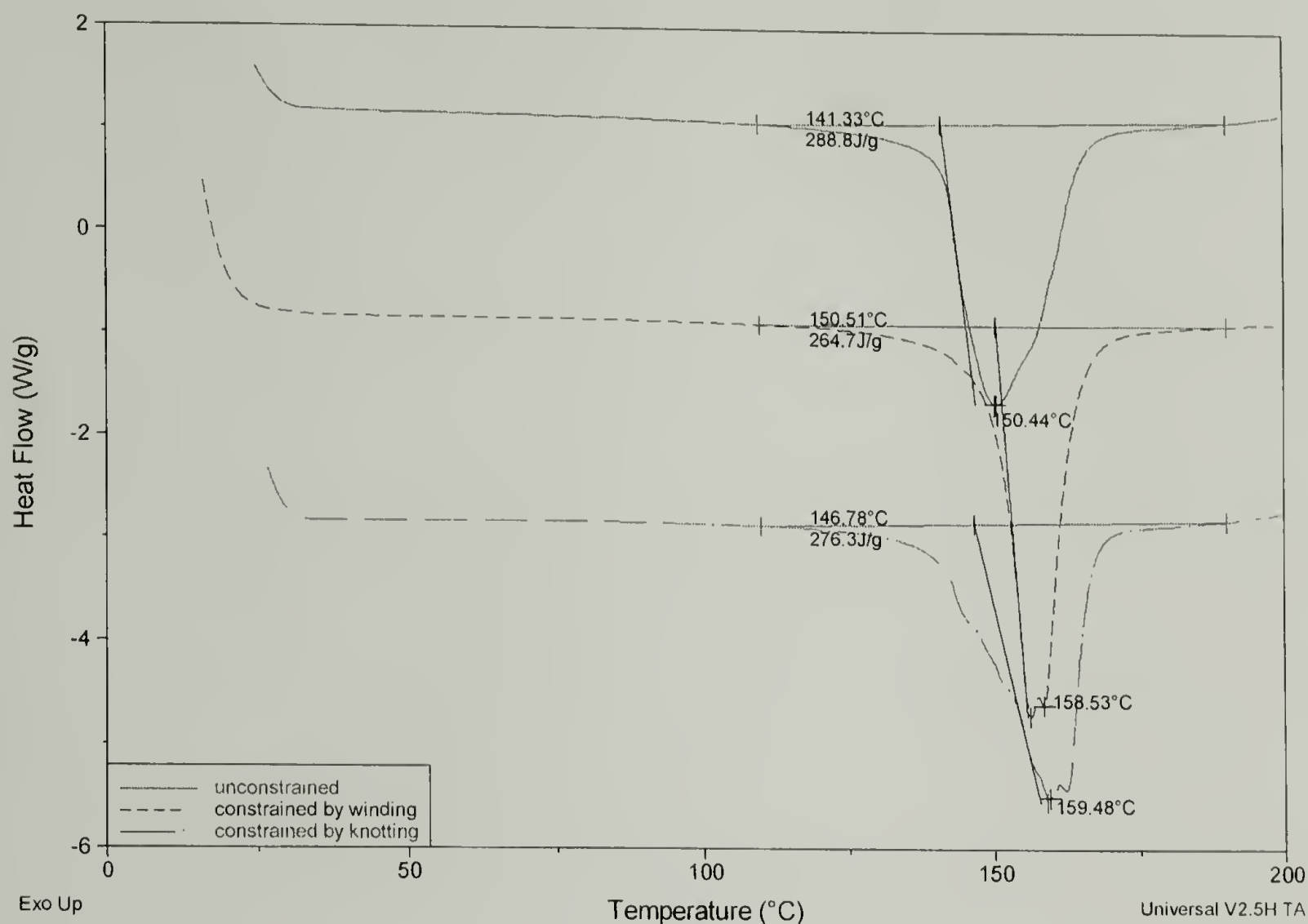


Figure 2.8 DSC traces of Spectra<sup>®</sup> fiber 900 in unconstrained and constrained states

Spectra<sup>®</sup> cloth 903 is made of Spectra<sup>®</sup> fiber 900 without any treatments. The first and second run DSC traces for Spectra<sup>®</sup> cloth 903 are shown in Figure 2.9 and 2.10, respectively. In the first trace, Spectra<sup>®</sup> cloth 903 and Spectra<sup>®</sup> fiber 900 have the same melting peak temperature at 150°C. In the second trace the melting peak temperature has shifted to 135°C, which is equivalent to the melting temperature of unoriented polyethylene. The recrystallized material, which was formed during quenching after the first run, is unoriented and the high orientation was destroyed during the melting process in the first run. High molecular orientation results in a high melting temperature due

largely to an increase in the crystallite  $c$  axis dimension.<sup>59</sup> High orientation of chains produces larger crystallites that melt at higher temperatures than smaller crystallites. High orientation requires the polyethylene chains adopt an extended conformation and pack side by side. The constraint imposed by the dense packing limits the relaxation and motion of the molecules and therefore deters the melting. The crystalline melting enthalpy from the first and second run of Spectra<sup>®</sup> cloth 903 differs, 288.9J/g and 191.3J/g, respectively, indicating that the original melted crystals are not fully transformed into new crystals. A large portion of the melt becomes part of the noncrystalline phase, either the amorphous phase or the intermediate phase,<sup>16</sup> and the recrystallized material has a much lower degree of crystallinity than the original material.

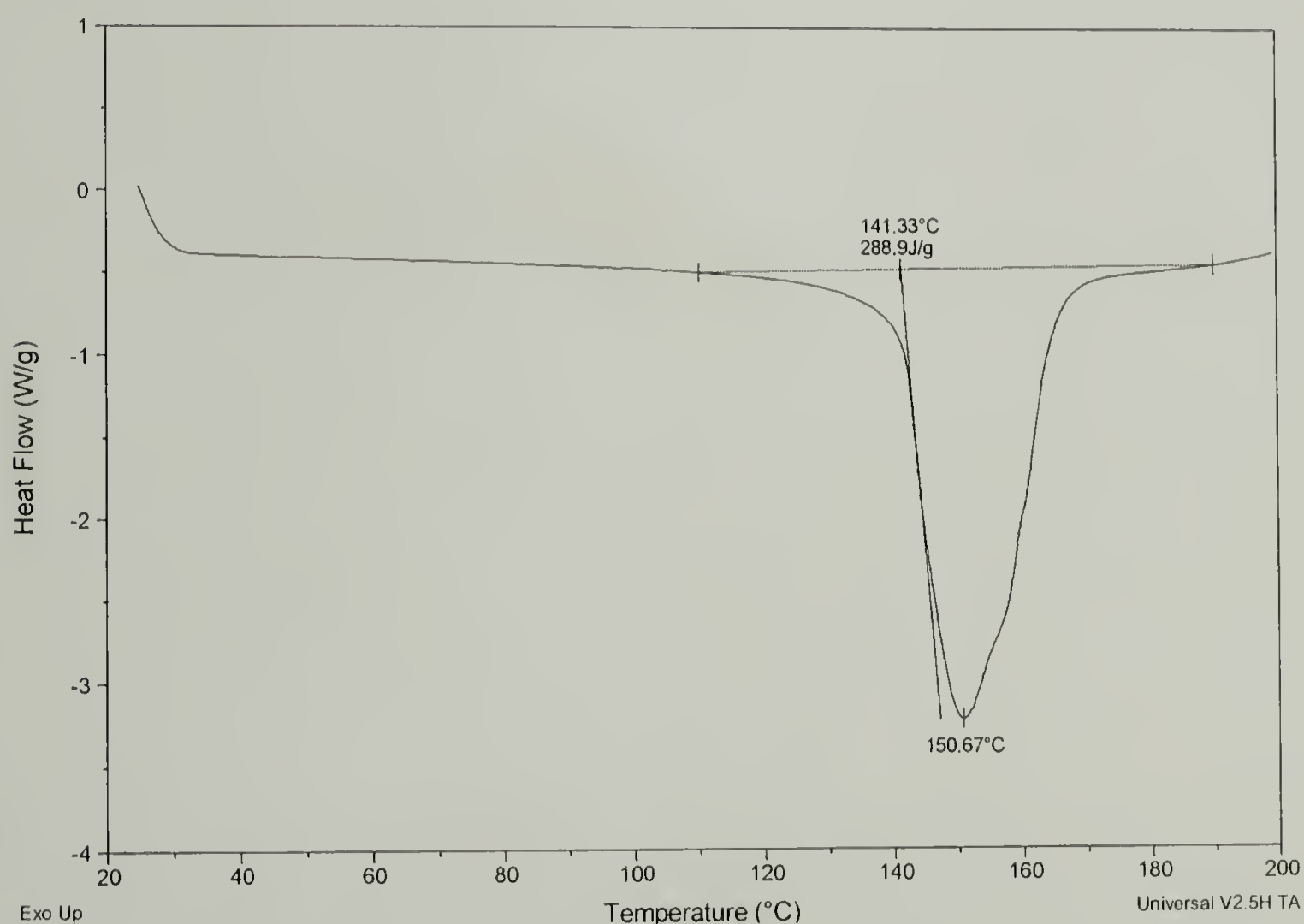


Figure 2.9 The first run DSC trace of Spectra<sup>®</sup> cloth 903



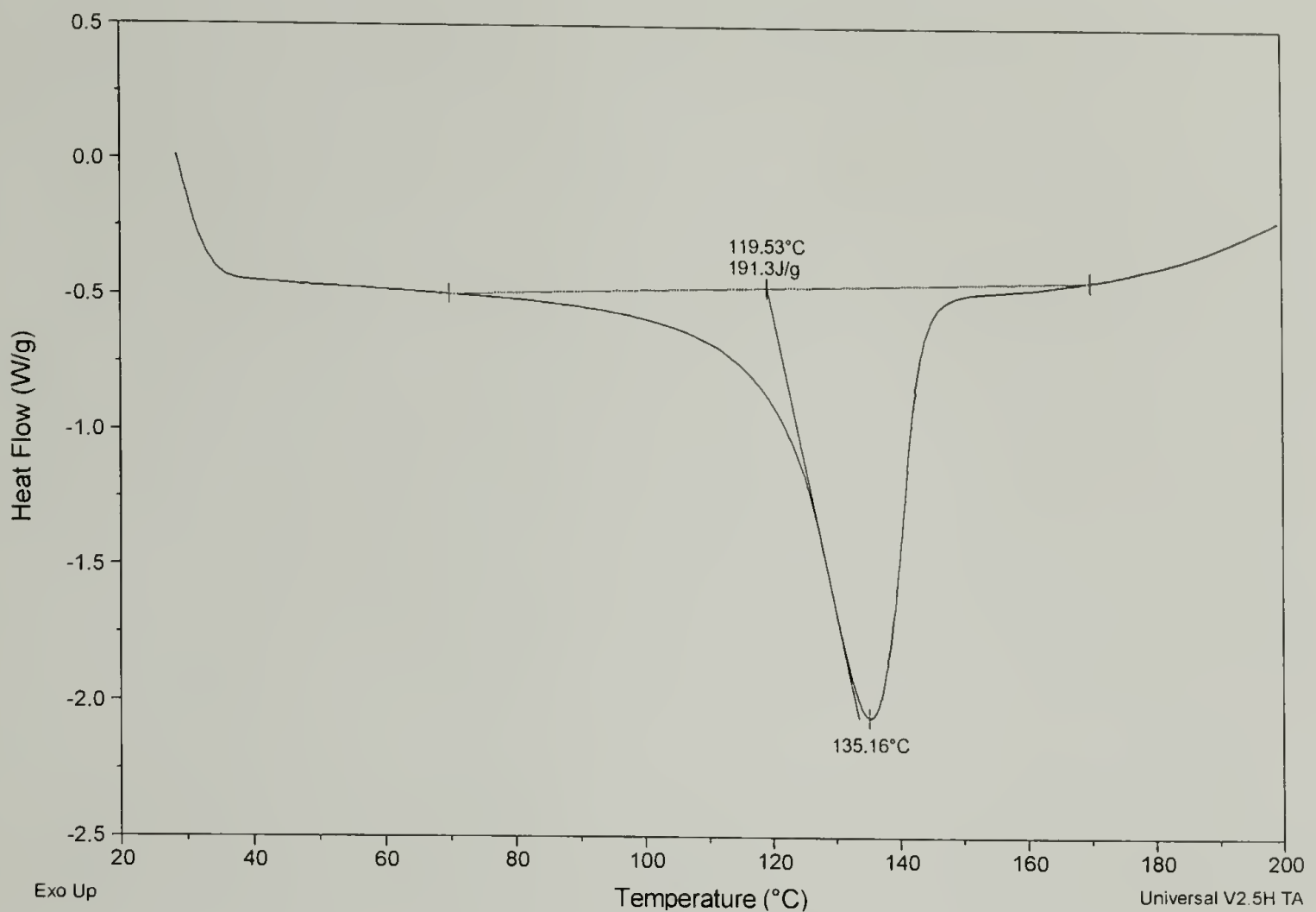


Figure 2.10 The second run DSC trace of Spectra<sup>®</sup> cloth 903 after quenching

High orientation and crystallinity are the keys to the high strength of Spectra<sup>®</sup> fiber and excessive melting during the sintering process should be avoided. The recrystallized phase, prepared from the melt upon cooling, has a lower degree of orientation and offers little to the longitudinal strength of the sintered products. Lower orientation within the recrystallized phase leads to lower crystallinity compared to the original material and decreases the strength of the sintered products.

### 2.3.5 Scanning electron microscopy images of Spectra<sup>®</sup> fiber 900 and Spectra<sup>®</sup> cloth 903

Scanning electron microscopy (SEM) image for the cross section of a fiber bundle in the cloth shows that the individual fibers have different shaped cross sections (Figure 2.11). The cross sections are not circular but rather irregular and polygonal, although

they do have similar diameters, or similar cross sectional areas in a strict sense. The SEM image for a section of Spectra<sup>®</sup> cloth shows the plain weaving pattern of the cloth very clearly (Figure 2.12). The fibers are nearly parallel to each other within a bundled yarn in either the warp or weft direction. There are a few fibers that deviate from the general direction, which could be the result of the twists applied to the yarn or the disturbance by the weaving process. The misalignments decrease the overall fiber orientation and lead to lower Hermans orientation function values, as illustrated in the following section.

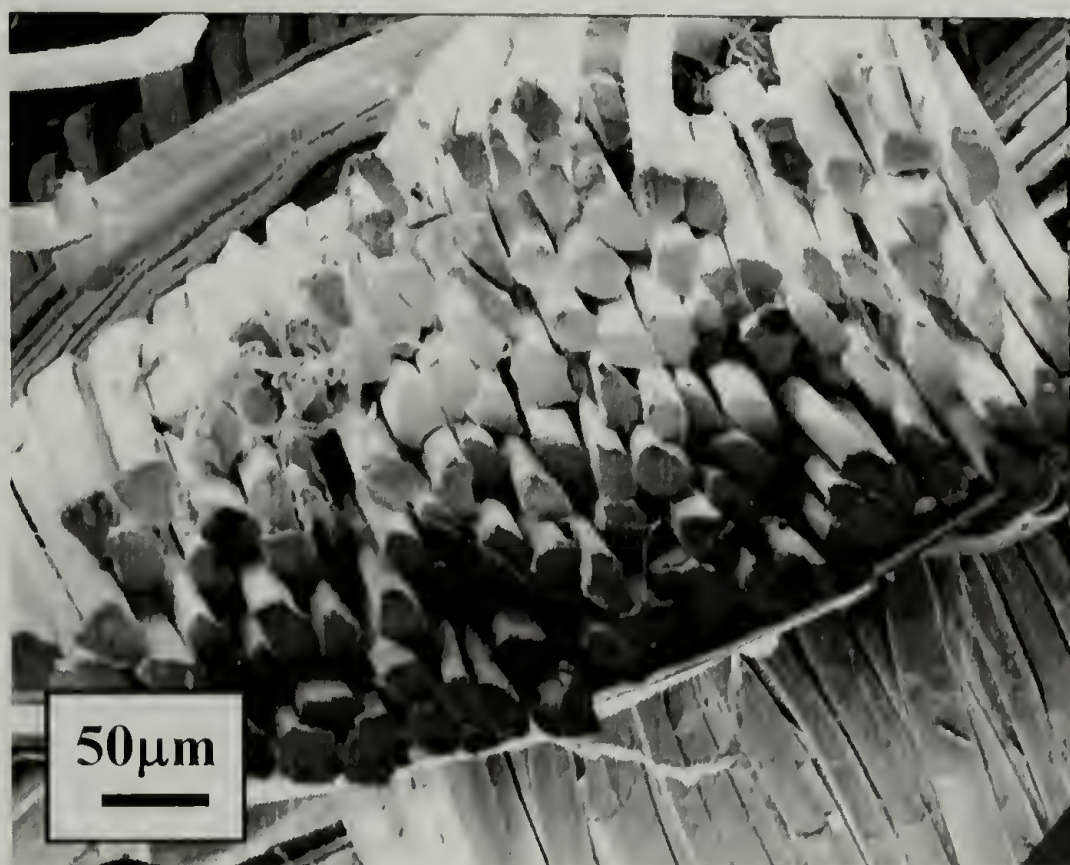


Figure 2.11 SEM image of a bundle of Spectra<sup>®</sup> fibers in the cloth



Figure 2.12 SEM image of Spectra® cloth 903

### 2.3.6 Wide angle X-ray diffraction of unidirectionally aligned Spectra® fiber and the as-received Spectra® cloth

Wide angle X-ray diffraction (WAXD) experiments revealed typical diffraction patterns of highly oriented polyethylene, characterized by the bright spot corresponding to the (110) and (200) reflections of the orthorhombic crystals.<sup>60</sup> Figure 2.13 and 2.14 show the diffraction pattern for unidirectionally aligned fibers and the plain woven cloth, respectively. The WAXD pattern of the cloth shows two sets of diffraction patterns corresponding to the 0/90 degree aligned fibers in the cloth. The Hermans orientation function was calculated in order to quantify the degree of orientation. The Hermans orientation function is a measure of the deviation of polymer chain alignment from the axis of interest (Figure 2.15). If Hermans orientation function,  $f = 1$ , the chains are fully



aligned and parallel to the axis. If  $f = 0$ , the chains are randomly oriented and if  $f = -1/2$ , all the chains are perpendicular to the axis.

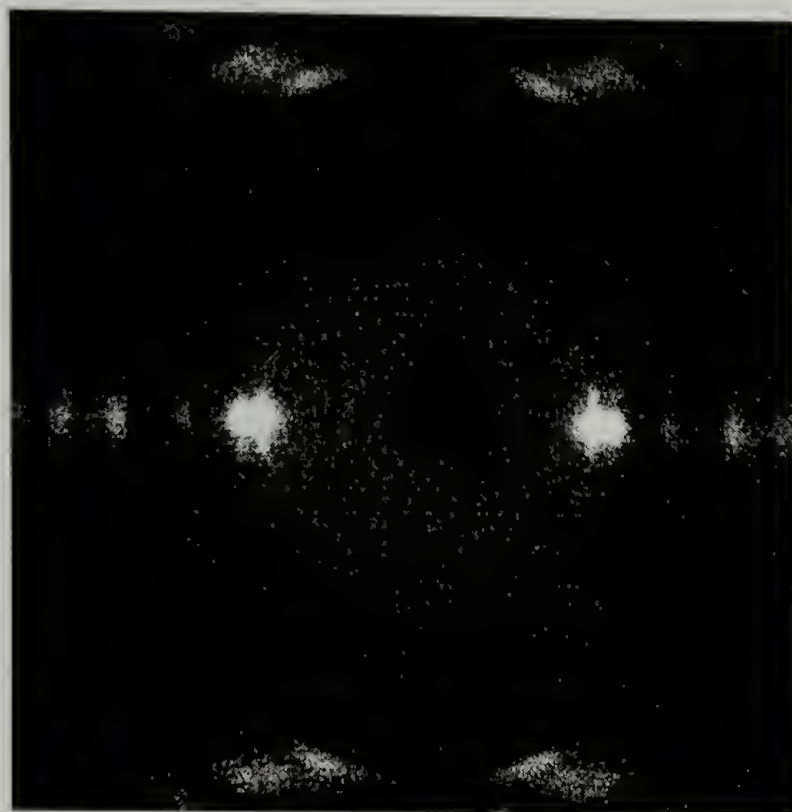


Figure 2.13 WAXD pattern of unidirectionally aligned Spectra<sup>®</sup> 900 fiber

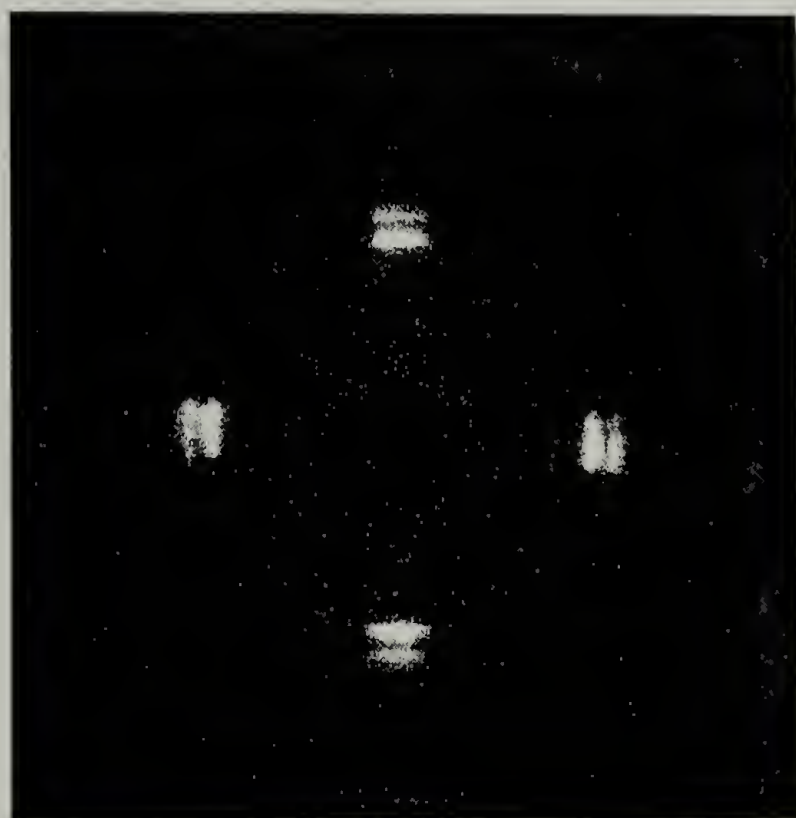


Figure 2.14 WAXD pattern of the as-received Spectra<sup>®</sup> cloth 903



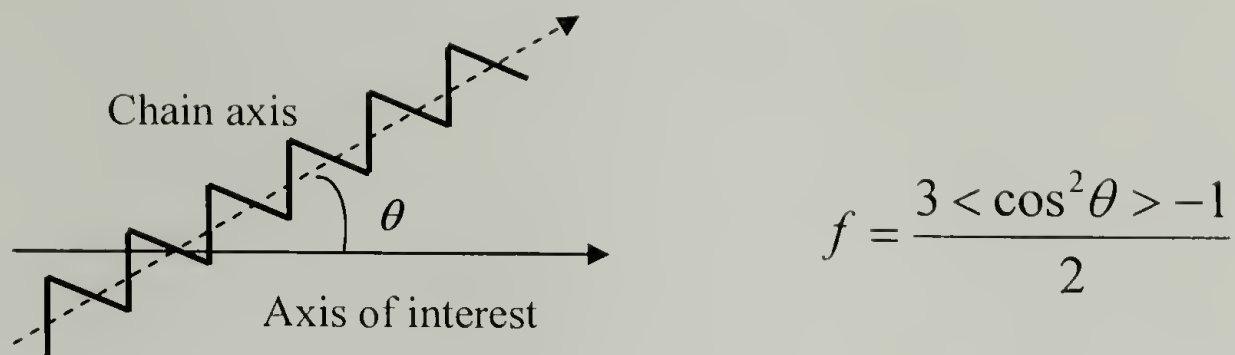


Figure 2.15 Hermans orientation function

From an integration of intensity over the azimuthal angle, Hermans orientation function was calculated and the results are shown in Table 2.6. Both materials are highly oriented. Unidirectionally aligned fibers have a higher degree of orientation than the woven cloth due to the inevitable misalignment of the fiber within the cloth as seen by SEM, previously. The results are also confirmed by well defined high order diffractions exhibited in the diffraction pattern of the unidirectionally aligned fiber.

Table 2.6 Hermans orientation function of unidirectionally aligned Spectra<sup>®</sup> fiber 900 and the as-received Spectra<sup>®</sup> cloth 903

Specimen type	Unidirectional fibers	Woven cloth
Hermans orientation function	0.942	0.887

## 2.4 Conclusion

As a high performance fiber, Spectra<sup>®</sup> fiber 900 has a high Young's modulus and tensile strength at ambient temperature although its strain at break is relatively low. Its tensile properties have strong temperature dependence and decrease rapidly with increasing temperature. As the fiber becomes more compliant at elevated temperatures,

its strain at break greatly increases. The tensile properties of the fibers annealed at high temperatures remain at a relatively high level even as the annealing temperature is raised near the melting temperature of the fiber. If a proper constraint on the fiber were used during the annealing process, the tensile properties could have been largely preserved after the fiber returned to ambient temperature. A constraint on the fiber can raise its melting temperature by 10°C. These facts lay the foundation for the high-temperature high-pressure sintering process, i.e., to preserve the superior properties of the original fiber and to translate them into the outstanding properties of the homocomposites.

Speetra<sup>®</sup> fiber 900 has a negative coefficient of thermal expansion, it shrinks dramatically at a temperature above 142°C and if constrained develops a large shrinkage force. X-ray diffraction results show that Speetra<sup>®</sup> fiber 900 has a very high degree of molecular orientation characterized by a high Hermans orientation function value. DSC demonstrated that the original highly oriented crystals have a considerably higher melting temperature than unoriented polyethylene. If these crystals are completely destroyed by melting, the recrystallized phase from melted fiber is unoriented. The melted phase does not fully crystallize upon cooling, resulting in a decrease in the degree of crystallinity. In order to preserve the high crystallinity and orientation, which are the two underlying reasons for the high properties of Speetra<sup>®</sup> fiber, a sufficient force is required to constrain the fiber throughout the sintering process to prevent the fiber from shrinking and to raise the melting temperature of the fiber.

## CHAPTER 3

### OPTIMIZATION OF THE HIGH-TEMPERATURE HIGH-PRESSURE SINTERING PROCESS FOR CONSOLIDATING SPECTRA<sup>®</sup> CLOTH

#### 3.1 Introduction

In the previous chapter, it was discovered that Spectra<sup>®</sup> fiber can sustain relatively high temperatures yet maintain its overall structure and properties, especially if it is constrained during heating. A constraint on the fiber can shift its melting temperature upwards by almost 10 degrees. It was proposed that Spectra<sup>®</sup> fiber and cloth could be consolidated using heat and pressure. If the processing conditions are tuned correctly, only small amount of the fiber will melt and recrystallize on cooling to fuse the material. The resulting product is a high modulus and strength “one-polymer” composite and this kind of material is a highly favorable candidate for ballistic shields. In a bid to explore a simple and effective approach to make body armor and helmets, a novel processing method called high-temperature high-pressure sintering was developed.

This chapter describes the processing procedures to consolidate Spectra<sup>®</sup> cloth 903 using high-temperature high-pressure sintering. Three key processing parameters are temperature, time and pressure and their influence on the structure and properties of the consolidated material were studied. The high temperature is in the vicinity of the fiber's normal melting point so as to induce adequate but not excessive melting. The time is important to allow for adequate heat transfer to promote interfiber and interlayer adhesion while conserving the fiber's high crystallinity and orientation. The high pressure exerted laterally on the fiber and cloth is required to constrain them and prevent shrinkage, as well as eliminate the voids and consolidate the materials. The crystallinity changes for



specimens processed under different conditions were measured by DSC; molecular orientation changes were studied by WAXD; and the impact properties were measured by puncture tests. The established process-structure-property relationship was used as a guideline to tune the processing conditions. Since impact resistance is important to ballistic protective apparatus, the processing conditions were optimized to achieve the best possible impact properties.

## 3.2 Experimental

### 3.2.1 Materials

Spectra<sup>®</sup> fiber was obtained from Honeywell and designated as Spectra<sup>®</sup> 900.<sup>57</sup> The yarn contains 120 filaments per tow and has a linear density of 1200 denier. The density of the fiber is 0.97g/cm<sup>3</sup>. Spectra<sup>®</sup> cloth was also provided by Honeywell and designated as Spectra<sup>®</sup> cloth 903. It is a plain woven cloth with an average thickness of 0.5mm and an areal density of 0.024g/cm<sup>2</sup>. Both materials were sampled and tested in the as-received state without any further treatments. Spectra<sup>®</sup> cloth 903 is the material of choice for ballistic protective hard armor.

### 3.2.2 Processing procedures

A single layer of cloth was sandwiched within aluminum foils and placed in between two steel plates. The hot press was preheated to a desired processing temperature, the temperature was allowed to equilibrate, and the sandwiched cloth was placed in the hot press. The upper and lower platens of the press were closed onto the specimen and the pressure was raised to the desired processing pressure. The pressure

and temperature were held constant for a period of processing time to execute the sintering process. The hot press and the specimen were quenched by running tap water through the press platens while pressure was maintained. The sintered specimen was removed from the press at ambient temperature and separated from the aluminum foil; no mold release agent was used.

### 3.2.3 Measurement of crystallinity changes by DSC

A TA Instrument DSC 2910 was used to observe the melting behavior of single layers Spectra<sup>®</sup> cloth consolidated under various processing conditions. ~10 mg of the samples in hermetically sealed pans were heated at 10°C/min from room temperature to 200°C under nitrogen (50 ml/min.).

### 3.2.4 Measurement of orientation changes by WAXD

Wide Angle X-ray Diffraction (WAXD) patterns were collected using pin hole collimated, monochromatic Cu K $\alpha$  radiation and a Bruker<sup>®</sup> “High Star” two dimensional detector. The diffraction patterns of a series of single layer Spectra<sup>®</sup> cloth sintered under different processing conditions were collected. The cloth was oriented “flat-on” so that the incident X-ray beam was perpendicular to the cloth and the weft or warp yarn was aligned parallel to the horizon. A radiation time of 300 seconds was used and diffraction patterns were captured digitally. The integration of the intensity was preformed using GADDS commercial software.

### 3.2.5 Measurement of impact properties by puncture test

Impact tests were performed using a dynatup<sup>®</sup> 8250 with the pneumatically powered shooting dart mode of puncture test since the consolidated Spectra<sup>®</sup> cloths are rather strong. The dart weighs 2.38kg and is pneumatically assisted by house nitrogen. The dart speed at penetration into the specimen was approximately 10 m/s. The specimens were 100mm × 150mm consolidated single layer Spectra<sup>®</sup> cloth 903 sheets which had experienced different processing conditions. Each specimen was secured on the sample stage by pneumatic clamps, the dart was then fired perpendicular to the surface of the specimen, and the cloth was punctured. The instrument recorded the load detected on the dart tip and the deflection of the specimen as soon as the shooting dart touched the specimen until total penetration. The total energy of impact was calculated from the integrated area under the load vs. deflection curve.

## 3.3 Results and Discussion

### 3.3.1 Overall and original crystallinity

There is a certain amount of fiber melting associated with the high-temperature high-pressure sintering process and the processing temperature plays a major role in determining the extent of the melting. A small amount of surface melting is needed to bond the fibers and cloth to develop the lateral strength of the structure. Excessive melting destroys the original highly oriented crystals and forms less oriented crystals that offer much less in the longitudinal strength of the structure. The goal was to find the proper sintering temperature at which a compromise between longitudinal and lateral strength was achieved. Single layer cloth specimens were sintered at temperatures



between 148°C and 160°C, while the processing pressure and time were kept constant at 7.6MPa and 30 minutes, respectively. The specimens show two melting endotherms in their DSC thermographs after sintering (Figure 3.1). The higher temperature peak at 150°C corresponds to the melting of the original highly oriented crystals and the lower temperature peak at 135°C corresponds to the melting of newly formed crystals from the melt upon cooling. They are less oriented and melt at a lower temperature. With increasing sintering temperatures, the higher temperature peak area decreases and the lower temperature peak area increases, indicating the gradual loss of the highly oriented crystals, accompanied by the gradual increase in the formation of unoriented crystals.

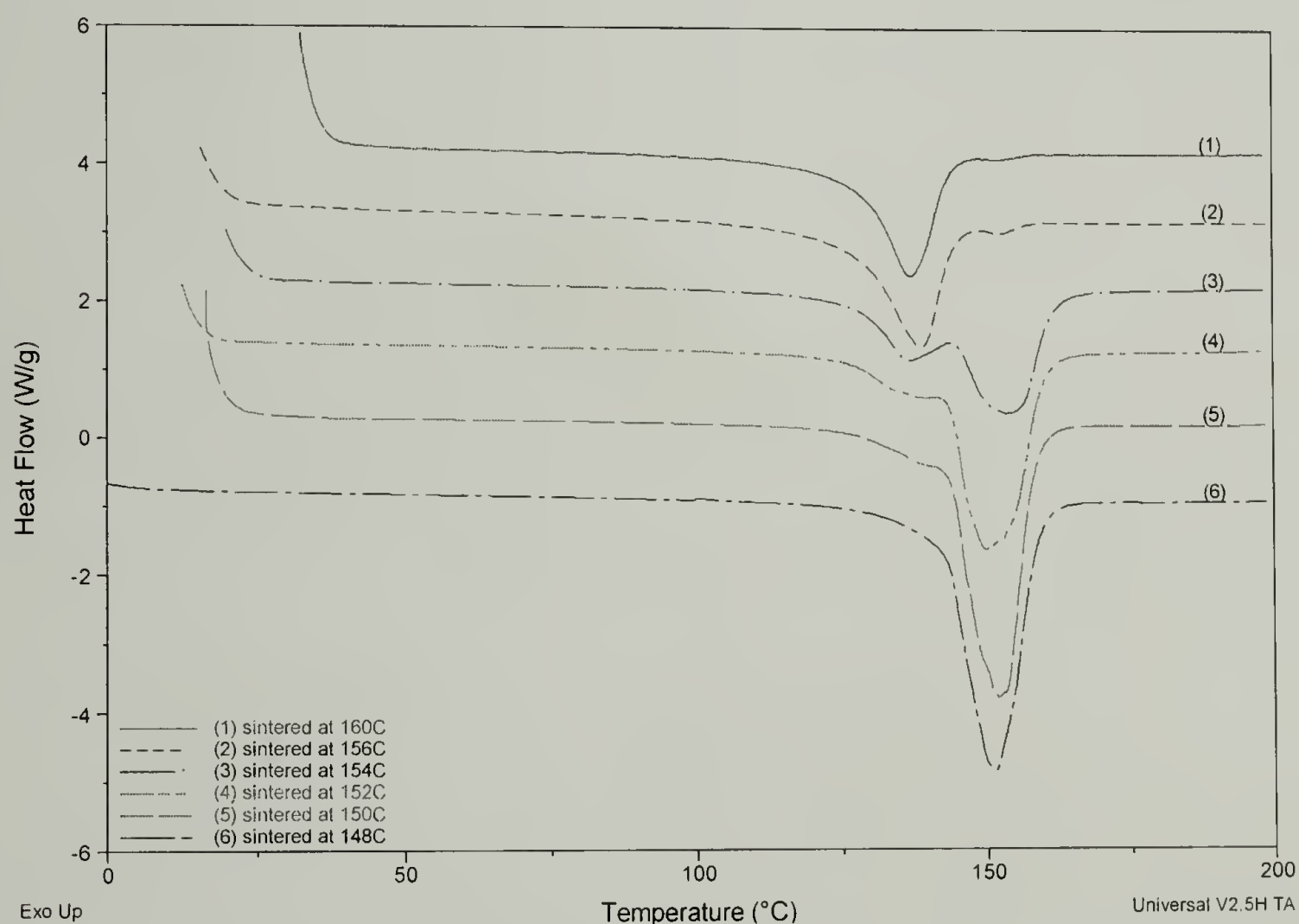


Figure 3.1 DSC trace overlay for single layer Spectra<sup>®</sup> cloth 903 sintered under 7.6MPa for 30 minutes at different temperatures

In theory, a 100% polyethylene crystal has a melting enthalpy of 293.6J/g.<sup>61,62</sup>

The melting enthalpy of the consolidated specimens was obtained by integration of the melting peak area. The degree of crystallinity was calculated according to Equation 3.1.

$$\text{Degree of crystallinity} = \frac{\text{Melting enthalpy of the specimen}}{\text{Melting enthalpy of 100\% polyethylene crystal}} \times 100\% \quad (3.1)$$

Since the two melting endotherms overlap, the integration consists of both peak areas.

The calculated crystallinity is the overall crystallinity with contributions from both the original crystals and the newly formed crystals (Table 3.1 and Figure 3.2). The overall crystallinity decreases with increasing processing temperature, indicating that not all the melted crystals are recrystallized on cooling, some are transformed into an amorphous or an intermediate phase. The physical appearance of the consolidated cloth confirms this observation (Figure 3.3). The cloths sintered at lower temperatures maintain the visible weaving pattern and the white color of the original cloth, while those sintered at higher temperatures have almost no visible weaving patterns and became translucent. The overall crystallinity remains up to a processing temperature of 152°C, suggesting that high crystallinity is maintained after sintering at this temperature due to the large lateral pressure constraining the fiber and raising its melting temperature. The crystallinity for the specimen sintered at 148°C is higher than that of the original cloth due to pressure induced crystallization. At higher temperatures the increased melting of the crystals overcomes the effect of pressure induced crystallization and results in the net decrease of overall crystallinity.

Table 3.1 Overall crystallinity of the as-received and consolidated Spectra<sup>®</sup> cloth 903 sintered under 7.6MPa for 30 minutes at different sintering temperatures

Specimen	as-received	148°C	150°C	152°C	154°C	156°C	160°C
Enthalpy (J/g)	279.5	286.3	278.4	265.9	246.9	186.6	165.2
Crystallinity	95.2%	97.5%	94.8%	90.6%	84.1%	63.6%	56.3%

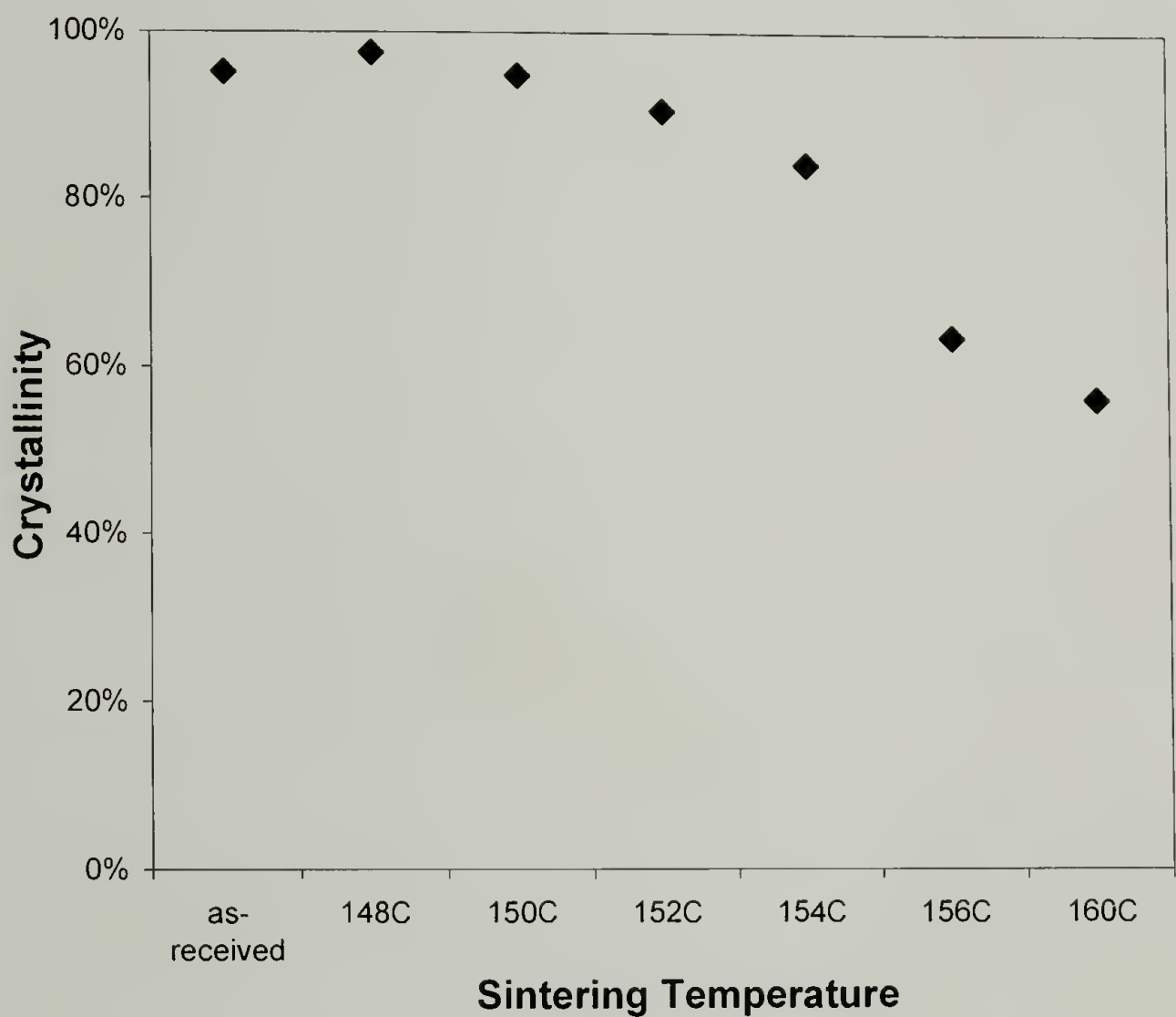


Figure 3.2 Overall crystallinity of the as-received and consolidated Spectra<sup>®</sup> cloth 903 sintered under 7.6MPa for 30 minutes at different sintering temperatures



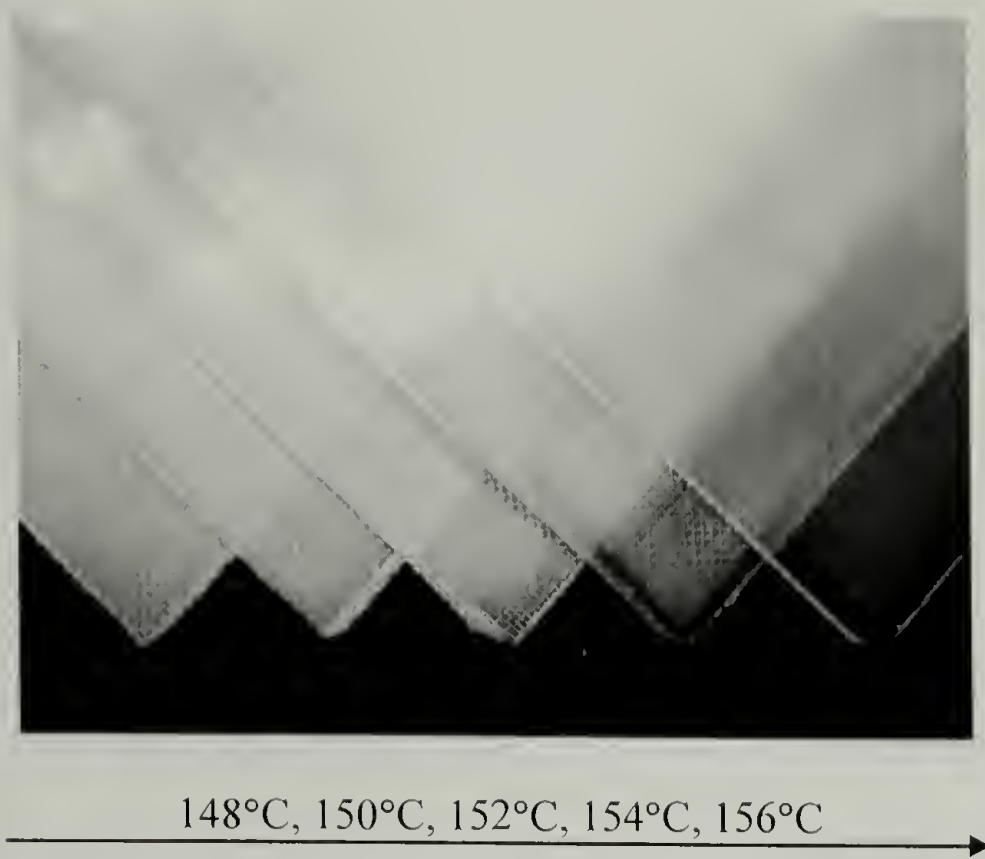


Figure 3.3 Picture of single layer Spectra® cloth 903 sintered under 7.6MPa for 30 minutes at different sintering temperatures

The two overlapping melting peaks can be mathematically deconvoluted and integrated separately to give the melting enthalpy for the two crystals: the original highly oriented crystals and the newly formed less oriented crystals. The amount of retained original crystals, referred to as “original crystallinity”, was calculated (Table 3.2 and Figure 3.4). There is an increase loss of the original crystals with increased processing temperature and at 160°C nearly all the original crystals are destroyed. About 13% of the original crystals melt at the normal melting point of the material (150°C), showing that constraint deferred the crystal melting.

Table 3.2 Changes in crystallinity corresponding to the original crystals for single layer Spectra<sup>®</sup> cloth 903 sintered under 7.6MPa for 30 minutes at different sintering temperatures

Specimen	148°C	150°C	152°C	154°C	156°C	160°C
Retained	92.0%	86.8%	76.9%	56.1%	5.8%	2.8%
Melted	8.0%	13.2%	23.1%	43.9%	94.2%	97.2%

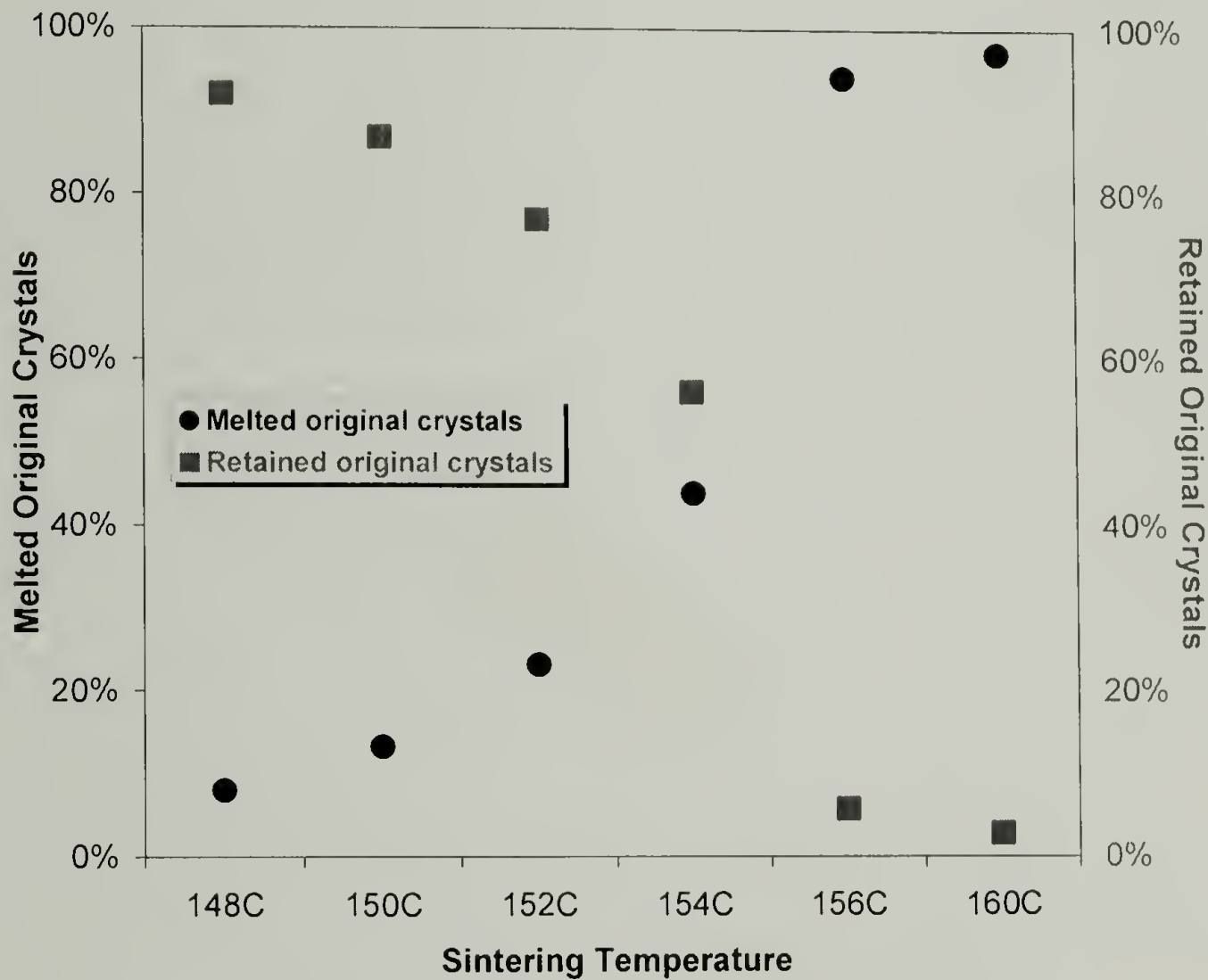


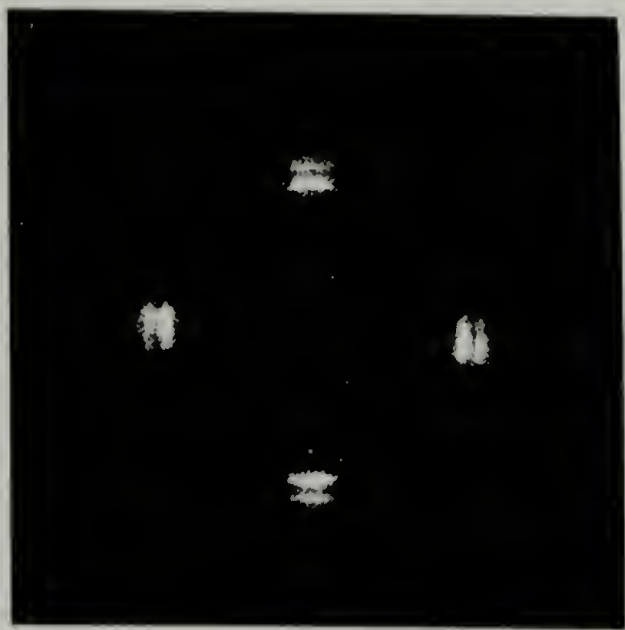
Figure 3.4 Changes in crystallinity corresponding to the original crystals for consolidated Spectra<sup>®</sup> cloth 903 sintered under 7.6MPa for 30 minutes at different sintering temperatures

High crystallinity is essential to the outstanding mechanical properties of Spectra<sup>®</sup> fiber 900. It has to be preserved as much as possible to achieve the high performance of

the sintered products. DSC suggests that the temperature range of 150°C – 152°C would be an ideal processing temperature; at these temperatures a minimum of 13% of the original crystals are melted and a 95% overall crystallinity is maintained after consolidation. The melted phase is sufficient to serve as the bonding mechanism to hold the consolidated structure together upon cooling and recrystallization.

### 3.3.2 WAXD patterns and Hermans orientation function

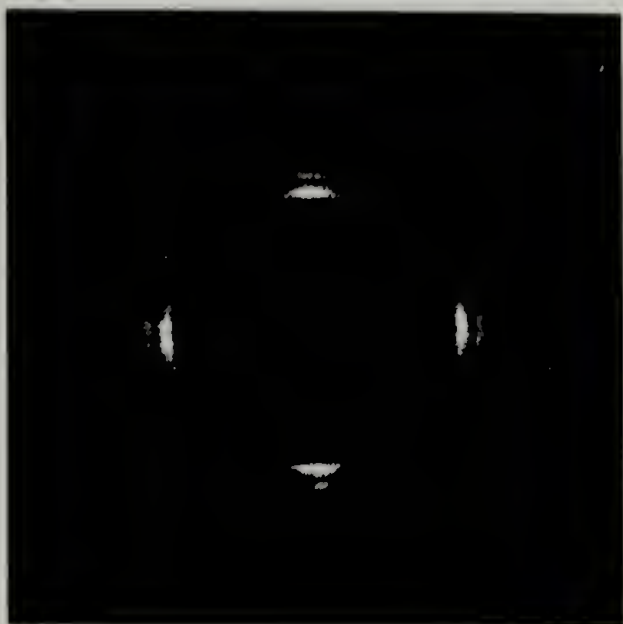
In the high-temperature high-pressure sintering, the molecules tend to relax towards their preferential random coil conformation at high temperatures even though they are under substantial constraint. The outcome is the loss of crystalline and chain orientation, resulting in a decrease of longitudinal strength. WAXD patterns for consolidated single layer Spectra<sup>®</sup> cloths sintered at different temperatures under constant pressure and time of 7.6MPa and 30 minutes are compared (Figure 3.5). Specimens sintered at lower temperatures, up to 150°C, have diffraction patterns similar to those of the as-received cloth, suggesting that high orientation is preserved even after the specimens experienced near-melting temperatures due to effective constraint. As the sintering temperature increases, the diffraction pattern of the consolidated cloth undergoes a series of changes. The spot-like diffraction pattern becomes arcs, the arcs broaden, and distinct diffraction rings eventually emerge due to the loss of molecular orientation.



as-received cloth



148°C



150°C



152°C



154°C



156°C

Figure 3.5 WAXD patterns for the as-received Spectra<sup>®</sup> cloth and Spectra<sup>®</sup> cloth consolidated under 7.6MPa for 30 minutes at different processing temperatures



The degree of orientation was calculated using Hermans orientation function for single layer Spectra<sup>®</sup> cloths consolidated at different temperatures (Table 3.3 and Figure 3.6). As the sintering temperature increases, degree of orientation decreases due to melting of the crystalline regions and relaxation of the polymer molecules to the entropically favorable random coil conformation. The Spectra<sup>®</sup> cloth maintains a relatively high orientation up to 152°C, beyond that temperature, the decrease in orientation is rather significant. Specimens sintered at 148°C have a higher degree of orientation than the original cloth due to pressure induced crystallization forcing the molecules to adopt a more oriented conformation in order to be incorporated into the crystal lattice. The studies on orientation changes confirm that the optimal processing temperature should not be higher than 152°C, above this temperature the properties of the consolidated structures significantly degrade.

Table 3.3 Hermans orientation function for unidirectional fibers, as-received Spectra<sup>®</sup> cloth, and Spectra<sup>®</sup> cloth consolidated under 7.6MPa for 30 minutes at different processing temperatures

Specimen	Unidirectional fiber	as-received cloth	148°C	150°C	152°C	154°C	156°C
Orientation	0.938	0.887	0.911	0.873	0.857	0.760	0.651

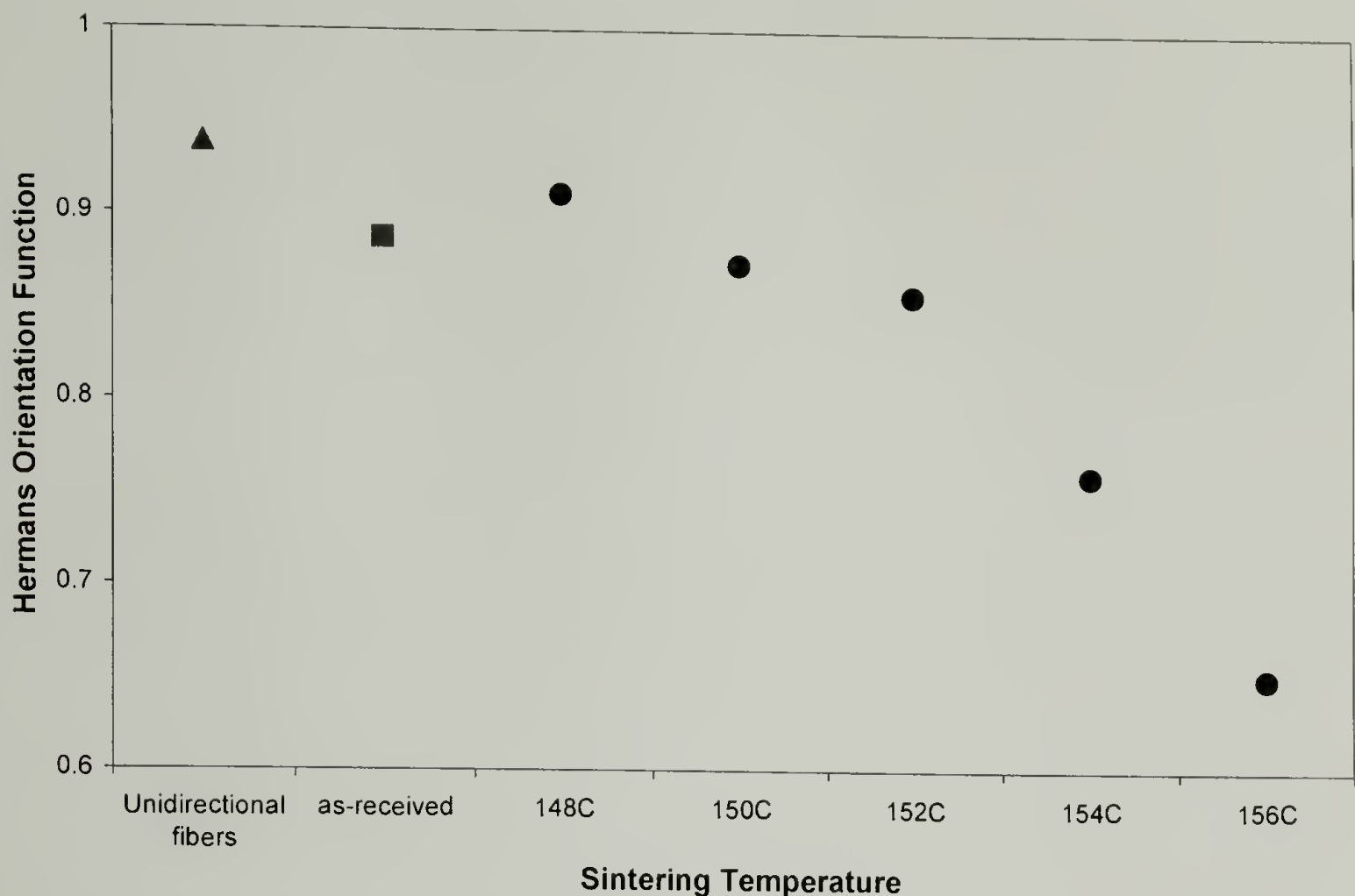


Figure 3.6 Degree of orientation calculated using Hermans orientation function for unidirectional fibers, as-received Spectra<sup>®</sup> cloth, and Spectra<sup>®</sup> cloth consolidated under 7.6MPa for 30 minutes at different processing temperatures

### 3.3.3 Correlation between crystallinity and orientation

High molecular orientation does not necessarily have a parallel relationship with high crystallinity. In a semicrystalline polymer the overall orientation of the crystalline domains can be far from perfect even though the polymer chains are nearly perfectly aligned within a single crystal; these domains can be randomly oriented. Molecular orientation is generally not correlated with crystallinity. Spectra<sup>®</sup> fiber has a unique structure and morphology; the polyethylene chains adopt a dominant extended chain conformation. The chains are parallel to the fiber axis and form nearly perfect needle-like crystalline domains (Figure 3.7).<sup>15</sup> As a result, the molecular orientation has a strong linear relationship with the degree of crystallinity (Table 3.4). If the values of Hermans

orientation function are plotted against the degree of crystallinity for the specimens processed at different temperatures, almost all the data points lay on a straight line (Figure 3.8). The greater the crystallinity, the higher the Hermans orientation function.

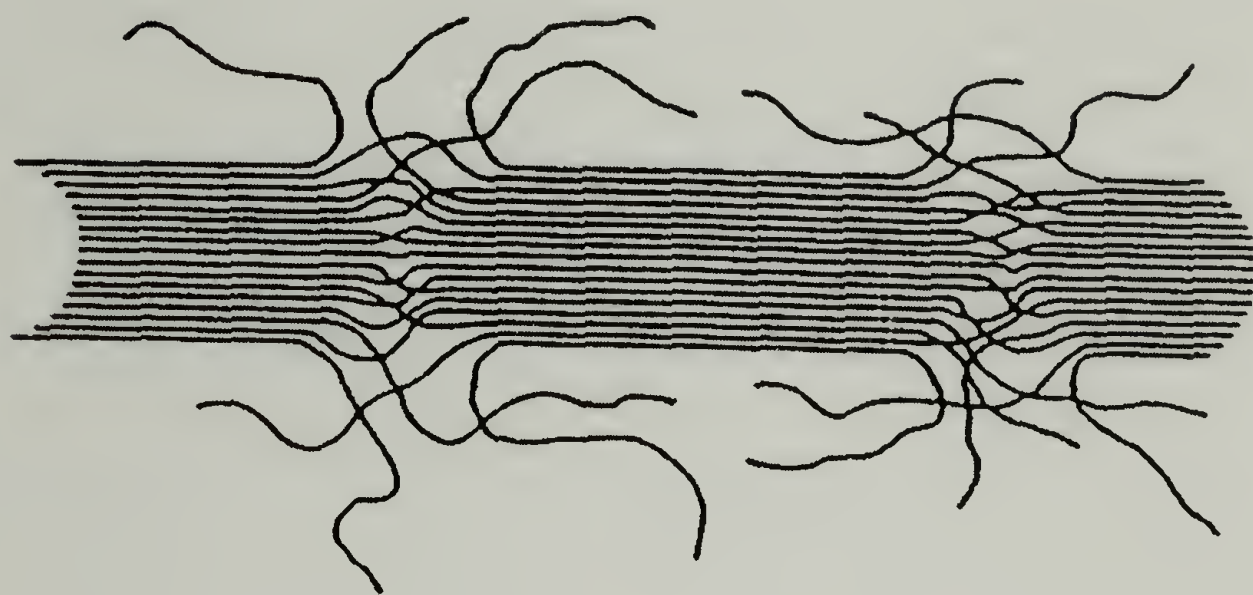


Figure 3.7 Schematic of Spectra<sup>®</sup> fiber microfibrils

Table 3.4 Degree of crystallinity and Hermans orientation function of the as-received Spectra<sup>®</sup> cloth and Spectra<sup>®</sup> cloth consolidated under 7.6MPa for 30 minutes at different processing temperatures

Specimen	as-received	148°C	150°C	152°C	154°C	156°C
Crystallinity	95.2%	97.5%	94.8%	90.6%	84.1%	63.6%
Orientation	0.887	0.911	0.873	0.857	0.760	0.658

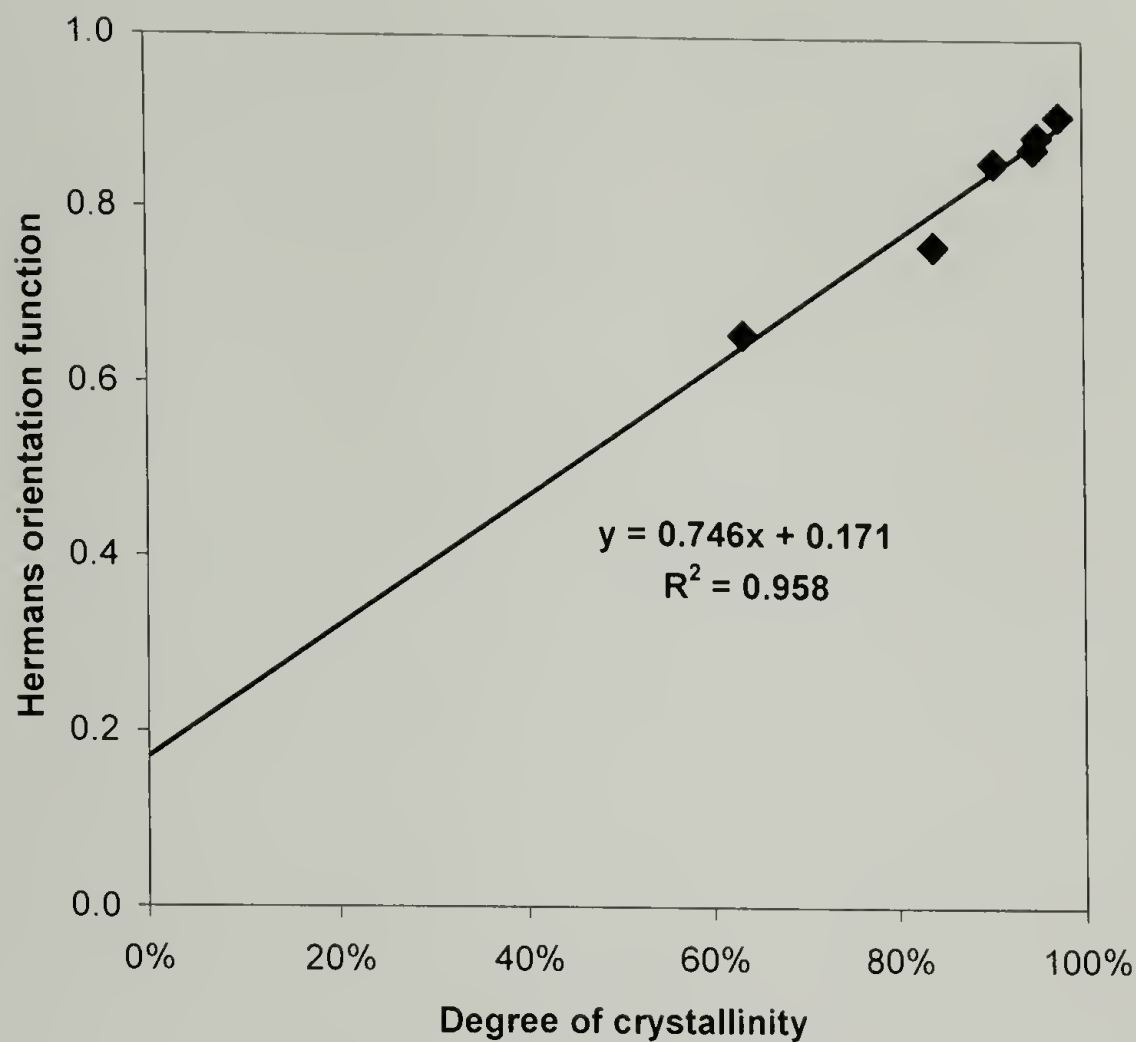


Figure 3.8 Linear correlation between the degree of crystallinity and Hermans orientation function

If the line is extrapolated to zero crystallinity, orientation has a value of 0.171.

Fu<sup>16</sup> et al. concluded in their studies that there are three different phases in the Spectra<sup>®</sup> fiber structure: a crystalline phase, an amorphous phase and an intermediate phase. The crystalline phase consists of orthorhombic crystals and monoclinic crystals and they make up ~75% and ~10% of the total fiber, respectively. The amorphous phase counts for ~5% of the fiber and the remaining ~10% is the so-called intermediate phase. The intermediate phase is made of polyethylene chains that adopt trans conformation and orient preferentially parallel to the fiber axis. The axial distance between the layers of neighboring carbon atoms in the intermediate phase is similar to that in the crystalline domain except the lateral packing is not as perfect and ordered as within the crystals.



The mobility of the chains in the intermediate phase is one order of magnitude higher than and one order of magnitude lower than the crystalline and amorphous phase, respectively. Based on Fu's model, the extrapolated orientation at zero crystallinity comes from the orientation of the intermediate phase.

#### 3.3.4 Normalized to thickness total energy of impact

The total energy of impact, the work done to puncture a consolidated Spectra<sup>®</sup> cloth was calculated from the load vs. deflection curve (Figure 3.9). Only the first peak is considered as the remaining responses are artifacts caused by the bouncing of the dart in the test. Since the specimen thickness is one of the factors that determine the total energy, the results were normalized to thickness (NTT). The NTT impact energy was used as the measure for impact resistance.

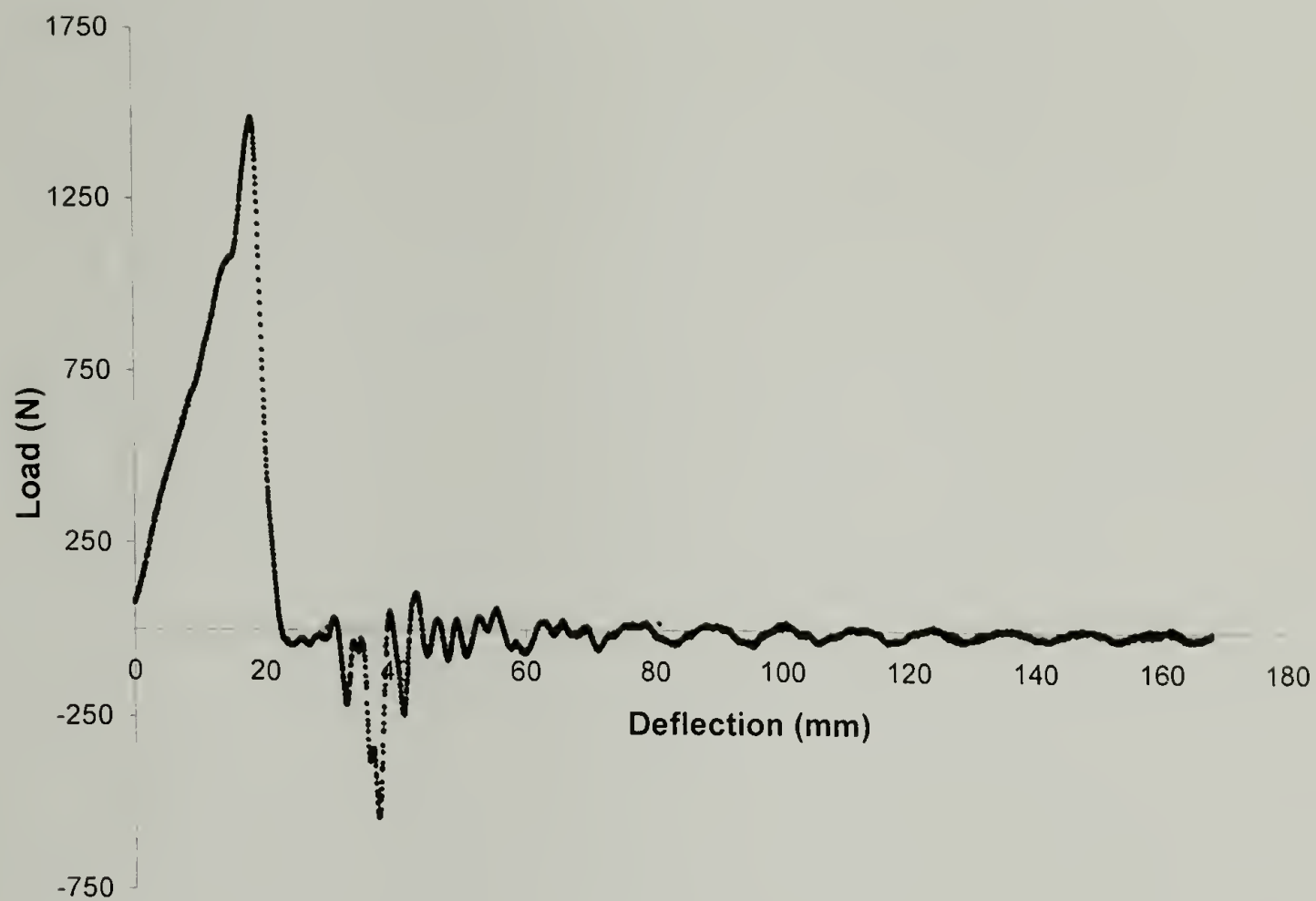


Figure 3.9 Typical Load vs. Deflection curve from an impact test of single layer of consolidated Spectra<sup>®</sup> cloth

A series of single-layer samples were produced at different processing temperatures and times under a constant pressure (7.6MPa) and their impact properties are compared with the impact properties of the as-received cloth and ultra high molecular weight polyethylene (UHMWPE) sheet (Table 3.5). An unoriented, isotropic UHMWPE sheet was obtained by the compression molding of UHMWPE powder. Two types of failure were observed: yarns were pushed aside and pulled out by the shooting dart but not broken, designated as failure mode *A*; yarns were broken and specimen was fractured, designated as failure mode *B*.

Table 3.5 NTT total impact energy (KJ/m) and failure mode of Spectra<sup>®</sup> cloth consolidated under different processing conditions, as-received Spectra<sup>®</sup> cloth, and unoriented UHMWPE sheet

Temperature						as-received cloth	UHMWPE sheet
Time	148°C	150°C	152°C	154°C	156°C		
30 minutes	78.1	92.0	13.7	3.2	2.3	16.6	13.3
Failure mode	<i>A</i>	<i>A</i>	<i>B</i>	<i>B</i>	<i>B</i>	<i>A</i>	<i>B</i>
20 minutes	63.7	90.7	14.3	5.4	1.1	-	-
Failure mode	<i>A</i>	<i>A</i>	<i>B</i>	<i>B</i>	<i>B</i>	-	-
10 minutes	60.3	76.1	90.6	13.3	1.5	-	-
Failure mode	<i>A</i>	<i>A</i>	<i>A</i>	<i>B</i>	<i>B</i>	-	-

\* sintering pressure = 7.6MPa

The as-received cloth has a similar level of impact resistance to the unoriented material since there is no lateral adhesion between the yarns. The dart could easily pull out yarns and squeeze past the woven yarns despite the high longitudinal strength of the individual fiber. Consolidation at high temperature and pressure produces interfiber adhesion and greatly improves the impact properties of the cloth. In the best scenarios, the impact resistance is inereased by nearly 6 times that of the as-received eloth. The maximum impaet properties are achieved when the Spectra<sup>®</sup> cloth is sintered between 150°C – 152°C depending on the processing time. There is a time-temperature superposition; as time becomes shorter a slightly higher temperature is needed to produce a specimen with the same level of impaet resistance as the one prepared at longer time and a lower temperature. The impaet property study confirms that the optimal proecessing temperature range suggested by the previous DSC and WAXD results is valid. For

consolidated cloth, the specimens failed by mode *A* absorb higher impact energy than the specimens failed by mode *B*. The impact results suggest that the fiber strength is maintained after consolidation and that the adhesion between fibers is good. The transition from mode *A* failure to mode *B* failure agrees with the location of the obtainable peak impact properties.

If the NTT impact energy is plotted against processing temperature and processing time (Figure 3.10), the optimal processing window is obvious. Under a pressure of 7.6MPa, a single layer of Spectra<sup>®</sup> cloth 903 sintered at 150°C for 20 – 30 minutes, or at 152°C for 10 minutes has the best impact resistance.

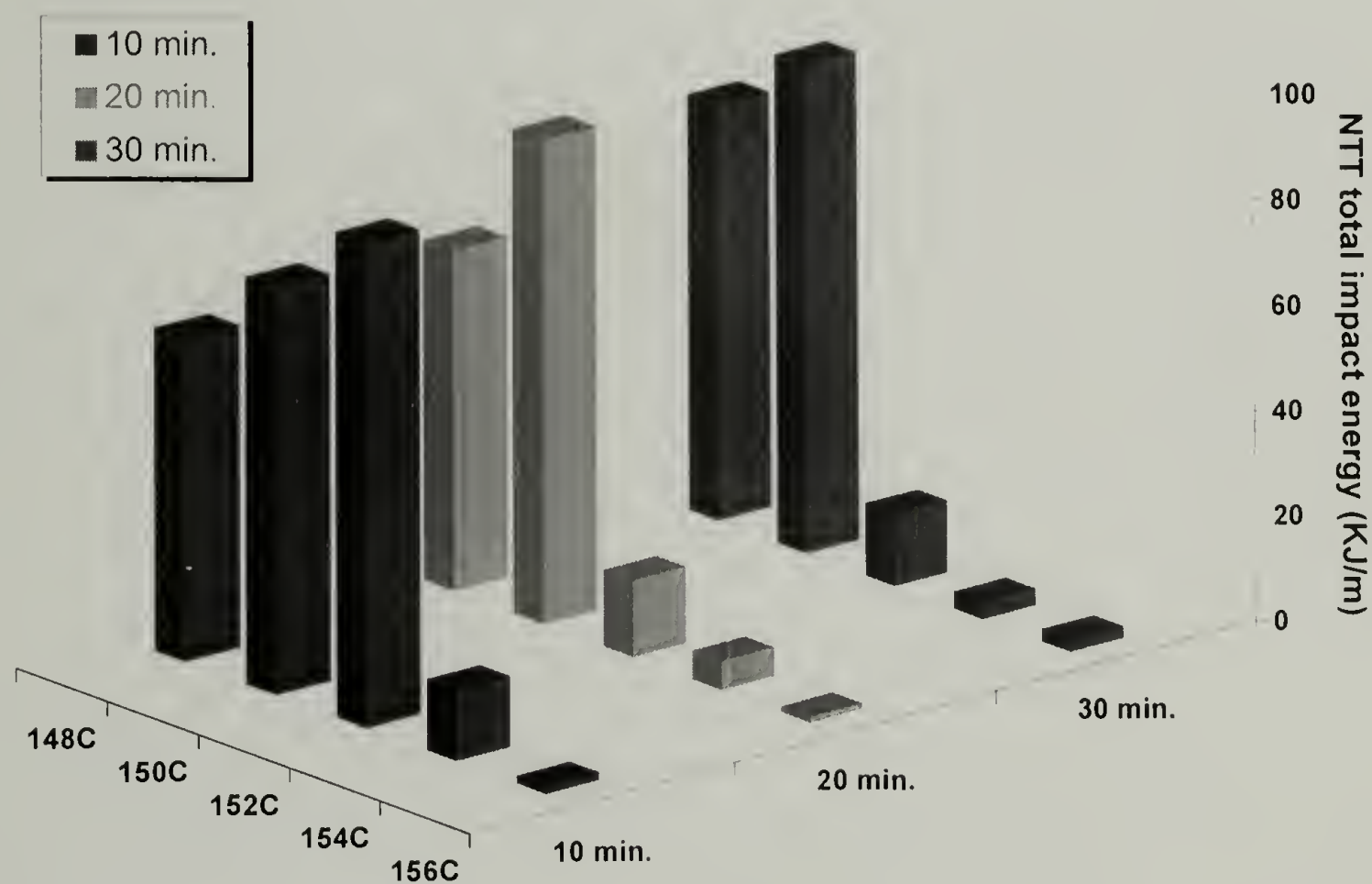


Figure 3.10 NTT total impact energy vs. temperature and time for single layer of consolidated Spectra<sup>®</sup> cloth 903 under 7.6MPa



The influence of pressure on the impact resistance was studied. Single layers of Spectra<sup>®</sup> cloth were sintered at 150°C for 30 minutes, under pressures ranging from 1.7MPa to 6.9MPa. The NTT impact energy was determined and there is a slight increase in impact resistance as the pressure is raised from 1.7MPa to 5.2MPa (Figure 3.11). At pressures greater than 5.2MPa, there is virtually no improvement in impact resistance. Impact resistance is not very sensitive to processing pressure, as opposed to time and temperature. Pressure is used to provide a constraint on the fibers and prevent them from shrinking, to eliminate voids, and to consolidate the structure. A minimum pressure is necessary for sintering but an excessive pressure does not help.

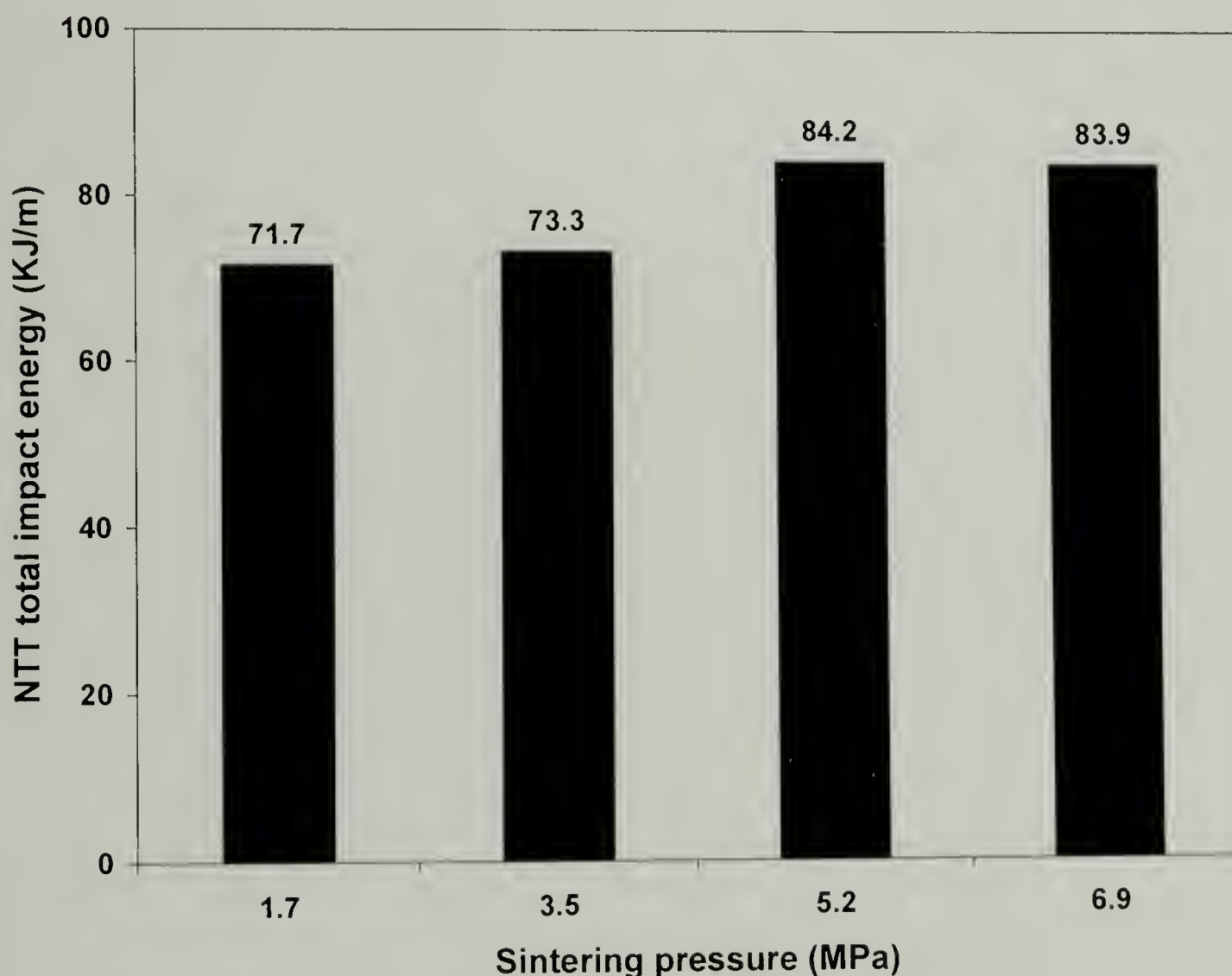


Figure 3.11 NTT total impact energy of single layer of consolidated Spectra<sup>®</sup> cloth 903 at 150°C for 30 minutes under various pressures

### 3.4 Conclusion

Single layers of Spectra<sup>®</sup> cloth were consolidated under various processing conditions by high-temperature high-pressure sintering. The resulting products have largely different physical properties and microstructure. At a given pressure and time, the extent of melting and recrystallization of the fiber increases with increasing processing temperature. Since not all of the melted phase recrystallizes on cooling, some is transformed to the amorphous and intermediate phase, the overall crystallinity decreases with increasing processing temperature. The original highly oriented crystals can be preserved if the sintering temperature is lower than 152°C. The relaxation of the molecular chains occurs at higher temperatures and becomes severe, indicated by the decreasing Hermans orientation function, with increasing processing temperature. The phenomenon of pressure induced crystallization happens to some extent as suggested by both DSC and WAXD. The Hermans orientation function shows a nearly perfect linear relationship with the degree of crystallinity due to the unique structure of Spectra<sup>®</sup> fiber. The impact resistance of Spectra<sup>®</sup> cloth is significantly improved after consolidation due to the development of interfiber adhesion. The processing temperature and time have a strong influence on the impact properties of the consolidated cloth while the processing pressure has little effect. The maximum impact properties are obtained when the cloths are sintered at 150°C – 152°C. The optimal processing windows is determined to be at 150°C for 20 – 30 minutes, or 152°C for 10 minutes under 7.6MPa. Under these conditions the consolidated cloths have the best impact resistance, indicative of the successful balance between the loss of longitudinal strength and the development of lateral strength.

## CHAPTER 4

### EVALUATION OF CONSOLIDATED STRUCTURES: PROCESS-STRUCTURE-PROPERTY RELATIONSHIP

#### 4.1 Introduction

The crystallinity and orientation of the consolidated Spectra<sup>®</sup> cloth determine the thermo-mechanical properties of the consolidated structures. They are greatly influenced by the processing conditions as confirmed by impact resistance observations. In this chapter, the consolidated Spectra<sup>®</sup> cloth is physically, thermally, mechanically, structurally, and morphologically characterized. Various characterization methods are used including mechanical testing, scanning electron microscopy (SEM), differential scanning calorimetry (DSC), and wide angle X-ray diffraction (WAXD) in this investigation.

The density of the sintered multilayer panels was measured to provide information on how well Spectra<sup>®</sup> cloth was consolidated under different processing conditions. The interlayer adhesion for sintered cloth was measured by T-peel test to characterize the lateral strength of the consolidated structures under different processing conditions. Flexural properties for multilayer flat panels sintered under different processing conditions were evaluated by three-point bend test to quantitatively illustrate the rigidity and stiffness of the consolidated structures. Ballistic performance of the flat panels was examined and compared with conventional matrix-containing Spectra<sup>®</sup> composites and other high performance fiber composites. The microstructure and morphology of the sintered cloth was investigated by SEM. Hermans orientation function was calculated for multilayer consolidated structures from WAXD results.

Differences between the surface and center layer of the multilayer sintered structure was probed by DSC and WAXD. The process-structure-property relationship is established to give an in-depth and better understanding of the high-temperature high-pressure sintering process for consolidating Spectra<sup>®</sup> cloth.

## 4.2 Experimental

### 4.2.1 Materials

Spectra<sup>®</sup> cloth 903 is made from Spectra<sup>®</sup> fiber 900 and was provided by Honeywell. It is a plain woven cloth with an average thickness of 0.5mm and an areal density of 0.024g/cm<sup>2</sup>. The material was sampled and tested in the as-received state without any further treatments. Spectra<sup>®</sup> cloth 903 is the material of choice for ballistic protective hard armor.

### 4.2.2 Density measurement

The effective consolidation of the Spectra<sup>®</sup> cloth was determined by comparing the literature value for the density of the Spectra<sup>®</sup> fiber with the determined density of the sintered structures. The weight of a specimen was measured both in air and immersed in 2-Propanol by a precision balance, then the density was calculated using Equation 4.1. 2-Propanol was used since its density (0.785g/cm<sup>3</sup>) is less than that of Spectra<sup>®</sup> fiber (0.97g/cm<sup>3</sup>).



$$\rho = \frac{w\rho_s}{w - w_s} \quad (4.1)$$

Where  $\rho$  is the specimen density

$\rho_s$  is the solvent density

$w$  is the specimen weight in air

$w_s$  is the specimen weight immersed in solvent

#### 4.2.3 T-peel test

Thermally bonded bilayer Spectra<sup>®</sup> cloth was prepared by sandwiching a 40mm × 150mm sheet of aluminum foil between two layers of 150mm × 150mm Spectra<sup>®</sup> cloth so that the aluminum foil was in line with one side of the cloth. The bilayer was consolidated by high-temperature high-pressure sintering, the aluminum foil was removed, and a 40mm wide gap was left with the remaining areas sintered. A series of bilayers were produced at different processing temperatures under constant pressure and time (7.6MPa and 30 minutes). Test specimens consisted of rectangular bilayer strips (12.5mm × 150mm) which had two “arms” due to the initial opening. T-peel tests were conducted on an Instron 5500R according to ASTM standard D1876. The two arms of the strip were attached to the upper and lower grips, and the crosshead was separated at the speed of 157mm/min. The peeling load and displacement distance were recorded. T-peel strength is reported as a measure of interlayer adhesion.

#### 4.2.4 Three-point bend test

Rectangular bars (100mm × 12.5mm × 3.2mm) prepared from twelve-layer Spectra<sup>®</sup> cloth panels consolidated under different processing conditions were used for three-point bend tests. The test was conducted using an Instron 5500R according to ASTM standard D790. A support span of 50mm and a crosshead speed of 1.35mm/min were used. The testing limit of 5% strain was used to ensure reliability of the data and the flexural modulus is reported as a measure of stiffness.

#### 4.2.5 Ballistic test

Ballistic tests on flat panels of consolidated Spectra<sup>®</sup> cloth were performed by the US Army at the Natick Soldier Center, MA. The panels were made from Spectra<sup>®</sup> cloth 903 according to our processing procedures and conditions and the testing protocol used was U.S. Military Standard 662F, a modified version of NATO V<sub>50</sub> ballistic test standard.<sup>63</sup> Multilayer sintered flat panels were shot by several different sized projectiles and the results were studied using a dimensionless analysis. The V<sub>50</sub> ballistic limits are related to the ratio of the area density of the armor systems to the presented area density of the projectiles.<sup>64</sup> The results are provided in comparison to composites using the same Spectra<sup>®</sup> cloth and a vinyl ester matrix, PBO fiber, and Kevlar<sup>®</sup> fiber reinforced composite armor systems.

#### 4.2.6 SEM and sample preparation

Consolidated Spectra<sup>®</sup> panels were etched according to Olley et al.<sup>65</sup> using 7% w/v potassium permanganate in a mixture of fuming sulfuric acid and phosphoric acid

mixture (1/2 v/v). Twelve-layer sintered Spectra<sup>®</sup> cloth panels prepared under different processing conditions were cut using a diamond knife to expose the cross section and were etched for one hour. At the end of the etching, the specimens were washed in a mixture of sulfuric acid and water (2/7 v/v) cooled near to its freezing point with dry ice. The solution was decanted and the specimens were washed in hydrogen peroxide, distilled water several times, and acetone for two minutes each. The specimens dried in air, were sputter-coated with gold, and examined under SEM. Peeled surfaces resulting from bonded bilayers which underwent the T-peel test were coated with gold and examined under SEM. JEOL 35CF and FESEM JEOL JSM-6320FXV were used in this study at magnifications of 100×, 1000×, and 1200×.

#### 4.2.7 WAXD of multilayer consolidated Spectra<sup>®</sup> cloth

Wide angle X-ray diffraction (WAXD) patterns were collected using pin hole collimated, monochromatic Cu K $\alpha$  radiation and a Bruker<sup>®</sup> “High Star” two dimensional detector. The diffraction patterns of a series of six-layer Spectra<sup>®</sup> cloth sintered under different processing conditions were collected. The cloth was oriented “flat-on” so that the incident X-ray beam was perpendicular to the cloth and the weft or warp yarn was aligned parallel to the horizon. A radiation time of 300 seconds was used and diffraction patterns were captured digitally. The integration of the intensity was preformed using GADDS commercial software.

#### 4.2.8 Studies on the surface and center layers

Surface and center layers were peeled and separated from the consolidated twelve-layer of Spectra<sup>®</sup> cloth prepared under different processing conditions. The crystallinity of the layers was determined by a TA Instrument DSC 2910 under nitrogen atmosphere (50 ml/min.). Hermetic pans containing ~10 mg samples of the peeled layers were heated at a rate of 10°C/min. from room temperature to 200°C. The molecular orientation of the layers was determined by WAXD and the procedure is described in the previous section.

### 4.3 Results and Discussion

#### 4.3.1 Density of the multilayer consolidated structure

Twelve layers of Spectra<sup>®</sup> cloth were sintered under 17.2MPa for 30 minutes at various temperatures and densities were calculated according to Equation 4.1. Figure 4.1 shows that the densities of the panels initially increase with increasing sintering temperature to a maximum at a sintering temperature of 154°C, and then decrease as the temperature increases above 154°C. Panels sintered at different temperatures have the densities similar to that of the original fiber (0.97g/cm<sup>3</sup>), suggesting that multilayer cloths are well consolidated with few voids; panels sintered at 154°C are nearly void-free (0.969g/cm<sup>3</sup>). The rise in density with sintering temperature from 150°C to 154°C is due to an increase in fiber lateral deformation which filled interstices. The drop in density with sintering temperature greater than 154°C is attributed to excessive fiber melting. The original highly oriented, dense crystalline regions of the fibers were destroyed during melting and the less dense amorphous regions were produced upon cooling. A large



decrease in crystallinity at a sintering temperature greater than 154°C was shown in the previous chapter (Section 3.3.1).

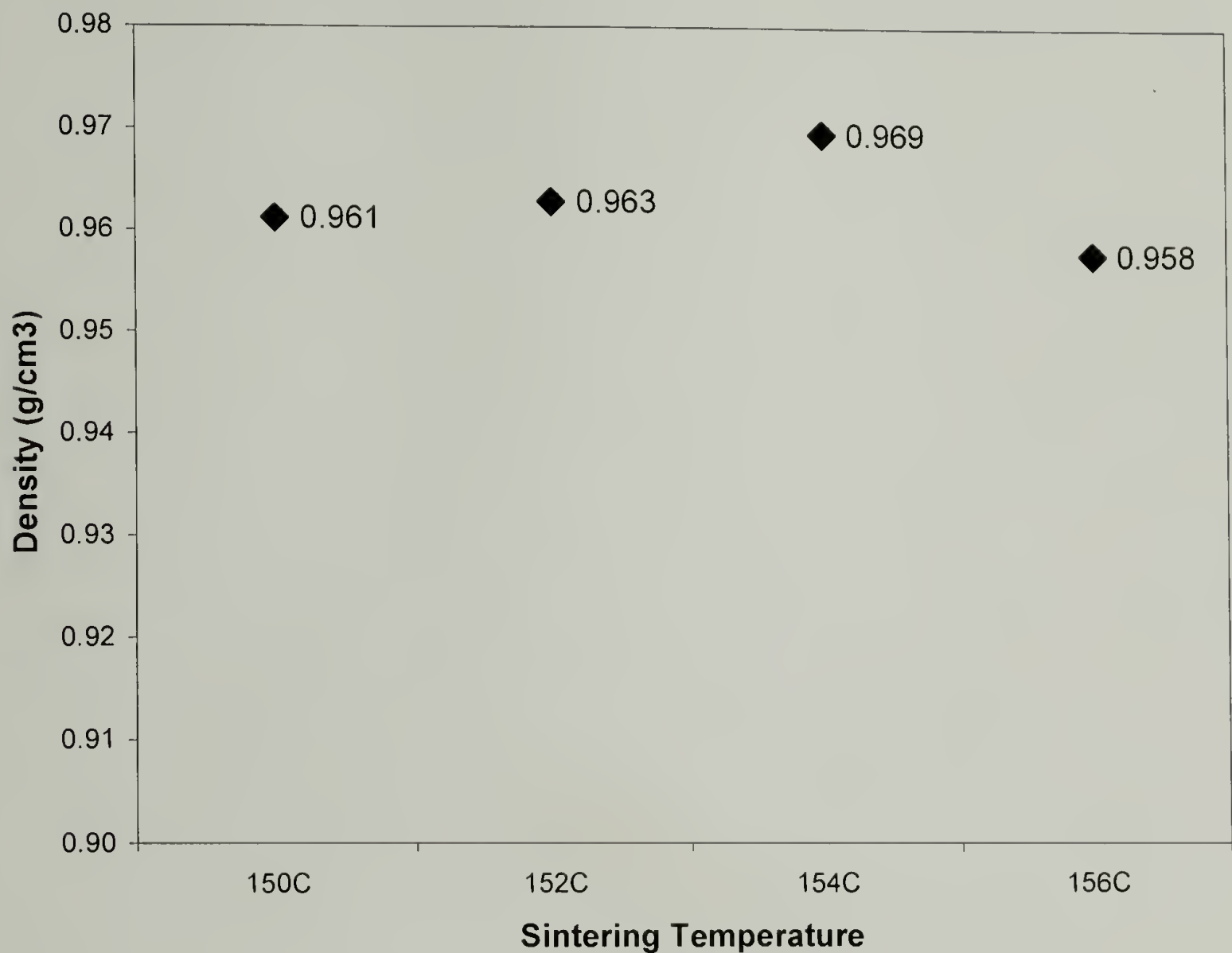


Figure 4.1 Density of multilayer Spectra<sup>®</sup> cloth panels sintered under 17.2MPa for 30 minutes at various processing temperatures

4.3.2 Interlayer adhesion

Interlayer adhesion facilitates stress transfer between fibers and matrix material, and provides lateral strength to the composites. The T-peel test is a simple and effective way to evaluate interface adhesion. T-peel strength is defined as the average peeling load in force per unit specimen width required to separate the adherends; a typical load vs. detachment plot is shown in Figure 4.2. The units are the same as separation energy per

unit area debonded. The fluctuation of data points in Figure 4.2 is due to non-uniform bonding. Since the surface of a woven cloth is not flat, with the yarns going up and down alternatively, the best adhesion is achieved when the high points of two cloths contact, the worst adhesion is suffered when the low points contact. Medium adhesion occurs when a high point and a low point are in contact.

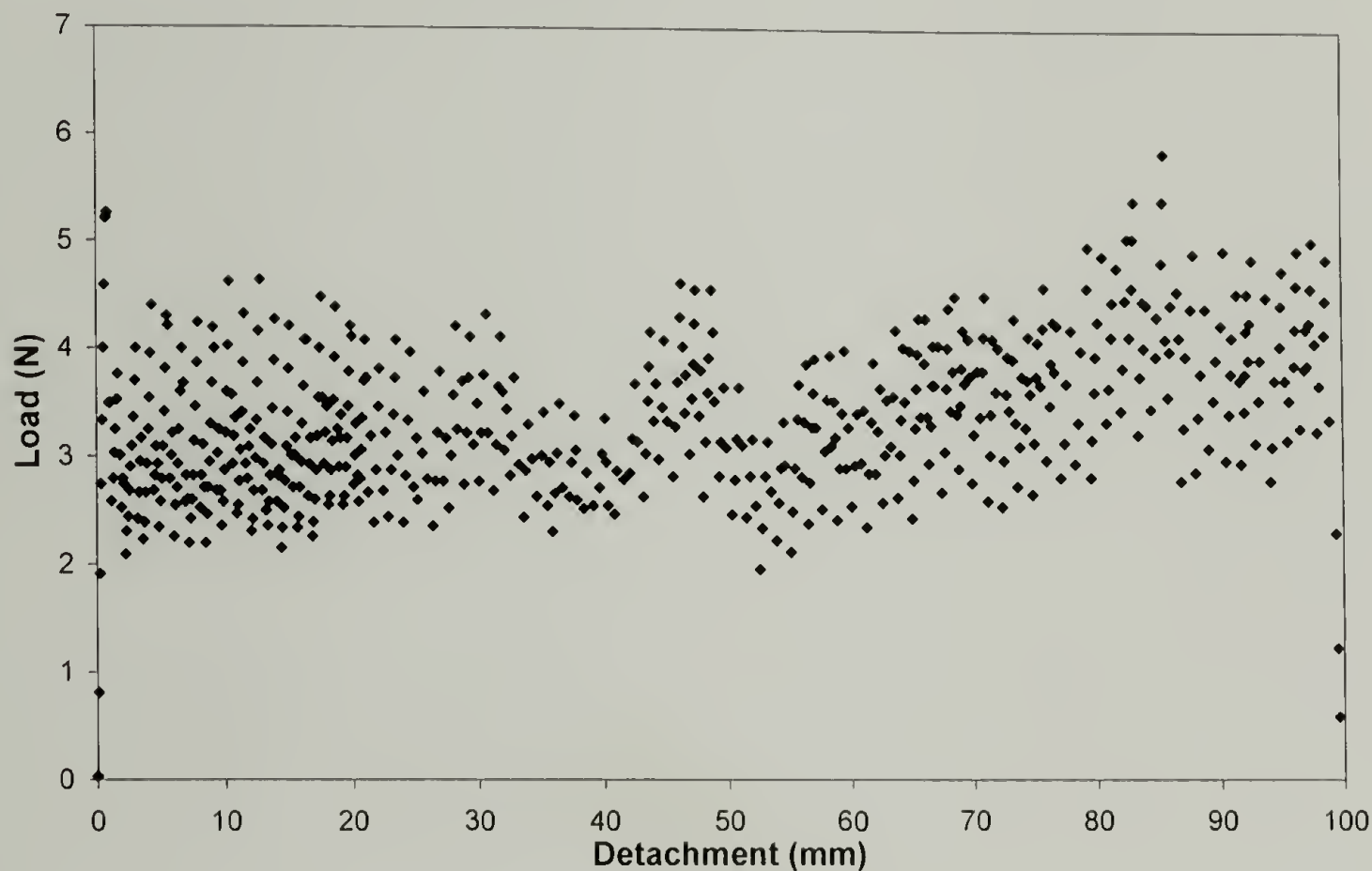


Figure 4.2 Typical load vs. detachment curve in a T-peel test

T-peel strengths for Spectra<sup>®</sup> cloth bilayers sintered at different processing temperatures are compared in Table 4.1. The peel strength increases monotonically over the temperature range since higher temperatures results in increased melting and recrystallization on cooling, hence better bonding. One would anticipate that consolidation at higher temperatures is required to make a good composite material as the better adhesion results in better load transfer. However, for laminated materials made for ballistic purposes, the stronger the adhesion the poorer the ballistic performance. When a

high speed projectile hits a target, its kinetic energy needs to be consumed in order to stop it and delamination between layers and fibers provides a good channel for the dissipation of energy. Excellent interface adhesion between layers and fibers worsens the ballistic protection and comes at the expense of the longitudinal strength since more crystalline melting and orientation loss happens at higher temperatures. It has been shown that the tensile failure of the fibers during ballistic impact absorbs a large portion of the kinetic energy,<sup>66</sup> therefore the preservation of the fibers' longitudinal strength is of great importance. A certain level of adhesive strength is desired to bond the material but excessive adhesion should be avoided.

Table 4.1 T-peel strength of two layers of Spectra<sup>®</sup> cloth 903 bonded under 7.6MPa for 30 minutes at different temperatures

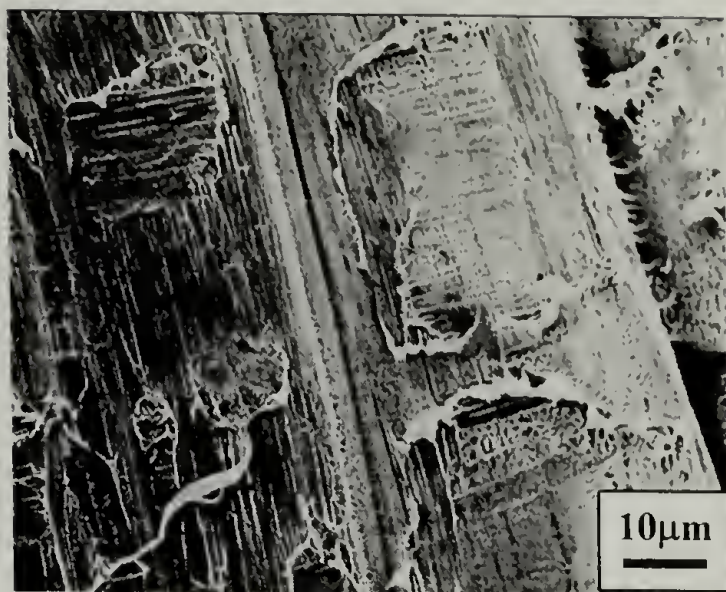
Sintering Temperature	148°C	150°C	152°C	154°C	156°C
T-Peel Strength (N/cm)	1.7	2.0	3.5	11.4	13.3

Peeled surfaces were examined under SEM (Figure 4.3) for the specimens sintered at different processing temperatures. At sintering temperatures between 148°C – 150°C, there is little adhesion between the bonded layers and few residues or detachments are left on the peeled surfaces. Individual fibers in the cloth are visible with no signs of fiber disturbance or lift, suggesting that the adhesion is only from the strength of the recrystallized thin layers between fibers. Adhesion becomes stronger at temperatures between 152°C – 156°C as indicated by the severe fibrillation resulted from peeling. Individual fibers are smeared out and not discernible.

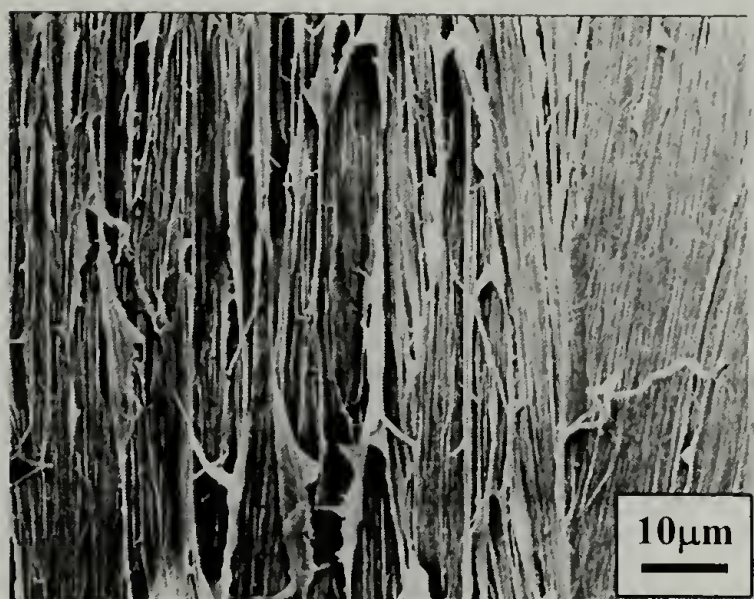




148°C



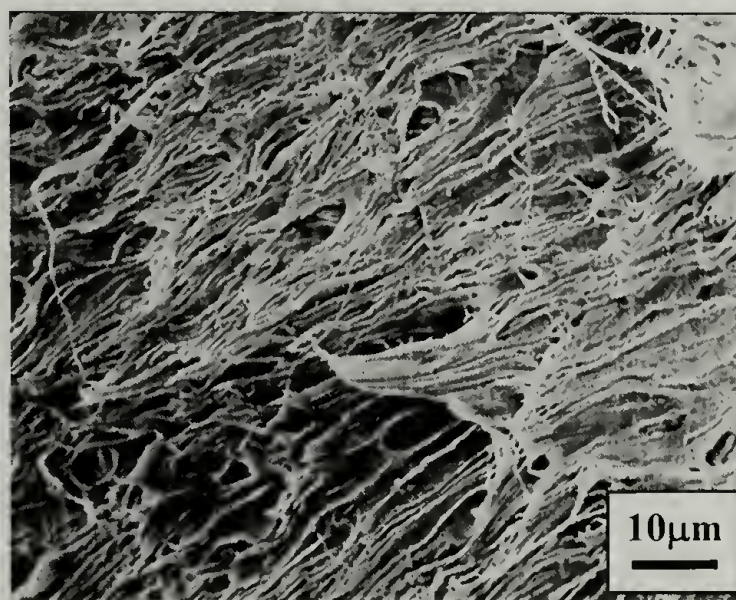
150°C



152°C



154°C



156°C

Figure 4.3 SEM images of peeled surfaces for specimens sintered under 7.6MPa for 30 minutes at different processing temperatures



4.3.3 Flexural properties

Flexural properties were measured by three-point bend tests to characterize the rigidity and stiffness of the materials. No specimens exhibited any failure or yield within the 5% strain limit set by ASTM D790, so no ultimate strength or yield strength is reported. At a much higher strain than 5%, the specimens sintered at lower temperatures showed delamination between the layers while the specimens sintered at higher temperatures showed no visible damage. Flexural modulus (Table 4.2 and Figure 4.4) was calculated by initial slope method according to Equation 4.2:

$$E = \frac{sL^3}{4wt^3} \tag{4.2}$$

- where  $E$  is the tangent modulus of elasticity
- $s$  is the initial slope of the load-deflection curve
- $L$  is the support span
- $w$  is the specimen width
- $t$  is the specimen thickness

Table 4.2 Flexural modulus (GPa) of twelve layers of Spectra<sup>®</sup> cloth 903 sintered at different processing conditions and unoriented UHMWPE panel

Processing condition	150°C	152°C	154°C	156°C	160°C	UHMWPE
30 minutes	3.33	4.52	5.18	4.31	0.80	0.74
45 minutes	3.57	5.23	4.24	3.27	0.81	-
60 minutes	4.87	5.98	4.45	1.95	0.78	-

\* Sintering pressure = 17.2MPa

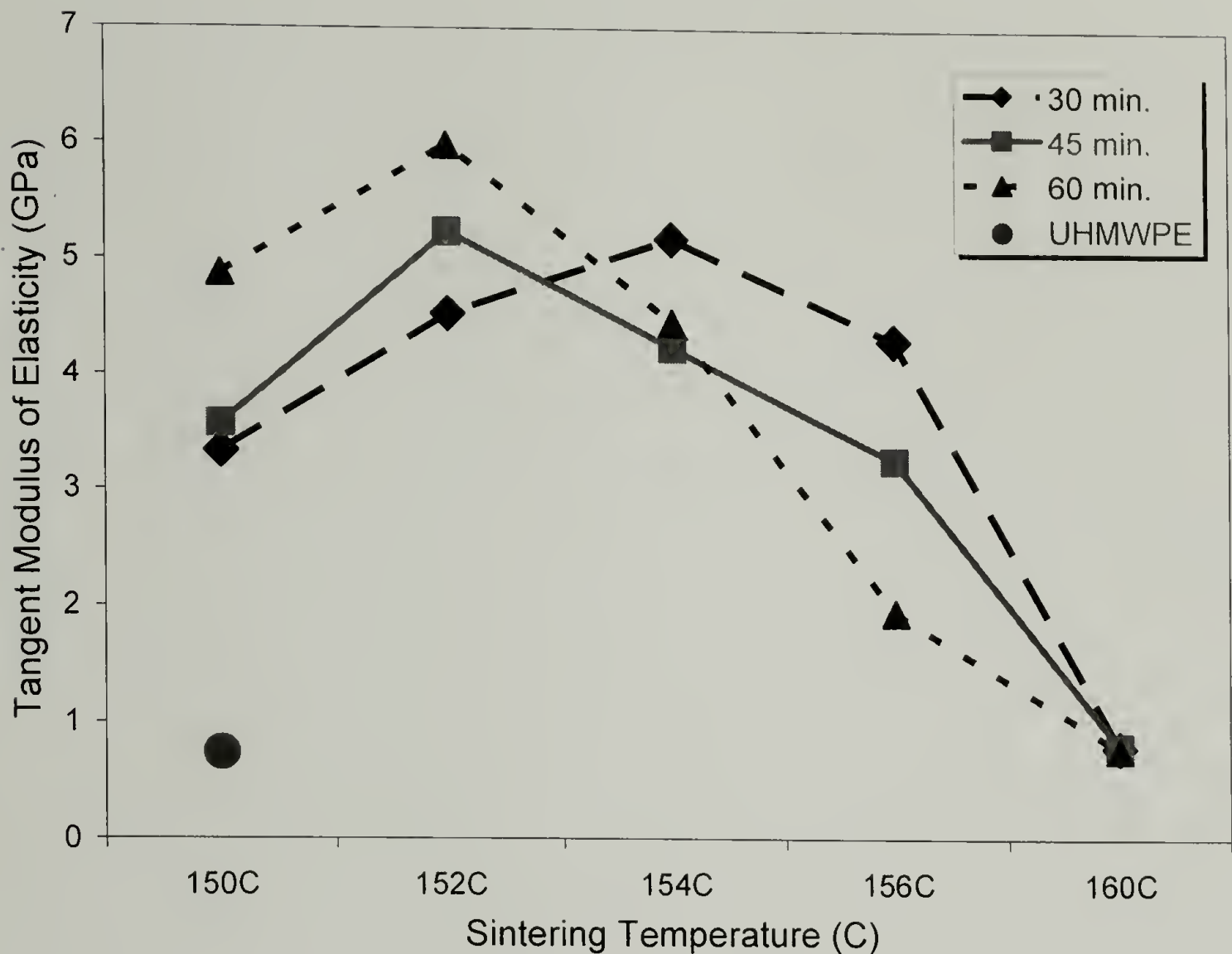


Figure 4.4 Flexural modulus of twelve layers of Spectra® cloth 903 sintered at different processing conditions (sintering pressure = 17.2MPa) and unoriented UHMWPE panel

The flexural modulus increases with increasing sintering temperature to 152°C and decreases with increasing sintering temperatures above 154°C. For all different sintering times, the flexural modulus is maximized for the specimens consolidated at 152°C or 154°C. Spectra® cloth panels sintered at 160°C have a measured flexural modulus similar to that of unoriented UHMWPE. The loss in rigidity is the result of the loss of crystallinity and molecular orientation due to excessive melting at the processing temperature of 160°C.

Consolidated multilayer Spectra® cloth panels are very stiff and rigid. Strain wave propagation speed is proportional to the square root of the ratio of the material

modulus and density ( $\sqrt{E/\rho}$ ).<sup>15</sup> The high modulus and low density of Spectra<sup>®</sup> material allows for fast wave propagation; the impact energy generated by a projectile can spread quickly and more material will be involved in the energy dissipation process. If a bullet hits an isotropic target material, the shock wave caused by impact travels in all directions at the same speed. A fiber reinforced armor system is highly anisotropic; the modulus in plane is much higher than the modulus through the thickness. A large  $\sqrt{E/\rho}$  value means the impact energy can spread quickly in the plane rather than through the thickness which is very good for ballistic protection.

In comparison to the tensile modulus 70GPa for the original Spectra<sup>®</sup> fiber 900, the measured flexural modulus seems low. The flexural modulus is limited by the 0°/90° weave of the cloth, since the fibers perpendicular to the specimens long direction do not significantly contribute to their rigidity based on the test geometry. Also, fibers in the cloth are not straight but nearly sinusoidal, there are voids in the specimens, and the partial melting of the fibers degrade their properties.

#### 4.3.4 Ballistic performance

Ballistic tests were performed using the  $V_{50}$  standard test:  $V_{50}$  ballistic limit is the velocity at which the probability of penetration of an armor material is 50 percent.  $V_{50}$  ballistic limits of matrix free Spectra<sup>®</sup> fiber composite, Spectra<sup>®</sup> fiber and vinyl ester matrix composites and plain woven Spectra<sup>®</sup> cloth against different projectiles are compared in Table 4.3. Matrix free Spectra<sup>®</sup> fiber composite was made by consolidation of 62 layers of Spectra<sup>®</sup> cloth according to our procedures, designated as “62-ply no resin”. Four Spectra<sup>®</sup> fiber/vinyl ester composites were also tested, designated as “66-ply

composite”, “61-ply composite”, “44-ply composite”, and “41-ply composite”. In addition, 62 layers of Spectra<sup>®</sup> plain woven cloth (base fabric) were stacked without any processing and used as a test specimen, designated as “62-ply fabric”. The projectiles were right circular cylinders and differed by their weights in the units of “grain” (1 grain = 64.799 milligrams). As expected, the composites do not perform as well as the base fabric at lower areal densities and against heavy projectiles due to fiber property degradation during processing and the high rigidity of the panels. At higher areal densities and against low-mass projectiles the results are reversed since the introduction of interfiber and interlayer adhesion hinders the penetration of the small projectiles.

Table 4.3  $V_{50}$  ballistic limits of matrix free Spectra<sup>®</sup> composite, Spectra<sup>®</sup> fiber/vinyl ester matrix composites, and Spectra<sup>®</sup> cloth against different sized projectiles

$V_{50}$ (m/s)	62-ply	66-ply	61-ply	44-ply	41-ply	62-ply
Projectile	no resin	composite	composite	composite	composite	fabric
2 grain	-	1099.0	1098.8	851.5	884.5	809.2
4 grain	761.0	-	-	-	-	753.6
16 grain	-	694.0	-	549.0	568.3	639.3
64 grain	457.3	-	-	-	-	541.3

\* 62-ply no resin - matrix free Spectra<sup>®</sup> fiber composite made of 62 layers of Spectra<sup>®</sup> cloth  
66-ply, 61-ply, 44-ply and 41ply composites - Spectra<sup>®</sup> fiber/vinyl ester composites  
62-ply fabric - stacked 62 layers of Spectra<sup>®</sup> cloth

In Figure 4.5, the ordinate is  $V_{50}$  velocity and the abscissa is the ratio of the presented areal density of the armor system to the areal density of the projectile.  $A_d$  refers to the area density of the specimen,  $A_p$  is the presented area density of the projectile, and  $m_p$  is the projectile’s mass. The filled symbols correspond to the matrix



free Spectra<sup>®</sup> cloth composites and the unfilled symbols correspond to the composites using Spectra<sup>®</sup> cloth with the vinyl ester matrix. All the data are plotted using appropriate symbols representing different projectiles. RCC stands for right circular cylinder type projectile. Also, plotted in the figure are today's state of the art Kevlar<sup>®</sup> KM2 (PVB-Phenolic) armor performance and the expected PBO composite armor performance, the best armor system that the Army can offer to date. Higher  $V_{50}$  values at a given areal density level indicate higher ballistic resistance. Matrix free Spectra<sup>®</sup> composites perform as well as, or slightly better than the system containing matrix, and better than the Kevlar<sup>®</sup> system at the same areal density level. Matrix free Spectra<sup>®</sup> composites are lighter in weight than the Spectra<sup>®</sup> and matrix or the Kevlar<sup>®</sup> system due to the elimination of the matrix and the low density of the fiber. Also the manufacturing process is simpler for the matrix free Spectra<sup>®</sup> composites than for the other two systems. Ballistic test results confirm that matrix free Spectra<sup>®</sup> fiber reinforced composite made by high-temperature high-pressure sintering is a promising candidate for high performance light weight body armor and helmets.

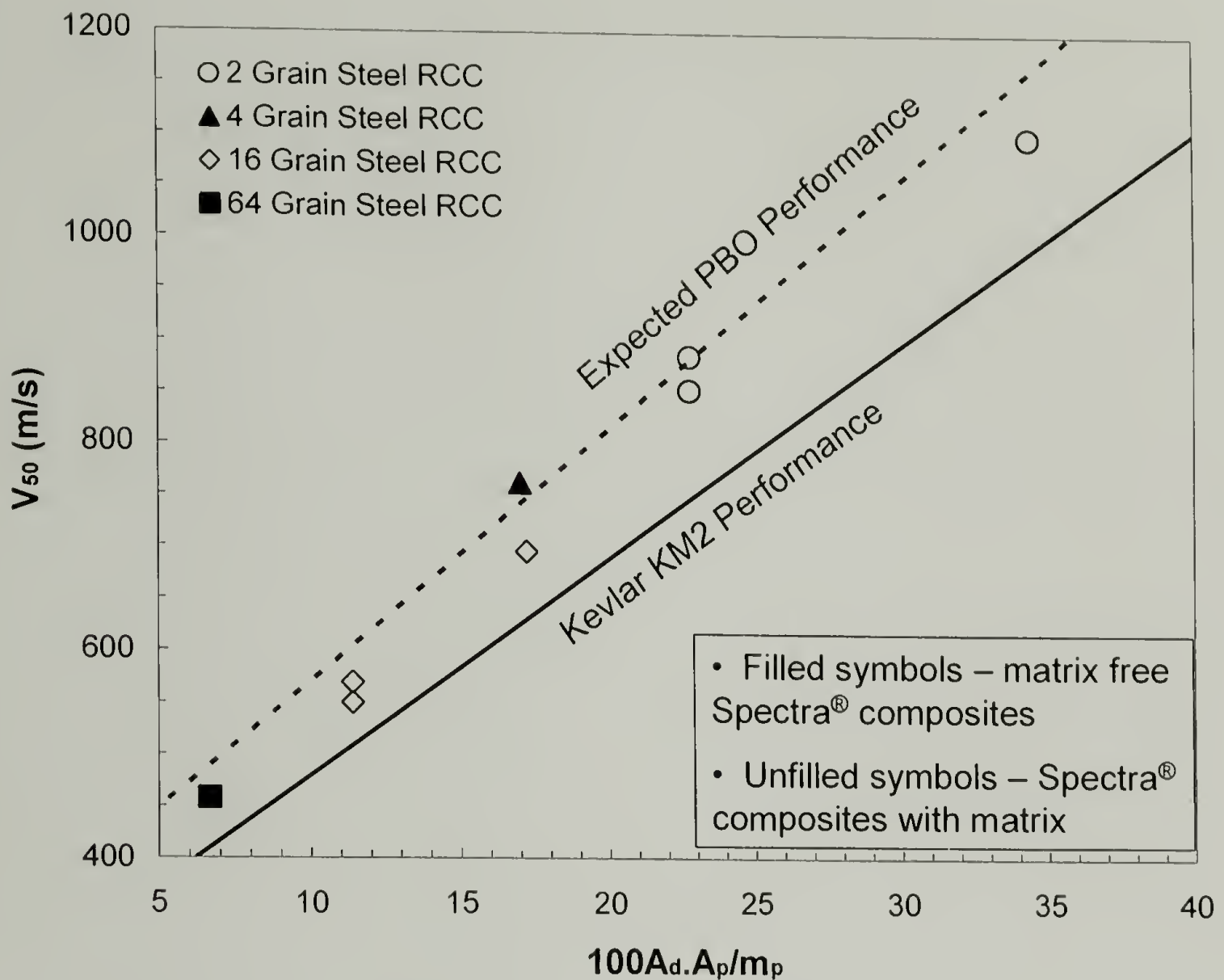


Figure 4.5 Ballistic performance of the multilayer consolidated Spectra® cloth compared with other composites (from the US Army)

#### 4.3.5 Morphology and sintering mechanism

SEM images at low magnification reveal the cross section of twelve layers consolidated Spectra® cloth (Figure 4.6). Bright regions correspond to fibers perpendicular to the plane of the page and dark regions correspond to fibers parallel to the plane of the page. Overall the multilayer cloths are well consolidated, although some crevices and voids can be seen due to knife damage or etching. The voids mostly appear at the junction regions between the warp and weft yarns, which indicate weak adhesion in these regions. The junction regions are more susceptible to knife damage and etching



reagent. There are fewer visible voids with increasing sintering temperature of the multilayer cloths.

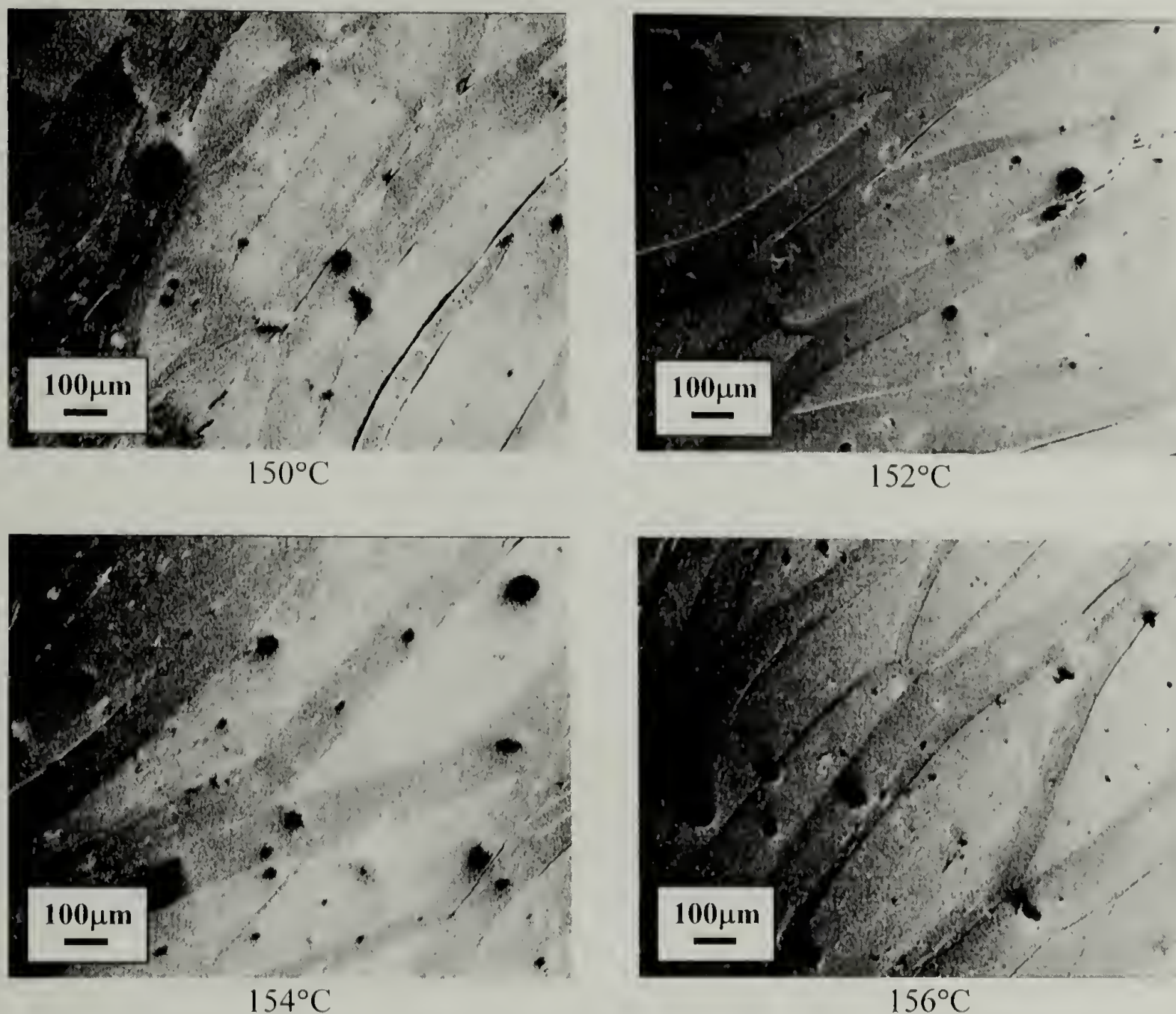
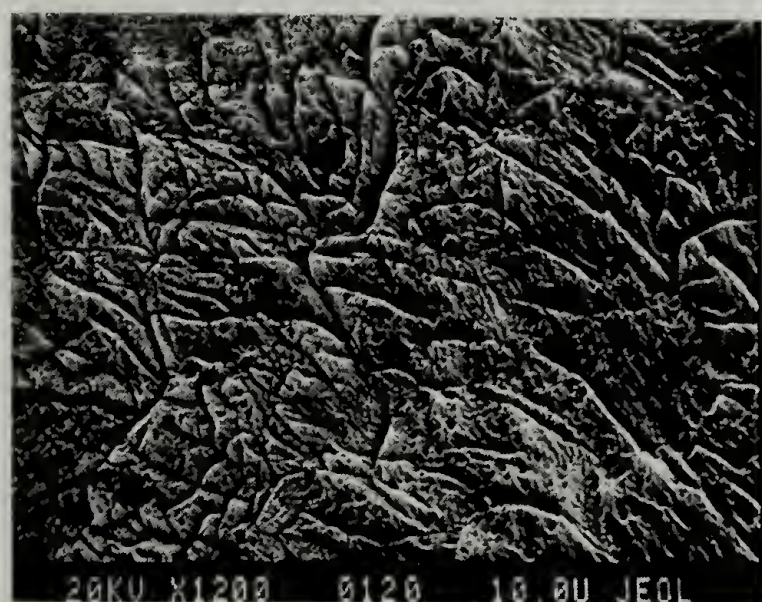


Figure 4.6 Low magnification SEM images showing the cross sections of multilayer Spectra<sup>®</sup> cloth sintered under 17.2MPa for 30 minutes at different processing temperatures

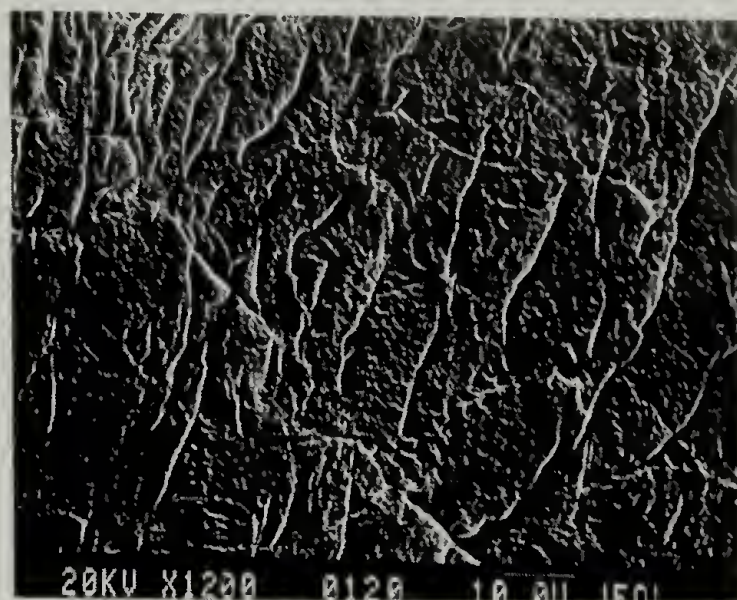
The cross sections of individual fibers can be seen under high magnification (Figure 4.7); the topology is quite different for the specimens sintered at lower and higher temperatures as a result of the etching process prior to investigation. The etchant removes the density deficient regions: the amorphous regions and the recrystallized phases, but not the original highly oriented crystals. Melting and recrystallization that



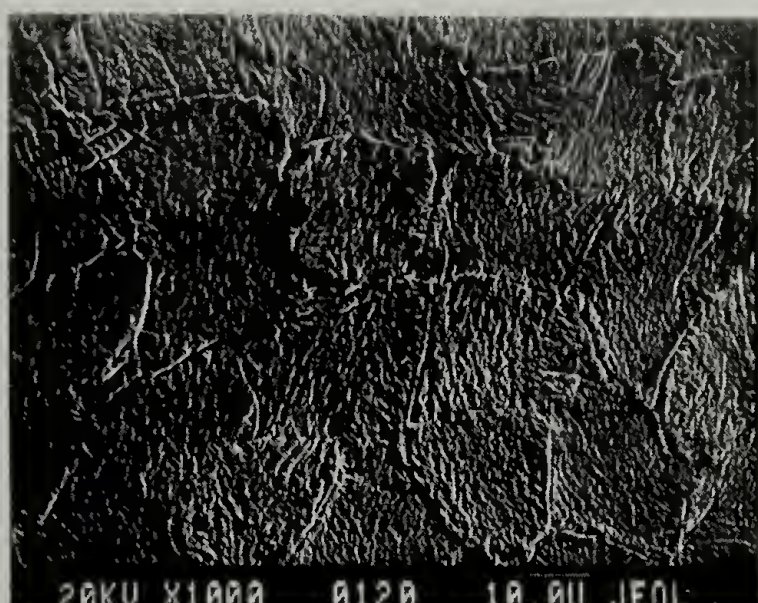
produces the less dense phases increases at higher processing temperatures at the fiber surface and core. Hill and valley like features are present in the cross section of the samples processed at lower temperatures. In addition, numerous conical pits are seen inside individual fibers since there are longitudinal density deficient region within Spectra<sup>®</sup> fiber. On the contrary, relatively smooth surfaces are seen in the samples processed at higher temperatures as a result of uniform etching.



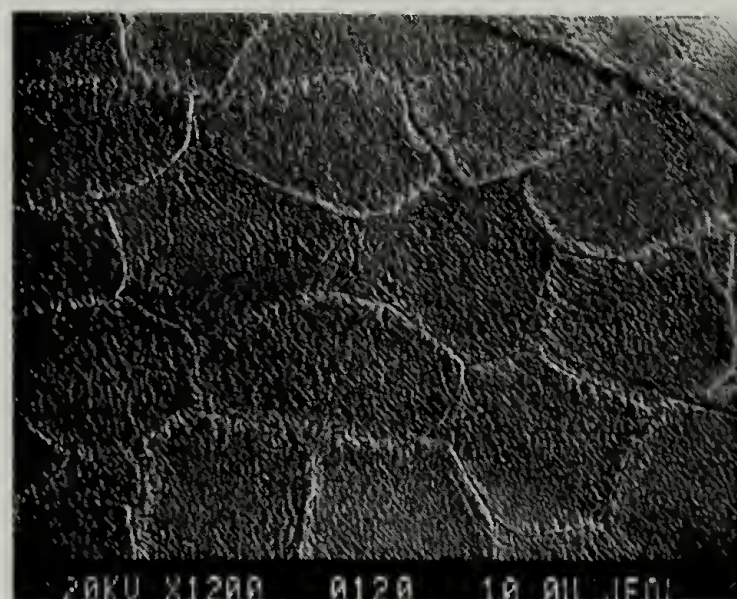
150°C



152°C



154°C



156°C

Figure 4.7 High magnification SEM images showing the cross sections of multilayer Spectra<sup>®</sup> cloth sintered under 17.2MPa for 30 minutes at different processing temperatures

Figure 4.8 shows SEM images of the boundary between two orthogonal yarns. In the transverse direction, there is no significant fiber melting to fill the voids. Instead, the



voids are filled by fiber deformation and impingement; there are signs of local welding at the boundary. The consolidation mechanism of fiber lateral deformation to fill voids and spot welding by the recrystallization of melted fiber surfaces is confirmed by SEM images and schematized in Figure 4.8.

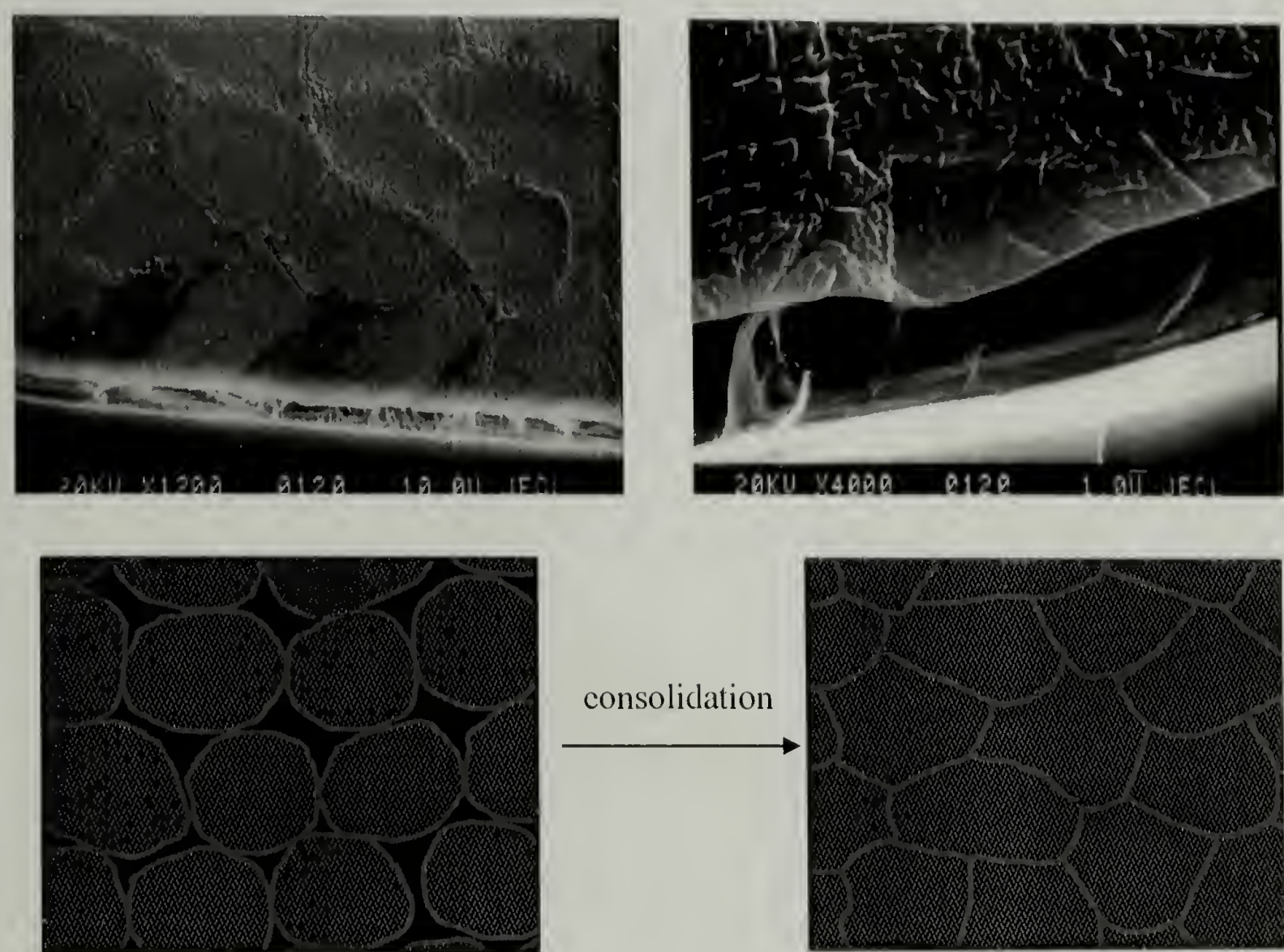


Figure 4.8 SEM images of the boundary between two orthogonal yarns in a multilayer consolidated Spectra<sup>®</sup> cloth and schematic of consolidation mechanism

#### 4.3.6 Molecular orientation

The molecular orientation within multilayer consolidated Spectra<sup>®</sup> cloth was examined by WAXD. Due to the limited penetration of X-ray, six layers of Spectra<sup>®</sup>

cloth were sintered at different processing temperatures and tested and the Hermans orientation function was calculated (Figure 4.9). Multilayer cloth specimens seem to maintain higher molecular orientation compared to single layer cloth sintered at the same temperature since the same molding time was used on both single layer and multilayer samples. The multilayer samples suffer less melting and chain relaxation since more material experiences the same amount of heat flow as the single layer samples. The low thermal conductivity of polyethylene may have reduced the time that multilayer samples experience the actual processing temperature. Also the multilayer samples are thick and more efficiently constrained under pressure as opposed to the thinner single layer cloth and as a result, have a higher degree of orientation even after sintering at high temperatures. Multilayer sintered material is not as highly oriented as the unidirectionally aligned fibers (0.938). The maximum orientation is obtained for the specimen consolidated at 154°C. The initial increase in Hermans orientation function at sintering temperature below 154°C is due to pressure induced crystallization, as described previously (Section 3.3.2).

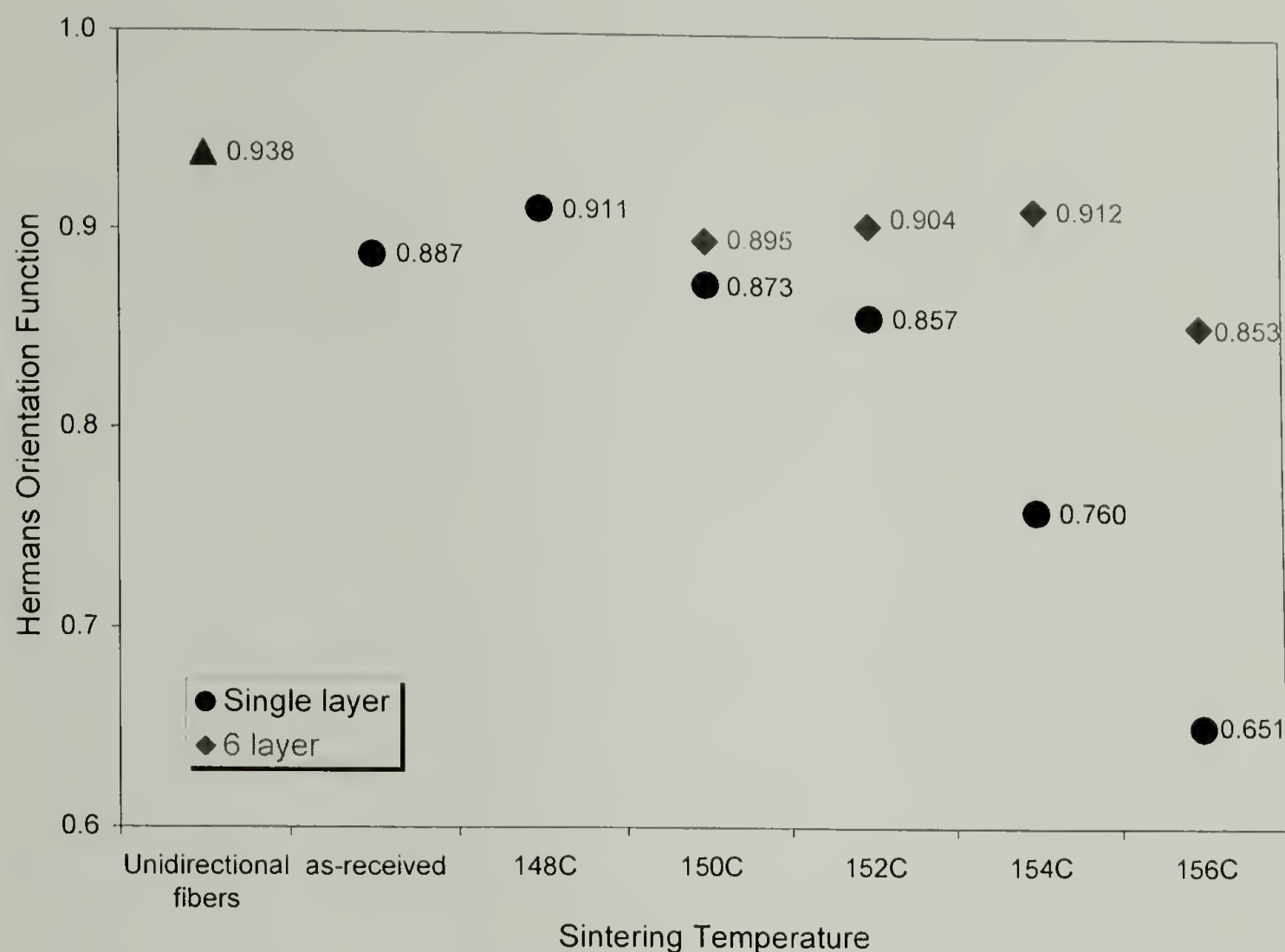


Figure 4.9 Hermans orientation function for single and six layer Spectra<sup>®</sup> cloth sintered under 7.6MPa for 30 minutes at different processing temperatures

#### 4.3.7 Comparison of the surface and center layers

In a multilayer consolidated Spectra<sup>®</sup> cloth panel, the surface layer and the inside layer may be differ due to different thermal histories experienced during heating and cooling cycles. In order to probe the possible difference, the surface and center layers were separated from twelve-layer Spectra<sup>®</sup> cloth panels consolidated at different processing temperatures. The crystallinity and molecular orientation of each layer were determined since these two parameters are the determining factors for other material properties.

DSC trace overlays for the surface layers and for the center layers of panels sintered at different processing temperatures are shown in Figure 4.10 and 4.11,



respectively. The melting enthalpy for each specimen is listed on the figures. The melting and recrystallization increases with increasing sintering temperature, as seen previously for single layer consolidated cloth. The extent of the change in melting and recrystallization is not as dramatic as the single layer consolidated cloth since the twelve-layer samples had the same sintering time as the single layer samples. As more material is involved, less melting happens at the same temperature.

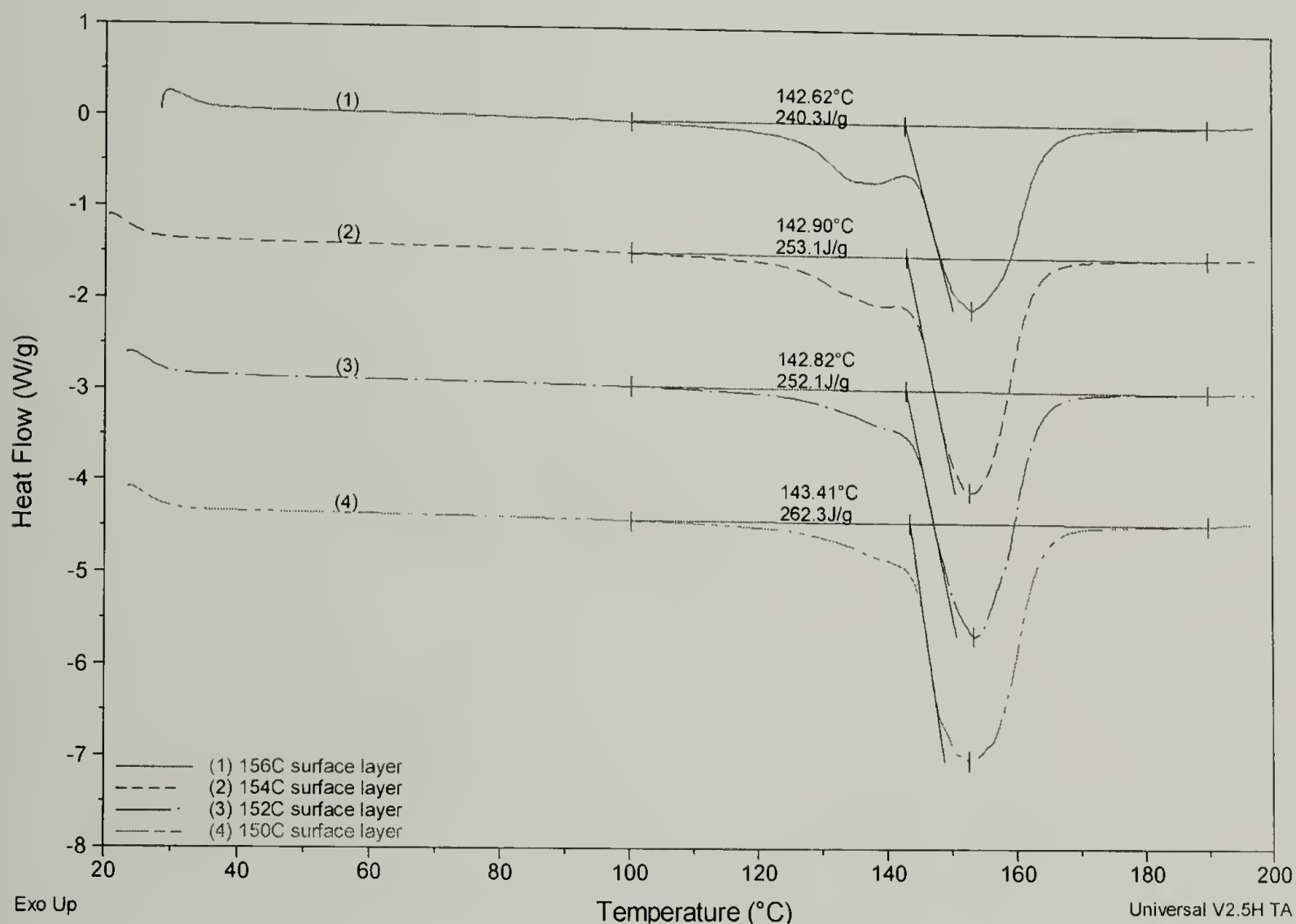


Figure 4.10 DSC trace overlay for the surface layers from twelve-layer Spectra® cloth panels sintered under 17.2MPa for 30 minutes at different processing temperatures

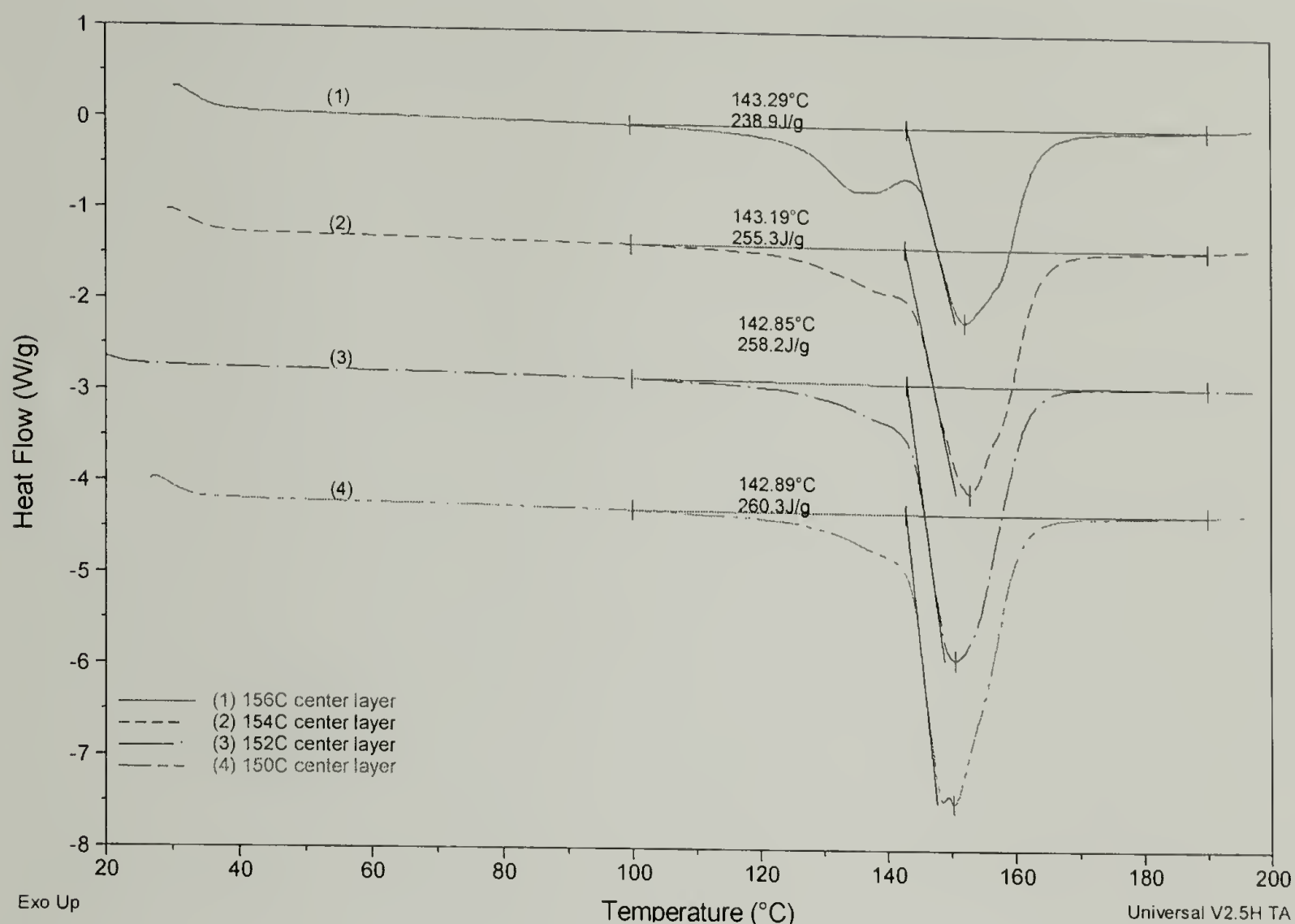


Figure 4.11 DSC trace overlay for the center layers from twelve-layer Spectra<sup>®</sup> cloth panels sintered under 17.2MPa for 30 minutes at different processing temperatures

The overall crystallinity for each surface and center layer was calculated as previously described (Section 3.3.1) in Table 4.4. There is a slight decrease in crystallinity with increasing sintering temperature for both the surface and center layers. At a given sintering temperature, the surface and center layers have approximately the same degree of crystallinity, suggesting that the multilayer cloth reached a uniform temperature throughout the entire sample during the 30 minute sintering time. Heat transfer needs time; although the surface layers were heated first at the beginning of the sintering process, they were also cooled first during quenching. The surface layer and center experienced the true sintering temperature for approximately the same amount of

time. The effects of the sintering time and quenching cancel each other out and result in a similar degree of crystallinity in the surface and center layers.

Table 4.4 Overall crystallinity for the surface and center layers from twelve-layer Spectra<sup>®</sup> cloth panels sintered under 17.2MPa for 30 minutes at different processing temperatures

Specimen	150°C	152°C	154°C	156°C
Surface layer	89.3%	85.9%	86.2%	81.8%
Center layer	88.7%	87.9%	87.0%	81.4%

Hermans orientation function for the surface and center layers was calculated from WAXD (Table 4.5 and Figure 4.12). As sintering temperature increases, both the surface and center layers maintain a constant level of molecular orientation and do not show a large decrease in orientation with increasing processing temperature as the consolidated single layers. Since the molding time was the same for both single layer and multilayer samples, multilayer samples experienced less chain relaxation, less time at the actual processing temperatures, and more efficient constraint, as previously described. The processing pressures were different for the single layer and multilayer samples at 7.6MPa and 17.2MPa, respectively. Greater pressure would provide better constraint and prevent chain randomization. At any given sintering temperature, the surface layer has almost the same orientation as the center layer, in agreement with the DSC results. Since crystallinity and orientation dictate the mechanical properties of Spectra<sup>®</sup> fiber, it may be concluded that multilayer consolidated structures have uniform thermo-mechanical properties throughout their layers when sintered under any given processing conditions.



Table 4.5 Hermans orientation function for the surface and center layers from twelve-layer Spectra<sup>®</sup> cloth panels sintered under 17.2MPa for 30 minutes at different processing temperatures

Specimen	150°C	152°C	154°C	156°C
Surface layer	0.878	0.870	0.868	0.866
Center layer	0.883	0.873	0.871	0.872

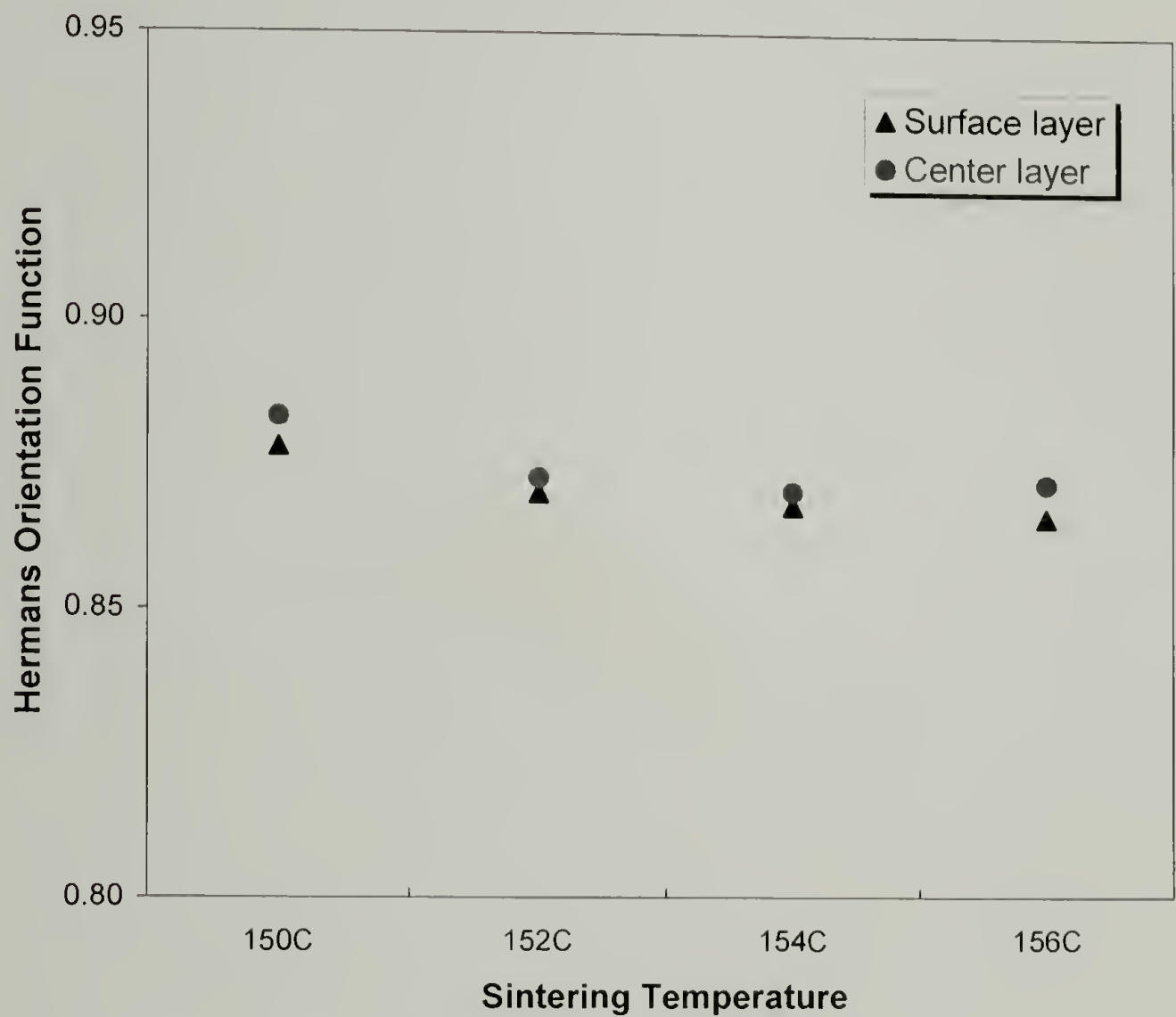


Figure 4.12 Hermans orientation function for the surface and center layers from twelve-layer Spectra<sup>®</sup> cloth panels sintered under 17.2MPa for 30 minutes at different processing temperatures

#### 4.4 Conclusion

The mechanical properties of multilayer consolidated Spectra<sup>®</sup> cloths were studied. Interlayer adhesion increases with increasing sintering temperature although medium adhesion may be sufficient for ballistic application. The multilayer cloth panels are very stiff and strong, and their flexural properties achieve maxima between 152°C – 154°C. The specimens did not fail three-point bend test within 5% strain limit, however samples sintered at low temperature exhibited shear failure at higher strains indicated by delamination, agreeing with results from T-peel tests indicating low interlayer adhesion. Ballistic performance for sintered multilayer thick panels shows that they are as good as the Spectra<sup>®</sup> fiber/matrix system and better than Kevlar<sup>®</sup> system at the same density level. Matrix free Spectra<sup>®</sup> fiber reinforced composites is very promising for making ballistic shields. The microstructure and morphology of multilayer consolidated Spectra<sup>®</sup> cloth was investigated and the cross section of the sintered structures shows good consolidation with few voids. Selective etching of the consolidated structures reveals that more melting and recrystallization, accompanied by chain relaxation leading to less oriented and dense regions, happen significantly at higher processing temperatures. SEM studies also prove that the consolidation occurs by fiber lateral deformation to fill voids and that fiber surface melting and recrystallization fuses the fibers together. Multilayer consolidated Spectra<sup>®</sup> cloth shows very high molecular orientation even after sintering at high processing temperatures due to less relaxation and more efficient constraint. Finally, the surface and center layers of consolidated Spectra<sup>®</sup> cloth have similar crystallinity and orientation at given sintering conditions which suggest that the layers have similar structure and properties. Based on these comprehensive studies, a better

understanding is established regarding the process-structure-property relationship for making matrix free Spectra<sup>®</sup> fiber reinforced composites using this high-temperature high-pressure sintering process.



## CHAPTER 5

### THERMOFORMING OF SPECTRA<sup>®</sup> CLOTH AND THE PROPERTIES OF HEMISPHERICAL DOME STRUCTURES

#### 5.1 Introduction

It was demonstrated that the high-temperature high-pressure sintering process could successfully consolidate plain Spectra<sup>®</sup> woven cloth without using any fiber pre-treatment or additional matrix. The optimal processing conditions were determined and the resulting matrix free composite is a high strength and high impact resistance material. For practical applications this material has to be capable of being formed into shapes having double curvatures. This chapter describes the thermoforming process of Spectra<sup>®</sup> cloth using a simple hemispherical mold. The design features of the mold are discussed and different molding sequences and procedures are illustrated to show the versatility in manufacturing. The theoretical background for the thermoformability is explained in terms of molecular interaction, microstructure, and morphology. Selective thermo-mechanical properties of the molded structures are measured to show that the idea of using Spectra<sup>®</sup> cloth to make ballistic shields is indeed feasible and promising.

#### 5.2 Experimental

##### 5.2.1 Materials

Spectra<sup>®</sup> cloth 903 is made from Spectra<sup>®</sup> fiber 900 and was provided by Honeywell. It is a plain woven cloth with an average thickness of 0.5mm and an areal density of 0.024g/cm<sup>2</sup>. The material was sampled and tested in the as-received state

without any further treatments. Spectra<sup>®</sup> cloth 903 is the material of choice for ballistic protective hard armor.

### 5.2.2 Mold design

A two-piece mold containing a male and female part was created (Figure 5.1) to thermoform objects with double curvatures from Spectra<sup>®</sup> cloth. The male part is a hemispherical punch and female is a hemispherical socket. The two hemispheres have different diameters so that there is a gap when they are closed together. The gap defines the thickness of the products; using different sized punches could vary the dome thickness. An important design feature is the use of a blank holder, a washer shaped plate on top of the female part, which can be fastened onto the female part using 12 bolts. The cloth is placed between the holder and the female part and bolted tightly to create a constraint against fiber shrinkage during heating, and to facilitate stretching of the fibers and cloth during mold closure. The surface of the punch and socket are polished to give the product a smooth finish.

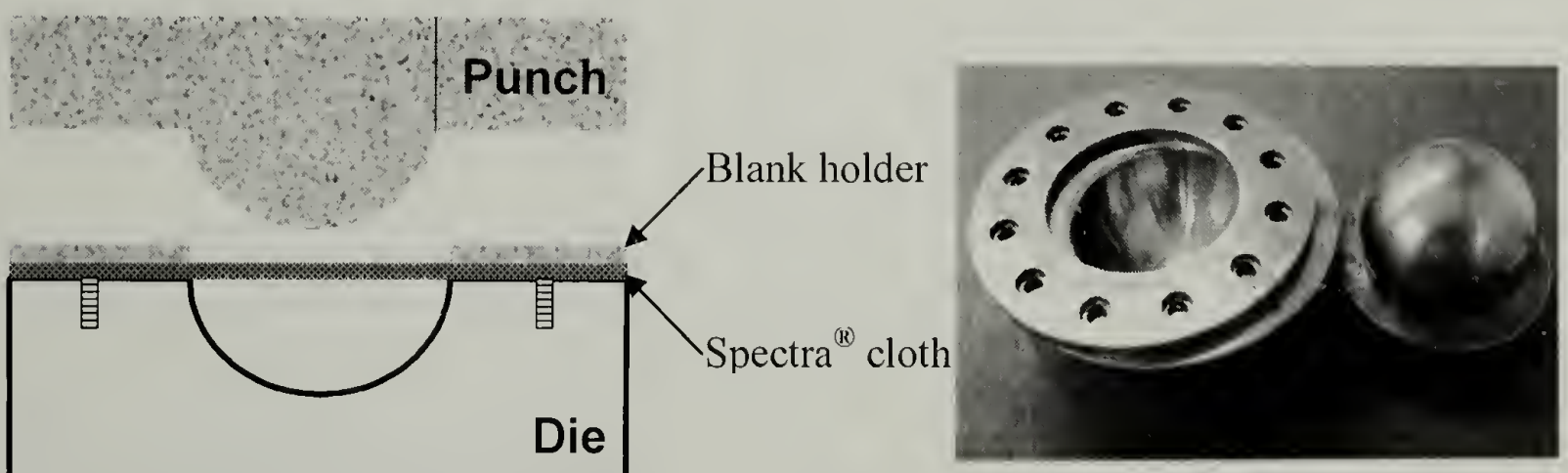


Figure 5.1 The design of the hemispherical mold

### 5.2.3 Molding schemes

Spectra<sup>®</sup> fiber is a thermoplastic polyethylene. An advantage of thermoplastics is their ability to be repeatedly heated, softened, and shaped provided the temperatures are not too high. In the previous sections we have demonstrated that in the optimum processing window, the fiber can be deformed without loss of orientation or crystallinity. Different shaping and molding schemes were proposed and used:

- Consolidate layers of Spectra<sup>®</sup> cloth to a thick flat panel, clamp the panel onto the mold, and apply heat and pressure to develop the shape
- Consolidate each layer of Spectra<sup>®</sup> cloth individually to make flat sheets, lay the consolidated sheets one on top of another and clamp them onto the mold, and apply heat and pressure to shape
- Shape individual layers of Spectra<sup>®</sup> cloth using the mold, stack the shaped layers one on top of another, and sinter them in the mold
- Consolidate and shape layers of Spectra<sup>®</sup> cloth directly in the mold to form the structure

In each approach the total time for the Spectra<sup>®</sup> cloth to experience heat and pressure was 30 minutes. The time for consolidating and/or shaping the cloth in the first stage was combined with the time for molding or sintering in the second stage for the first three methods. There is no need to use any type of mold release agent, since polyethylene is self-lubricating and does not stick to the steel mold.



#### 5.2.4 Typical procedures

A typical sequence is illustrated by the set of pictures using the “flat panel first” router as an example in Figure 5.2. A pre-consolidated flat panel, which consisted of 25 layers of cloth, was drilled and bolted tightly between the blank holder and the socket die. Meanwhile, the press was heated to the desired sintering temperature, for example 150°C. The punch was placed on top of the panel and carefully aligned in the press. A small initial force was applied to secure the position of the mold. Once the mold and the cloth reached the desired sintering temperature (about 10 minutes) the force was gradually increased up to 10 tons over a 5-minute period. The cloth conformed fully to the hemispherical shape of the mold and after 5 minutes was consolidated. The mold assembly was rapidly cooled to ambient temperature, by running tap water through the press’s platens, while maintaining pressure. The hemispherical dome could be easily removed after pressure was released and the blank holder was lifted away.

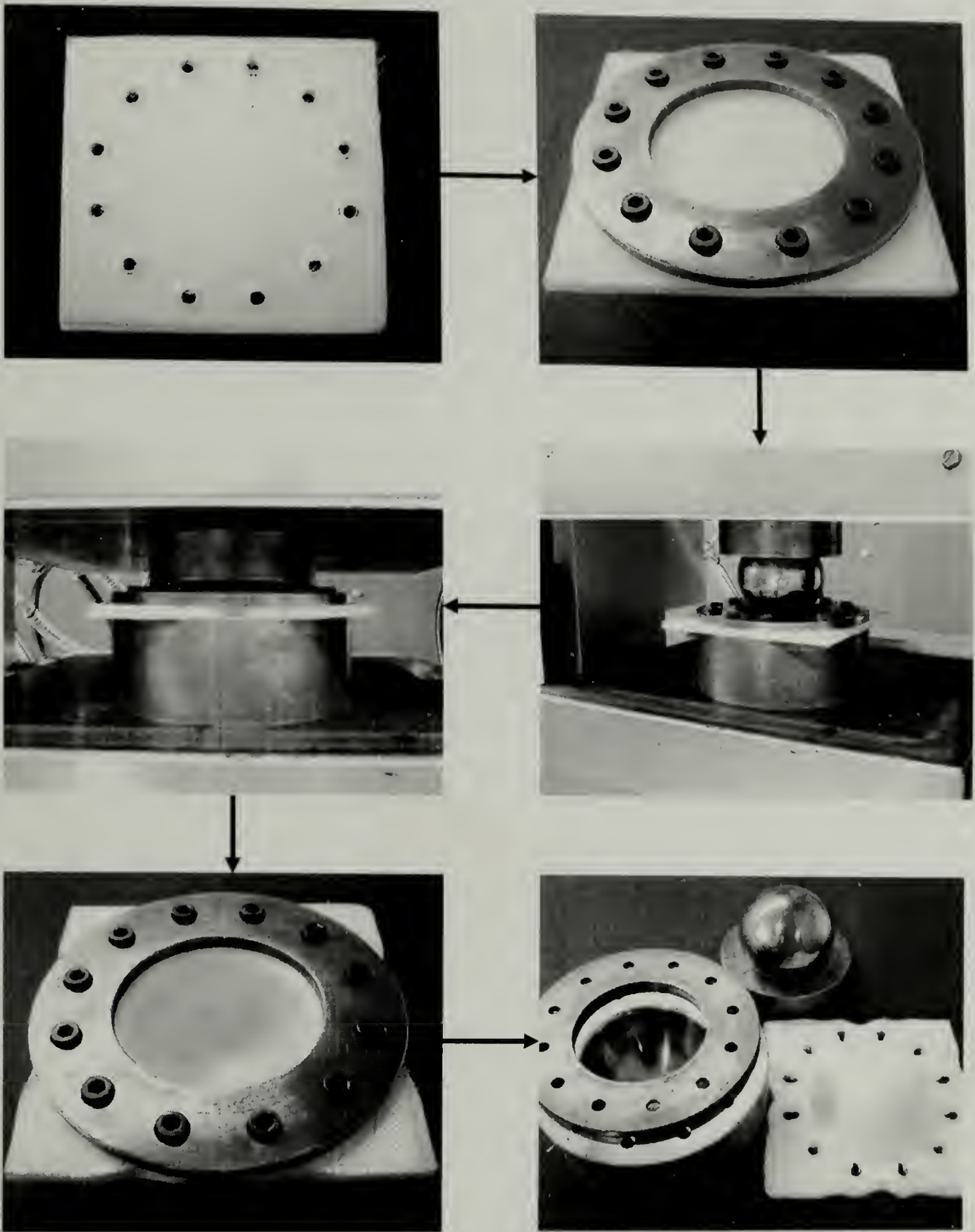


Figure 5.2 Typical molding procedures using a twenty-five layer consolidated Spectra<sup>®</sup> cloth flat panel

### 5.2.5 Property measurements

The typical dimensions of the hemispherical dome were averaged over several domes, which were cut into half using a band saw. To check thermal dimensional stability, the half domes were placed in a preheated oven set to various temperatures for 30 minutes, cooled to room temperature, and the dimensions were measured and compared to the original value. Compressive properties of the domes were evaluated using an Instron 5500R at a crosshead speed of 1mm/min. Since the stretching of the fibers may change their structure and morphology and the draw ratios are different for different positions in the dome, it was thought that the final properties might vary as a function of position. Specimens were sampled from the top and edge of a dome of a shaped and consolidated single layer cloth. Specimens were studied using DSC at a low heating rate in order to decipher possible changes in the crystalline structure; DSC results are used to indicate the effects of shaping on the mechanical properties.

## 5.3 Results and Discussion

### 5.3.1 Thermoformability

Spectra<sup>®</sup> fiber does not stretch significantly at room temperature with only about a 4% strain at break. At elevated temperatures, Spectra<sup>®</sup> fiber is quite “rubbery” and stretchy. Spectra<sup>®</sup> fiber has the unique extended chain morphology with minimum chain folds and entanglements (Figure 3.7). The polymer is chemically nonpolar and there are no strong secondary forces between molecules, and no strong intermolecular interactions. At higher temperatures, when chain mobility increases, the molecules slide past each other relatively easily under a large load. Shown on the macroscopic scale, Spectra<sup>®</sup>



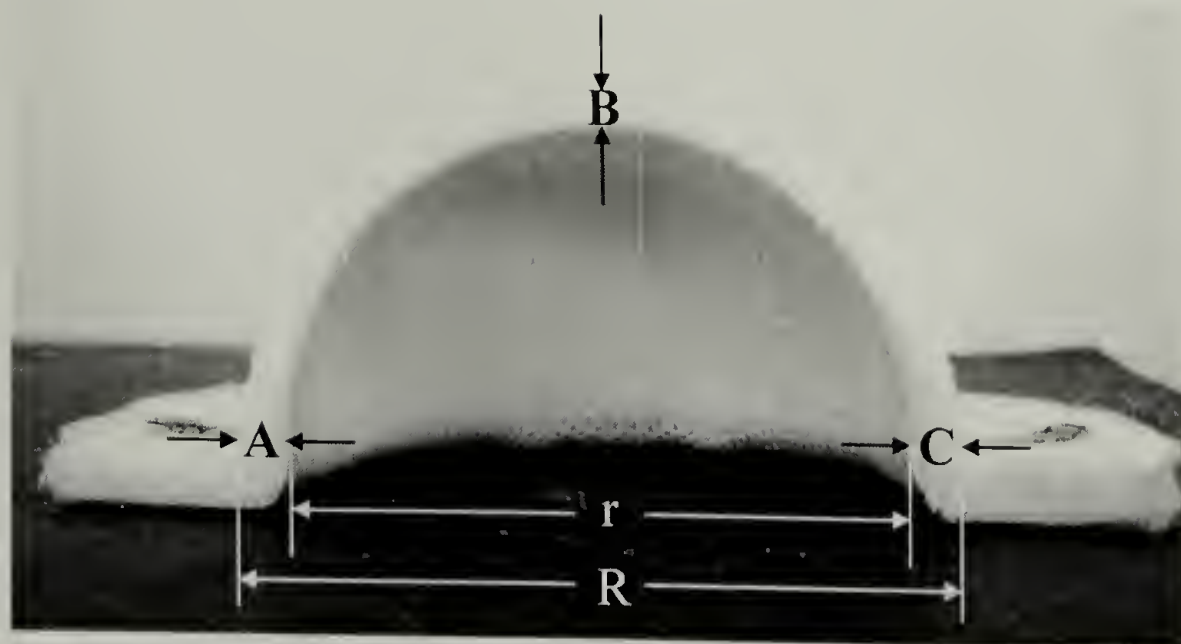
fiber can accommodate high deformation such as those produced in the formation of a hemispherical structure without failing.

Spectra<sup>®</sup> fiber pressurized at an elevated temperature induces a polyethylene crystal transformation, an orthorhombic phase to hexagonal phase transition (o-h transition) as reported by many researchers.<sup>68-70</sup> The pressure and temperature at which the transition occurs depends on the crystal dimension, viz., fold length.<sup>71</sup> Hexagonal crystals possess a relatively low viscosity compared to orthorhombic crystals and chain mobility is rather high in this so-called “mobile phase”. Due to the o-h transition at high pressure and temperature, Spectra<sup>®</sup> fiber is capable of undergoing large axial strains with relative ease via this metastable, transient hexagonal phase.

Due to its excellent thermoformability, all the aforementioned molding schemes work well with Spectra<sup>®</sup> cloth to produce stiff and strong solid domes, indicating the versatility in manufacturing schemes.

### 5.3.2 Dome dimensions and thermal dimensional stability

The dimensions of the domes were measured and a typical set of values measured on different positions of the dome is shown (Figure 5.3). The thickness of the dome is not uniform since the center section of the dome underwent increased stretching. The dome thickness decreases gradually from 4.05mm at the periphery to 2.85mm at the top, roughly 30% reduction. The variation of the thickness is symmetric with respect to the center of the dome. A uniform dome thickness can be achieved by adding compensating layers to the top area during molding.



Outer diameter  $R = 70.7\text{mm}$   
 Inner diameter  $r = 62.6\text{mm}$

Thickness  $A = 4.05\text{mm}$   $C = 4.05\text{mm}$   
 $B = 2.85\text{mm}$

Figure 5.3 Dimension and thickness of the dome

The dome halves were annealed in a precision oven at different temperatures starting from  $150^{\circ}\text{C}$ . At the end of the annealing, their dimensions were checked and the dimensions of the domes did not change much compared with the original dimension values. The domes have good thermal dimensional stability even after annealing at temperatures as high as  $156^{\circ}\text{C}$  and they had become soft. Based on the previous TMA and DSC studies (Section 2.3.3 and 3.3.1, respectively), it was expected that the dome size would change because of the development of a large shrinkage force and the partial melting at higher temperatures. It is possible that the annealing time was not long enough to allow for heat conduction. Relaxation of the molecular chains may require a longer time scale, or the structural stability of the dome geometry and the sufficient interlay adhesion maintain the shape.

### 5.3.3 Compressive properties

Compression tests on shaped hemispherical domes were performed by compressing the dome between two parallel metal plates. As the plates closed, the dome top was flattened, the flat area grew gradually, and at the end of the test the specimen was nearly flat. Dilatation of the dome diameter was not observed. Extensive delamination and buckling occurred in the dome region due to shear and compressive force. As the flattened area increased continuously during the test and the dome is non-uniform in thickness, it is difficult to define mathematically and calculate the stress and strain. The compressive modulus and strength are not available. The dome exhibits a yielding point under compression and the yield load is approximately 1.68kN. The total work done during the test is approximately 16.4J (Figure 5.4); the dome is very strong and rigid. The flattened dome can be re-shaped in the mold to maintain rather high stiffness and the cycle can be repeated.



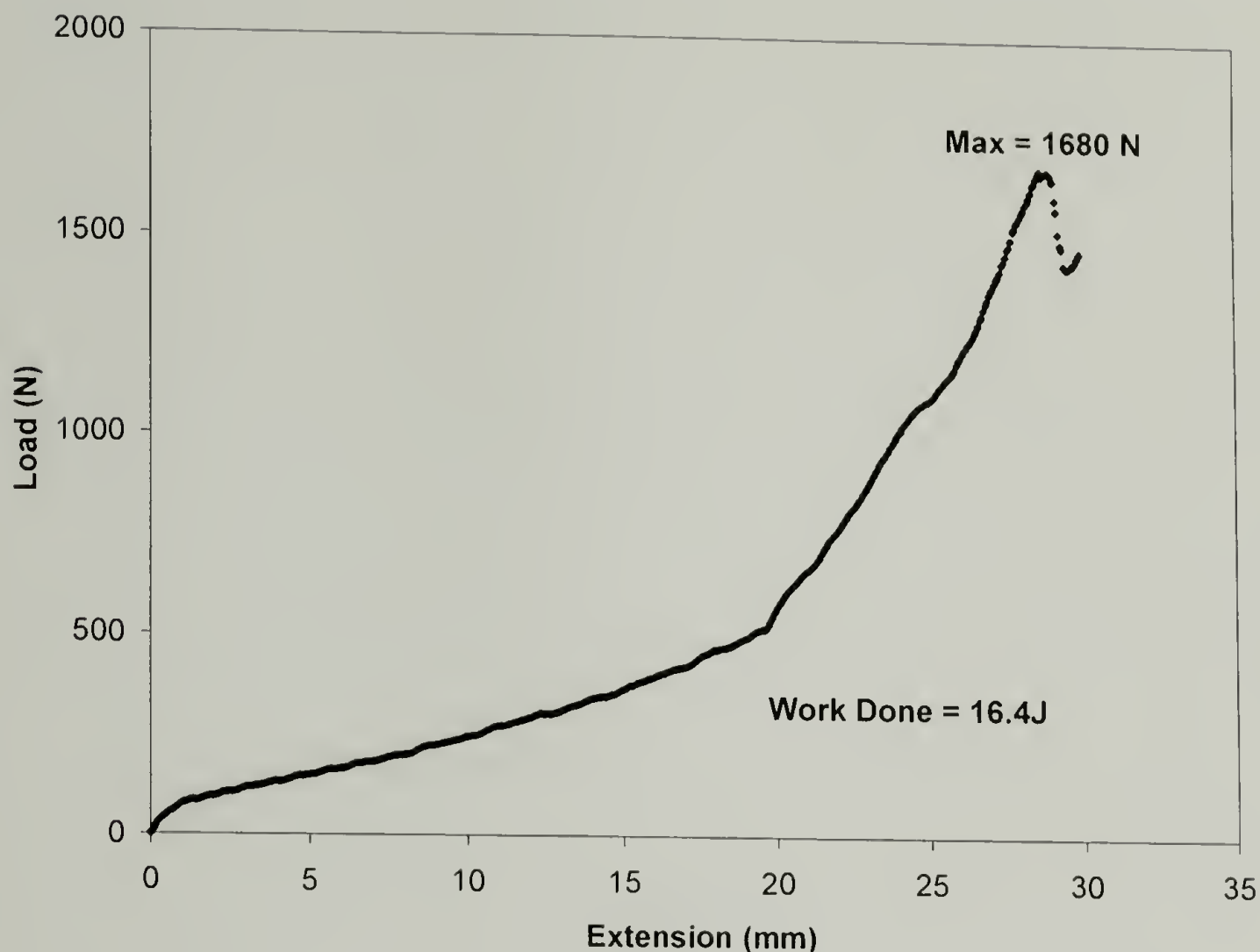


Figure 5.4 Compressive properties of the dome

#### 5.3.4 DSC studies of dome top and edge

DSC trace for the dome top and edge exhibits two melting endotherms for each sample (Figure 5.5). The large endotherm at  $144^{\circ}\text{C}$  corresponds to the melting of the orthorhombic crystals and the shoulder at  $151^{\circ}\text{C}$  is related to the melting of the hexagonal crystals.<sup>58</sup> The hexagonal phase is induced by constrained ultradrawing<sup>58,68</sup> or high pressure annealing<sup>71,72</sup> as described in the literature. Although there is little difference in overall crystallinity, the size of the endotherm at  $151^{\circ}\text{C}$  is clearly different for two samples. The dome edge appears to have more hexagonal crystal phase than the dome top. According to research by Garcia-Leiner<sup>73</sup>, the presence of the hexagonal phase is the result of a crystalline transition of the internally constrained orthorhombic

crystals. Internally constrained orthorhombic crystals are formed between the existing lamellae or as extended single chains via strain induced crystallization under pressure. They tend to transform to the “mobile” hexagonal phase during heating so that the stress can be relaxed. These constrained crystals undergo an o-h transition route during process of melting. It was also found that the development of the constrained crystals destroys the integrity of the original crystals and results in deterioration of the tensile properties. The DSC studies suggest that the mechanical properties of the dome at different positions may differ due to the difference in draw ratio and exerted pressure.

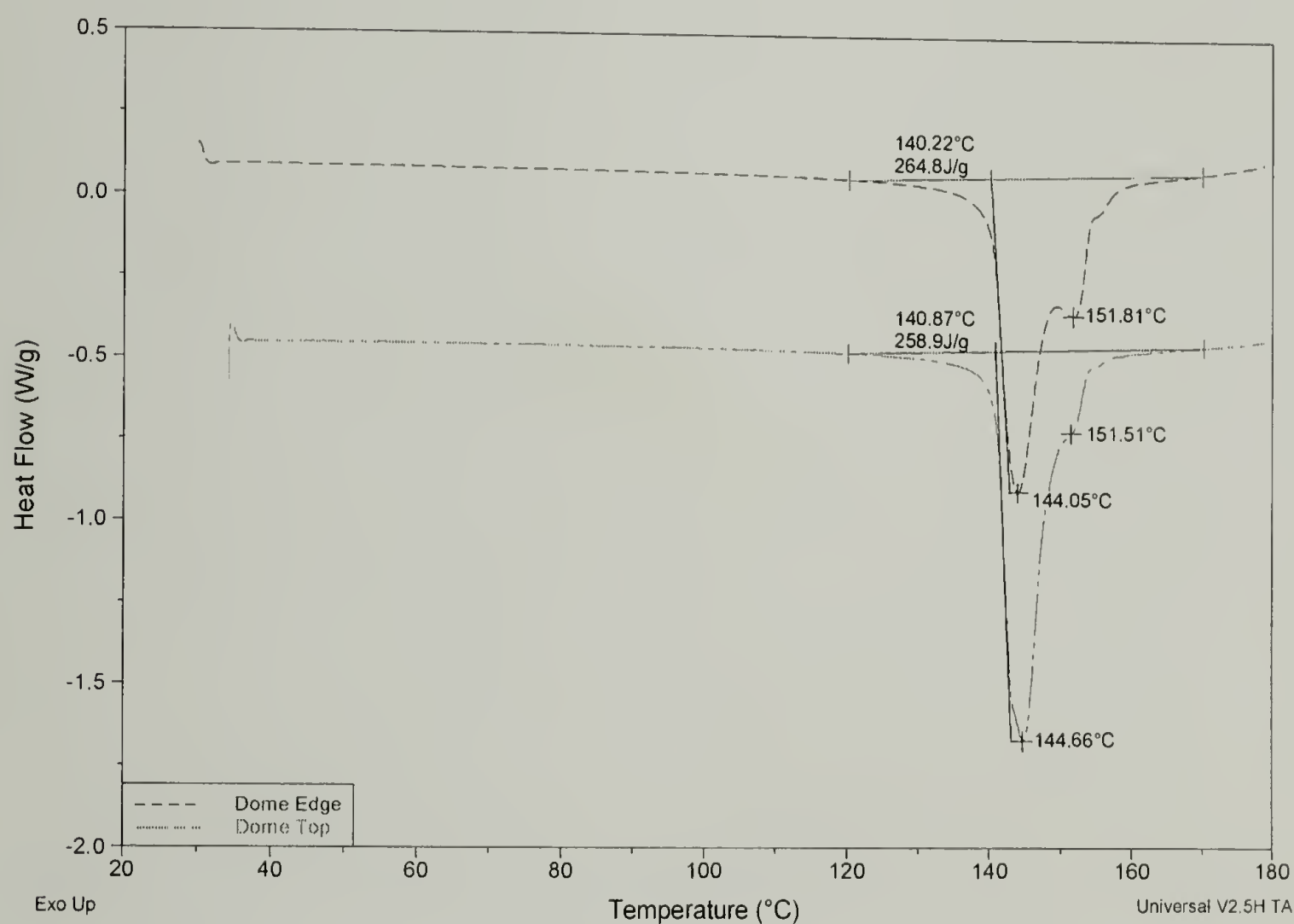


Figure 5.5 DSC trace overlay for samples taken from the top and edge regions of the dome

## 5.4 Conclusion

A two-piece hemispherical mold was designed to thermoform Spectra<sup>®</sup> cloth. Spectra<sup>®</sup> cloth was successfully molded to form a doubly curved structure using different shaping schemes. The exceptional thermoformability of Spectra<sup>®</sup> cloth is due to the unique microstructure and physical properties of the fiber as well as solid state crystal transformations during processing. Ballistic shields using Spectra<sup>®</sup> cloth and no matrix or cutting patterns has been proven to be possible. The dome-like products have non-uniform wall thickness due to different stretching ratios across the structure which can be corrected. The domes have good thermal dimensional stability even at 156°C and compressive properties of the domes are good. DSC studies of the dome reveal the o-h crystalline transition and imply that the mechanical properties of the dome at different positions may vary due to the spatial variation of degree of crystallinity and crystal type throughout the dome.



## CHAPTER 6

### STUDIES ON DYNEEMA FRAGLIGHT<sup>®</sup> NONWOVEN FELT AND SPECTRA SHIELD<sup>®</sup> PLUS PCR PREPREG

#### 6.1 Introduction

Matrix free Spectra<sup>®</sup> fiber reinforced composite made of Spectra<sup>®</sup> cloth 903 via high-temperature high-pressure sintering has been shown to be a promising approach to produce materials for ballistic shields. Various properties of the consolidated structures were analyzed and characterized and the optimal processing conditions were determined through the investigation of process-structure-property relationship. To complete the study, Dyneema Fraglight<sup>®</sup> nonwoven felt and Spectra Shield<sup>®</sup> Plus PCR<sup>74</sup> prepreg, commercially available materials designed specifically for ballistic applications, were chosen for parallel comparisons. The high-temperature high-pressure sintering process was applied, and the physical, thermo-mechanical and microstructural properties of the consolidated products were determined and compared to those of the sintered Spectra<sup>®</sup> cloth 903. It is concluded that matrix free Spectra<sup>®</sup> fiber reinforced composite has dominant advantages over the other two materials.

#### 6.2 Experimental

##### 6.2.1 Materials

Dyneema Fraglight<sup>®</sup>, a needle punched nonwoven felt with an areal density of 190 - 220g/m<sup>2</sup>, is made from Dyneema<sup>®</sup> fiber and designed for protection against fragments of exploding bombs and artillery shells. Dyneema<sup>®</sup> fiber is an UHMWPE fiber commercialized by DSM with similar properties to Spectra<sup>®</sup> fiber.

Spectra Shield<sup>®</sup> Plus PCR is a non-woven thermoplastic composite consisting of two plies of unidirectional Spectra<sup>®</sup> fiber tapes cross-plyed at 0°/90° and impregnated in a matrix. Spectra Shield<sup>®</sup> Plus PCR is made by Honeywell and is used in applications such as rigid armor and breast plates, vehicle and architectural armor, blast containment and shields. Its areal density is  $95\pm15\text{g/m}^2$  and thickness is  $0.13\pm0.05\text{mm}$ . The fiber weight fraction of Spectra Shield<sup>®</sup> Plus PCR is approximately 80%. The matrix is an undisclosed proprietary material.

## 6.2.2 Material processing and property measurements

### 6.2.2.1 Processing procedure

A single layer of felt or prepreg was sandwiched within aluminum foils and placed in between two steel plates. The hot press was preheated to a desired processing temperature, the temperature was allowed to equilibrate, and the sandwiched felt or prepreg was placed in the hot press. The upper and lower platens of the press were closed onto the specimen and the pressure was raised to the desired processing pressure. The pressure and temperature were held constant for a period of processing time to execute the sintering process. The hot press and the specimen were quenched by running tap water through the press platens while pressure was maintained. The sintered specimen was removed from the press at ambient temperature and separated from the aluminum foil; no mold release agent was used.

#### 6.2.2.2 Measurement of crystallinity changes by DSC

A TA Instrument DSC 2910 was used to observe the melting behavior of single layers felt or prepreg consolidated under various processing conditions. ~10 mg of the samples in hermetically sealed pans were heated at 10°C/min from room temperature to 200°C under nitrogen (50 ml/min.).

#### 6.2.2.3 Measurement of orientation changes by WAXD

Wide Angle X-ray Diffraction (WAXD) patterns were collected using pin hole collimated, monochromatic Cu K $\alpha$  radiation and a Bruker<sup>®</sup> “High Star” two dimensional detector. The diffraction patterns of a series of single layer Spectra Shield<sup>®</sup> Plus PCR sintered under different processing conditions were collected. The specimen was oriented “flat-on” so that the incident X-ray beam was perpendicular to the prepreg. A radiation time of 300 seconds was used and diffraction patterns were captured digitally. The integration of the intensity was preformed using GADDS commercial software.

#### 6.2.2.4 Measurement of impact properties by puncture test

Impact tests were performed using a dynatup<sup>®</sup> 8250 with the pneumatically powered shooting dart mode of puncture test since the consolidated felt or prepreg are rather strong. The dart weighs 2.38kg and is pneumatically assisted by house nitrogen. The dart speed at penetration into the specimen was approximately 10 m/s. The specimens were 100mm  $\times$  150mm consolidated single layer felt or prepreg sheets which had experienced different processing conditions. Each specimen was secured on the sample stage by pneumatic clamps, the dart was then fired perpendicular to the surface of



the specimen, and the specimen was punctured. The instrument recorded the load detected on the dart tip and the deflection of the specimen as soon as the shooting dart touched the specimen until total penetration. The total energy of impact was calculated from the integrated area under the load vs. deflection curve.

#### 6.2.2.5 Measurement of interlayer adhesion by T-peel test

Thermally bonded bilayers were prepared from two layers of Dyneema<sup>®</sup> felt, two layers of Spectra<sup>®</sup> prepreg, and one layer of Spectra<sup>®</sup> cloth and one layer of Dyneema<sup>®</sup> felt for T-peel tests. A series of bilayers were produced at different processing temperatures under constant pressure and time (7.6MPa and 30 minutes) and the T-peel tests were conducted on an Instron 5500R according to ASTM standard D1876 as described previously, Section 4.2.3.

#### 6.2.2.6 Measurement of flexural properties by three-point bend test

The flexural properties of multilayer consolidated Dyneema<sup>®</sup> felt and consolidated Spectra<sup>®</sup> prepreg sintered under different processing conditions were determined by three-point bend tests according to ASTM standard D790 with a support span of 50mm and a crosshead speed of 1.35mm/min, as described previously, Section 4.2.4. A testing limit of 5% strain was used to ensure the reliability of the data.

#### 6.2.3 Thermoforming of Dyneema Fraglight<sup>®</sup> and Spectra Shield<sup>®</sup> Plus PCR

Thermoforming of Dyneema Fraglight<sup>®</sup> and Spectra Shield<sup>®</sup> Plus PCR to make hemispherical domes was done by first making 250mm × 250mm multilayer flat panels at

150°C under 6.9MPa for 30 minutes. The resulting flat panels were cut into four 125mm × 125mm squares, twelve holes were then drilled into the panels, and they were bolted onto the hemispherical mold. The molding procedures and conditions were followed as described previously, Section 5.2.4.

## 6.3 Results and Discussion

### 6.3.1 Dyneema Fraglight<sup>®</sup> nonwoven felt

Dyneema Fraglight<sup>®</sup> felt is made of continuous Dyneema<sup>®</sup> fiber which has comparable mechanical properties to Spectra<sup>®</sup> fiber. Dyneema Fraglight<sup>®</sup> is a nonwoven felt and the fibers are unoriented and randomly aligned. It is an in-plane isotropic material and therefore it is expected that the consolidated structures of this material would have a lower rigidity and stiffness than the more oriented consolidated Spectra<sup>®</sup> cloth. The needle punching process, used to manufacture the felt, has introduced physical entanglements of the fibers. Good impact resistance is expected for the consolidated materials as these entanglements should make penetration difficult. Good interlayer adhesion is anticipated since the entanglements would hinder the separation of bonded layers. Studies on Dyneema Fraglight<sup>®</sup> felt were carried out by monitoring the crystallinity change with processing, measuring the impact properties, interlayer adhesion and flexural properties of the consolidated products and investigating the thermoformability of the felt.

#### 6.3.1.1 Crystallinity change

A single layer of Dyneema<sup>®</sup> felt was consolidated at a processing temperature ranging from 140°C to 156°C under a pressure of 7.6MPa for 30 minutes. DSC thermographs for the as-received Dyneema<sup>®</sup> felt and the consolidated felts are overlaid in Figure 6.1. As-received Dyneema<sup>®</sup> felt shows a distinct melting peak at 150°C as does Spectra<sup>®</sup> cloth. With increasing processing temperature, a lower temperature shoulder on the melting peak emerges and eventually evolves into a distinct peak at 135°C. The two endotherms correspond to the melting of the original highly oriented crystals and the newly formed crystals formed upon cooling, respectively. With increasing sintering temperature, the higher temperature endotherm decreases and the lower temperature endotherm increases, indicating the gradual loss of the original highly oriented crystals accompanied by the gradual formation of unoriented crystals.





Table 6.1 Overall crystallinity of single layer as-received and consolidated Dyneema<sup>®</sup> felt sintered under 7.6MPa for 30 minutes at different processing temperatures

Specimen	as-rec'd	140°C	145°C	148°C	150°C	152°C	154°C	156°C
Enthalpy (J/g)	271.2	273.8	275.0	270.9	266.0	240.9	220.4	131.5
Crystallinity	92.4%	93.3%	93.7%	92.3%	90.6%	82.1%	75.1%	44.8%

The melting enthalpy of the two types of crystals was calculated by deconvoluting the two overlapping melting endotherms and integrating the area under each curve; the amount of retained original crystals was determined (Table 6.2). The quantity of original crystals remains at approximately the same percentage as processing temperature is increased to 150°C and then decreases quickly as the temperature is further increased (Figure 6.2). High crystallinity needs to be preserved to assure the properties of the consolidated Dyneema<sup>®</sup> felt, so the suggested processing temperature should not exceed 150°C.

Table 6.2 Changes in crystallinity corresponding to the original crystals for single layer consolidated Dyneema<sup>®</sup> felt sintered under 7.6MPa for 30 minutes at different processing temperatures

Specimen	140°C	145°C	148°C	150°C	152°C	154°C	156°C
Retained	92.1%	91.6%	90.7%	88.1%	68.7%	57.2%	5.4%
Melted	7.9%	8.4%	9.3%	11.9%	31.3%	42.8%	94.6%

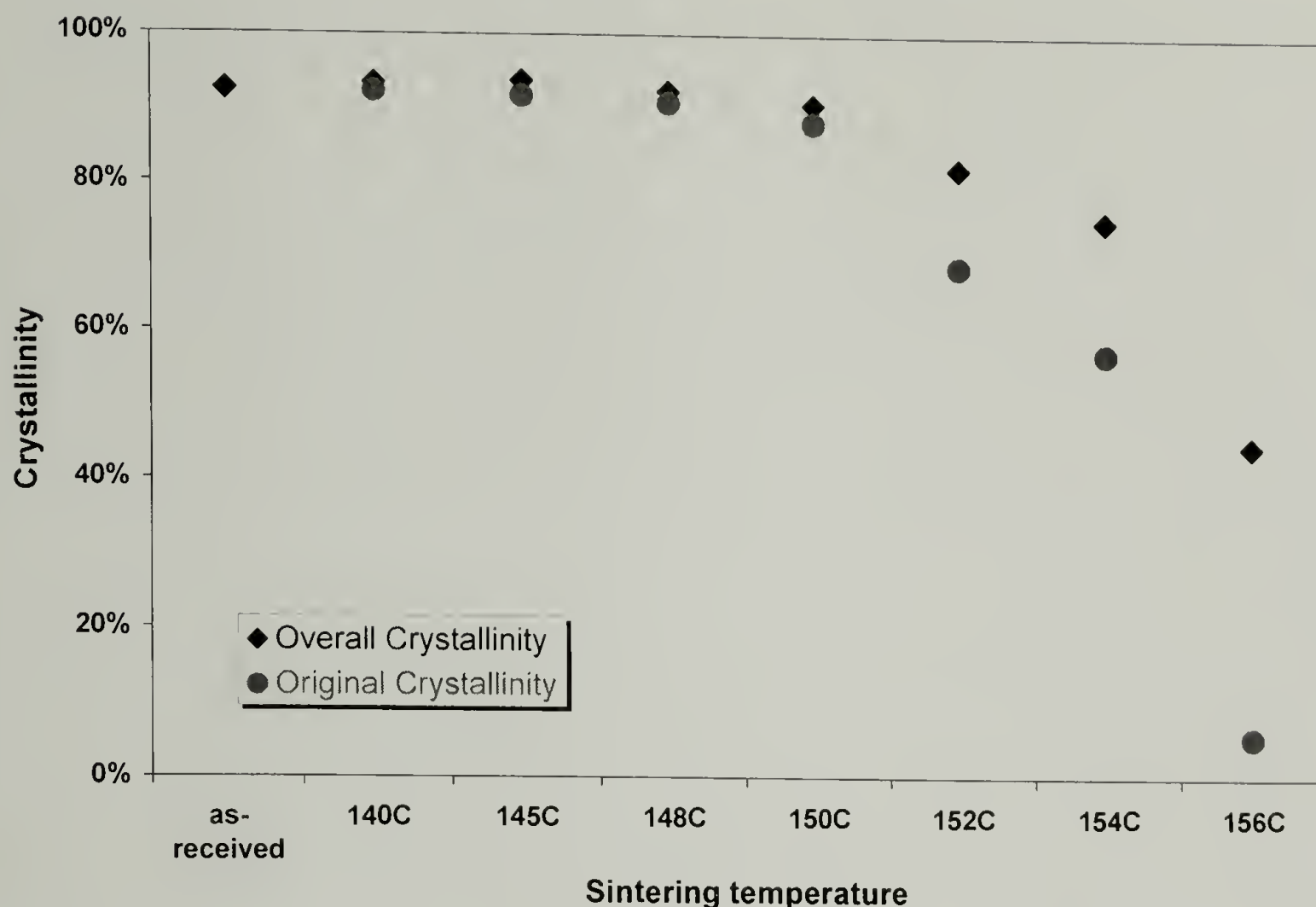


Figure 6.2 Changes in overall crystallinity and crystallinity from the original crystals for single layer as-received and consolidated Dyneema<sup>®</sup> felt sintered under 7.6MPa for 30 minutes at different processing temperatures

### 6.3.1.2 Impact properties

The impact resistance of single layer of Dyneema<sup>®</sup> felt consolidated under 7.6MPa for 30 minutes at different temperatures was measured and compared to that of the as-received felt; the NTT total impact energies are shown in Figure 6.3. As-received felt has good impact resistance due to the physical entanglements of its fibers which makes it difficult for the shooting dart to penetrate. Dyneema<sup>®</sup> felt consolidated at 148°C exhibits the best impact properties with a nearly 30% increase over the original felt. At sintering temperatures below 148°C, the impact resistance is hardly improved. At sintering temperatures above 148°C, the impact properties decrease rapidly due to



excessive melting. Up to 150°C the test specimens failed by pulling fibers out of the felt without visible signs of fiber breakage and above 150°C the specimens fractured and the fibers were broken. The best processing temperature to achieve the maximum impact properties of the felt is approximately 148°C.

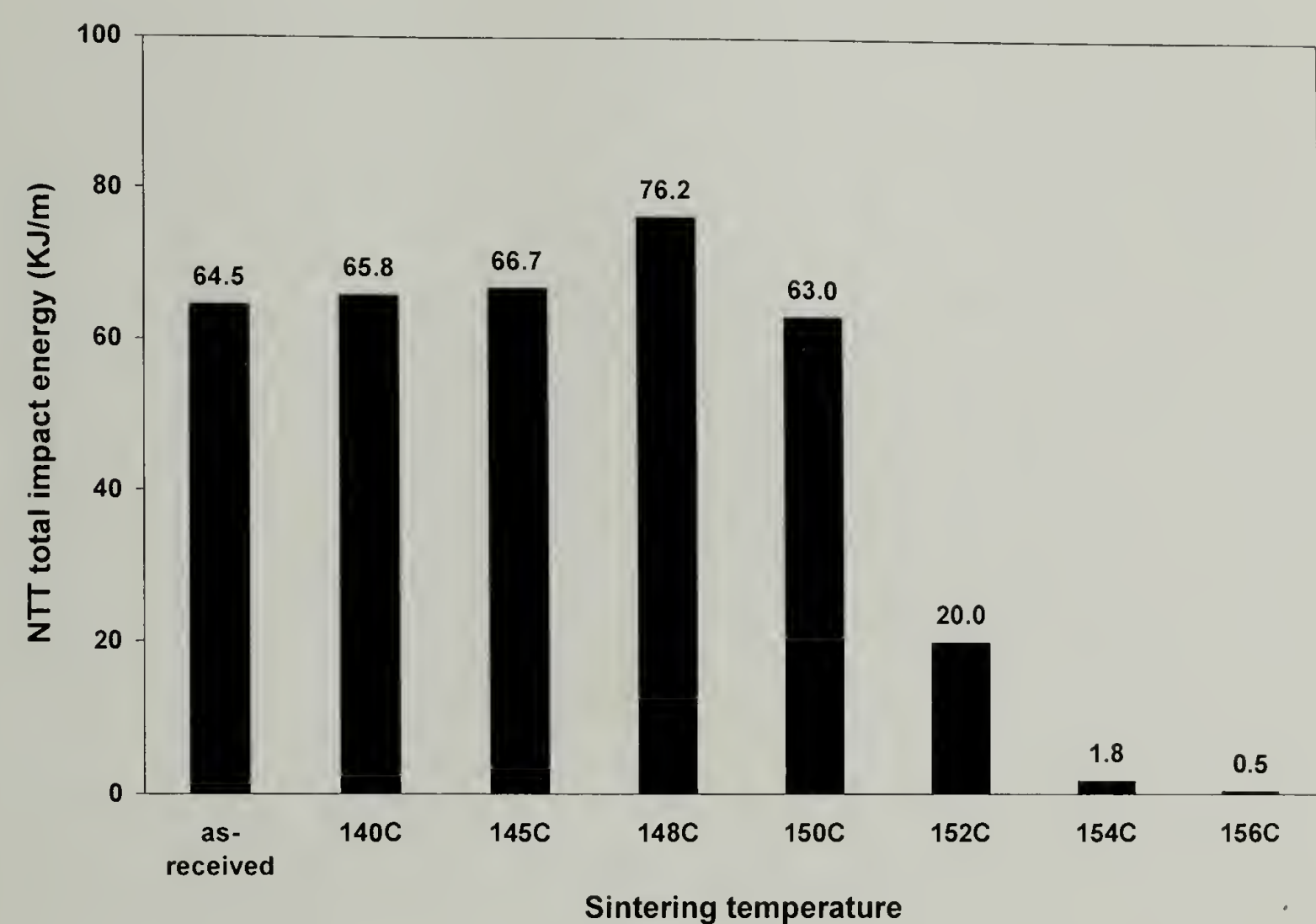


Figure 6.3 NTT total impact energy (KJ/m) of the as-received Dyneema<sup>®</sup> felt and single layer consolidated Dyneema<sup>®</sup> felt sintered under 7.6MPa for 30 minutes at different processing temperatures

6.3.1.3 Interlayer adhesion

Interlayer adhesion for Dyneema<sup>®</sup> felt sintered at different temperatures was determined by measuring the peeling load needed to separate bonded bilayers. T-peel strengths for samples bonded at 148°C, 150°C, 152°C and 154°C are shown in Figure

6.4. Dyneema<sup>®</sup> bilayers sintered at or above 156°C are completely fused and can not be separated without breaking the specimens. Interlayer adhesion increases with increasing sintering temperature, especially above 150°C, since more melting occurs at higher temperatures and more recrystallized material acts as binder.

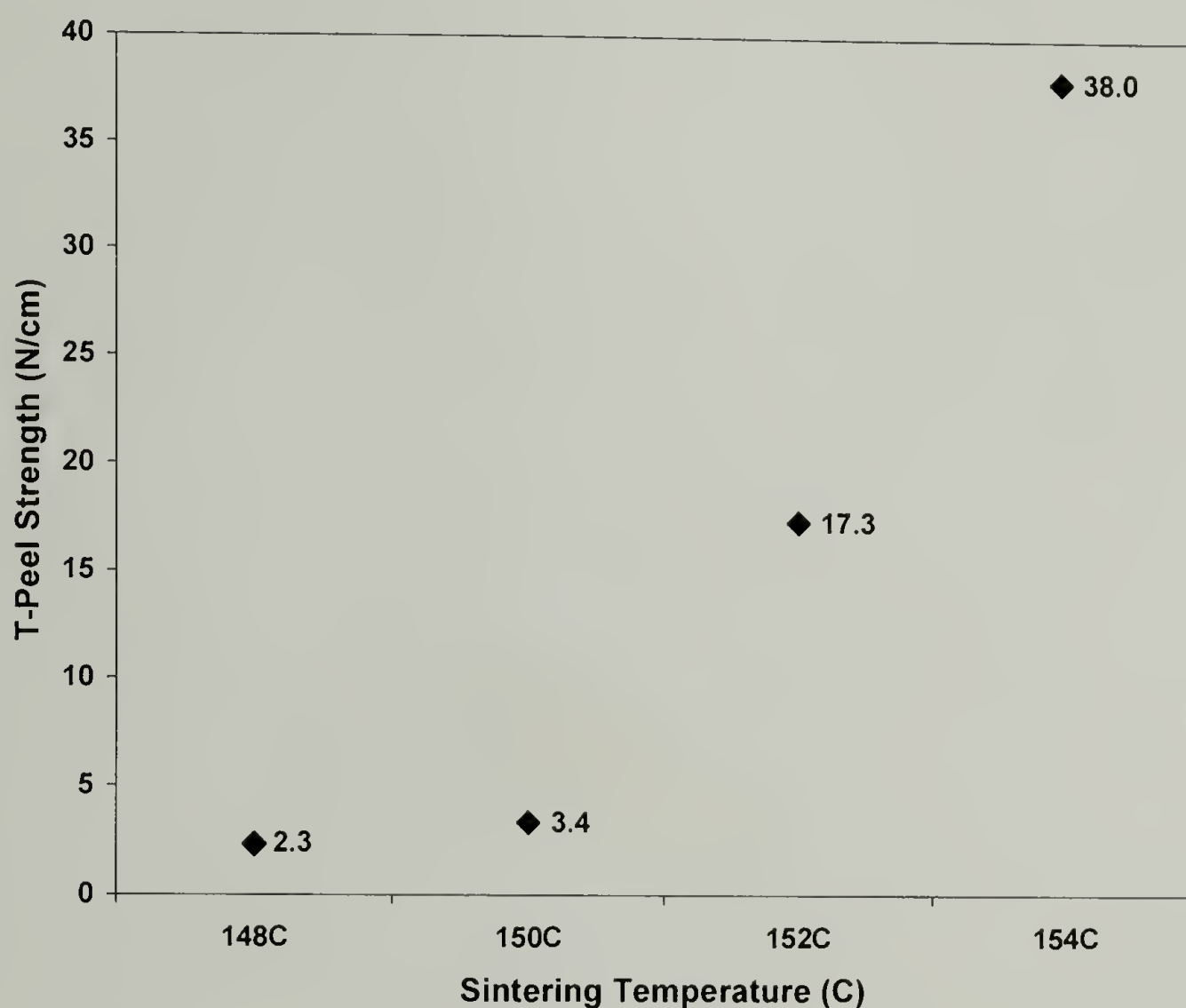


Figure 6.4 T-peel strength for Dyneema<sup>®</sup>-Dyneema<sup>®</sup> bilayers sintered under 7.6MPa for 30 minutes at different temperatures

#### 6.3.1.4 Flexural properties

Flexural properties of Dyneema<sup>®</sup> felt consolidated in 4 layer panels at different processing temperatures were measured by three-point bend tests (Figure 6.5).

Consolidated Dyneema<sup>®</sup> felt has relatively low flexural modulus due to random fiber alignment. No specimens showed any failure or yield within the 5% strain limit set by

ASTM standard. Panels sintered at 145°C have the highest rigidity. The lower temperature sintered felts were not sufficiently consolidated and interlayer adhesion is low. At higher sintering temperatures the felts melted excessively and fiber rigidity is lost. The existence of the optimal sintering temperature regarding flexural properties illustrates the importance of the balance between the lost longitudinal strength and the gained lateral strength.

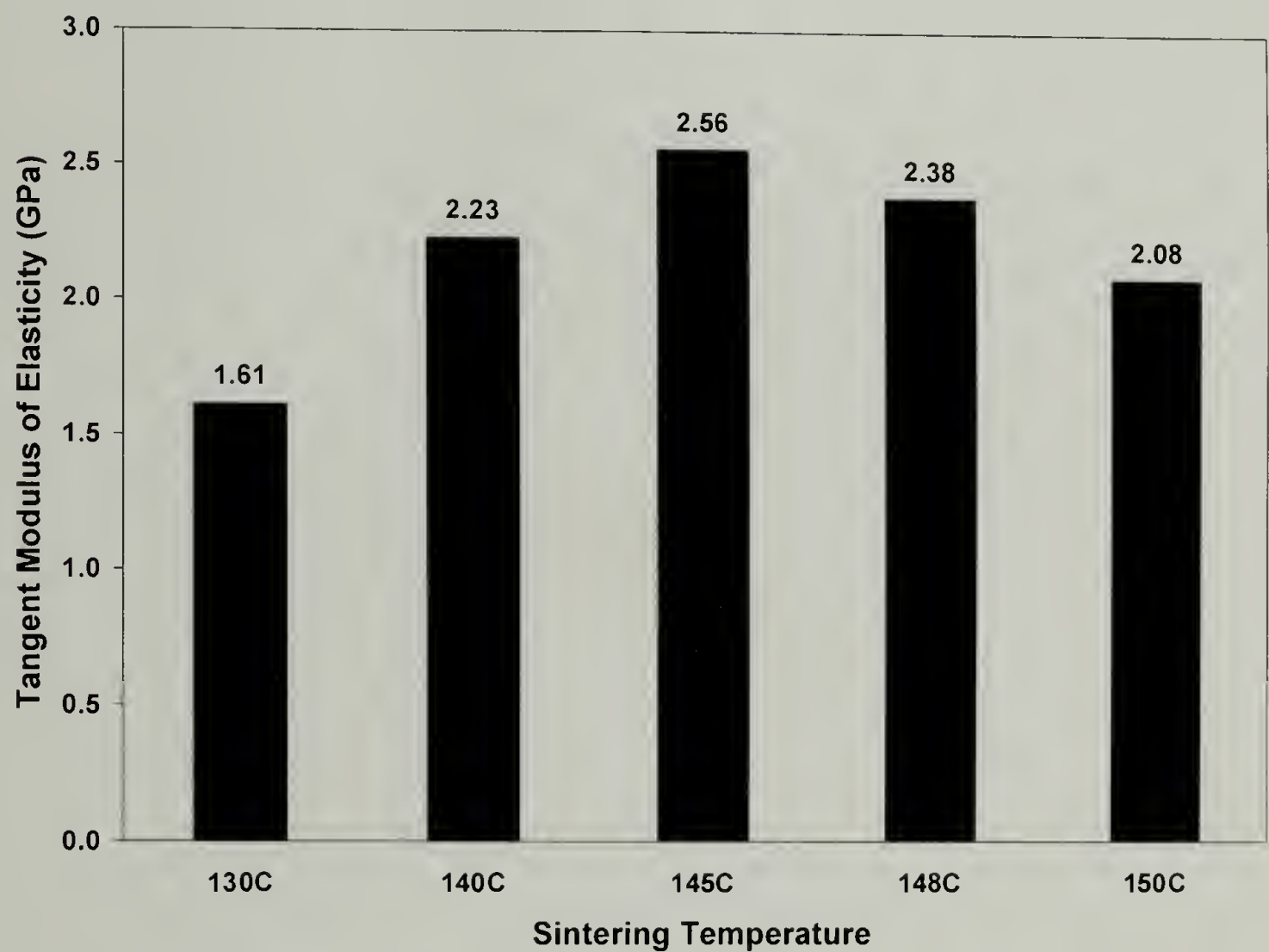


Figure 6.5 Flexural modulus of 14 layers Dyneema<sup>®</sup> felt panels consolidated under 17.2MPa for 30 minutes at different temperatures

6.3.1.5 Thermoformability

Multilayer Dyneema<sup>®</sup> felt can be molded to hemispherical domes using the same procedure as described for Spectra<sup>®</sup> cloth. Due to its simplicity, the consolidated flat

panel was prepared and then shaped, although other shaping schemes would also have worked. Due to the thickness of the felt, 20 layers of Dyneema<sup>®</sup> felt were used to produce a dome having dimensions similar to that of 25 layers of Spectra<sup>®</sup> cloth. Domes made from Dyneema<sup>®</sup> felt are strong and stiff. Looseness of the fibers in the felt resulted in the straightening of the previously curled fibers rather than the actual stretching of the fibers by the deformation of the felt in the mold. As a result, a relatively smaller force was used for molding as compared to the Spectra<sup>®</sup> cloth. Dyneema<sup>®</sup> felt has good thermoformability.

### 6.3.2 Spectra Shield<sup>®</sup> Plus PCR prepreg

Spectra Shield<sup>®</sup> Plus PCR is a nonwoven prepreg which contains two chemically different materials: Spectra<sup>®</sup> fiber and matrix. The matrix is used as a binding agent and good interfiber and interlayer adhesion is expected. In each layer of prepreg, either in the 0° or 90° direction, the fibers are aligned relative to each other. The ordered fiber alignment should be reflected in a high Hermans orientation function parameter. The unidirectional fiber alignment can also contribute positively to the impact resistance and flexural properties. However the soft matrix would contribute negatively to the impact and flexural properties. The net outcomes are difficult to predict and have to be carefully studied.

#### 6.3.2.1 Crystallinity change

A single layer of Spectra Shield<sup>®</sup> Plus PCR prepreps was consolidated under 7.6MPa for 30 minutes at various processing temperatures. The DSC thermographs are



overlaid in Figure 6.6 along with that of the as-received prepreg. The matrix appears to have no thermal transition within the range of testing temperatures. Prepregs sintered at temperatures up to 150°C have a melting endotherm at approximately 150°C with a shoulder at 135°C. Prepregs sintered above 150°C have two distinct melting endotherms at 135°C and at 150°C. The peak at 150°C corresponds to melting of the original oriented crystals and the peak at 135°C corresponds to the melting of recrystallized less oriented crystal phase. The trace for the as-received prepreg contains a shoulder on the melting peak, suggesting that the original material might have experienced a high temperature treatment previously in the manufacturing process.

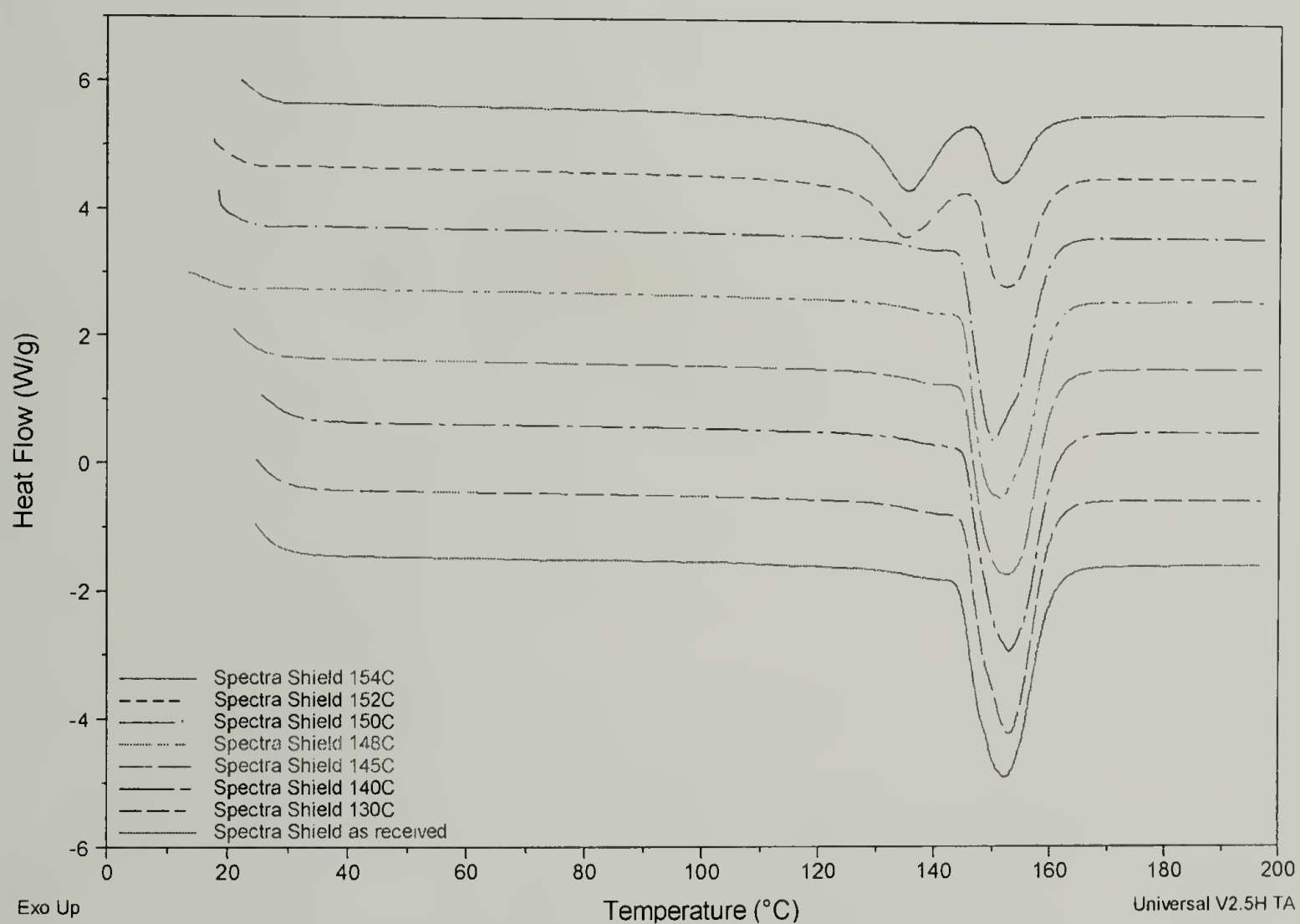


Figure 6.6 DSC trace overlay of the as-received Spectra Shield<sup>®</sup> Plus PCR and single layer Spectra Shield<sup>®</sup> Plus PCR consolidated under 7.6MPa for 30 minutes at different processing temperatures

The overall crystallinity and the retained original crystallinity were calculated as a function of processing temperature (Table 6.3 and Figure 6.7) and normalized with respect to the fiber weight fraction (80%). The starting material has a lower overall crystallinity than the Spectra<sup>®</sup> cloth due to manufacturing. The consolidated sheets maintain relatively constant crystallinity up to 148°C. Overall crystallinity decreases with increasing temperature above 148°C. Some of the consolidated prepregs have higher crystallinity than the as-received material due to the effect of pressure induced crystallization. The retained original crystallinity decreases with increasing processing temperature after 148°C. Above 150°C, the difference between the overall crystallinity and the original crystallinity becomes significant, indicating that a large amount of the original crystals were melted and the calculated overall crystallinity contains a great deal of newly formed crystals which are unoriented and imply lower properties for the materials sintered at these temperatures. At the same sintering temperature, consolidated Spectra<sup>®</sup> cloth has higher crystallinity than consolidated Spectra Shield<sup>®</sup> Plus PCR and better properties. Spectra Shield<sup>®</sup> Plus PCR has a much broader processing temperature window than Spectra<sup>®</sup> cloth within which the original crystallinity level is preserved, which could be a processing advantage.

Table 6.3 Overall crystallinity and retained original crystallinity for the as-received Spectra Shield<sup>®</sup> Plus PCR and single layer Spectra Shield<sup>®</sup> Plus PCR consolidated under 7.6MPa for 30 minutes at different temperatures

Specimen	as-received	130°C	140°C	145°C	148°C	150°C	152°C	154°C
Overall crystallinity	90.3%	93.9%	92.8%	92.0%	90.7%	85.9%	80.8%	70.0%
Original crystallinity	89.6%	90.9%	90.5%	88.1%	87.9%	83.5%	49.2%	27.9%

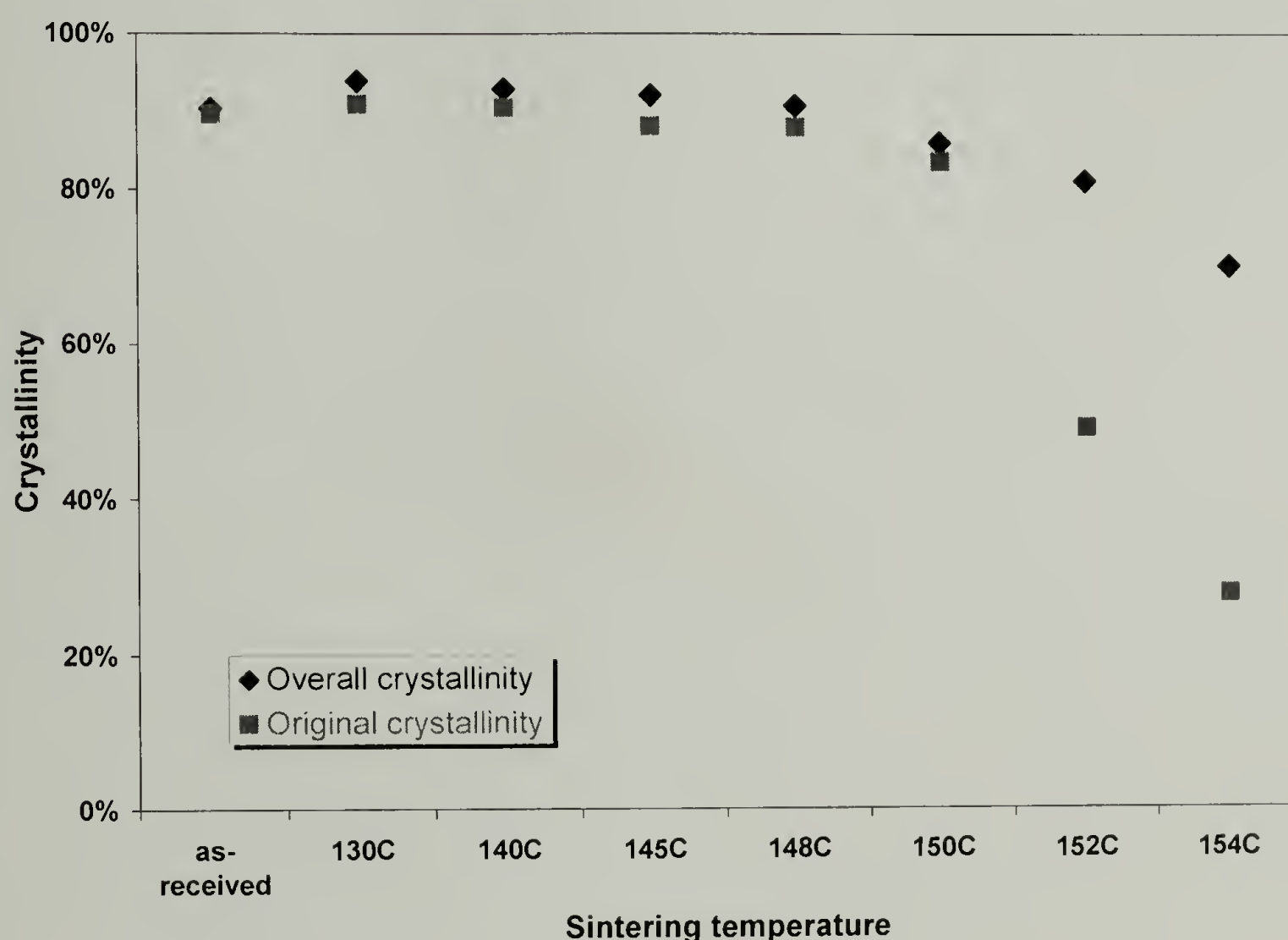


Figure 6.7 Overall and original crystallinity of the as-received Spectra Shield<sup>®</sup> Plus PCR and single layer Spectra Shield<sup>®</sup> Plus PCR consolidated under 7.6MPa for 30 minutes at different processing temperatures

### 6.3.2.2 Orientation change

The molecular orientation of the original and consolidated single layer Spectra Shield<sup>®</sup> Plus PCR was examined using WAXD. The calculated Hermans orientation function is shown in Figure 6.8 as a function of processing temperature. As fibers in the prepreg are unidirectionally aligned, one would imagine that Spectra Shield<sup>®</sup> Plus PCR would have had higher Hermans orientation function than that of Spectra<sup>®</sup> woven cloth due to the lack of fiber waviness in Spectra Shield<sup>®</sup> Plus PCR. The results are contradictory; the Hermans orientation function of the as-received Spectra Shield<sup>®</sup> Plus PCR is only 81% of that for the as-received Spectra<sup>®</sup> cloth 903. All consolidated Spectra Shield<sup>®</sup> Plus PCR have lower molecular orientation than consolidated Spectra<sup>®</sup> cloth under the same processing conditions. This may be due to the thermal history experienced by the fibers during the manufacturing of Spectra Shield<sup>®</sup> Plus PCR. Consolidated Spectra Shield<sup>®</sup> Plus PCR maintains a constant level of molecular orientation up to 150°C. Hermans orientation function decreases with increasing temperature at sintering temperature above 150°C. Since high molecular orientation translates to good mechanical properties, the apparent existence of a plateau in orientation provides for a broad processing temperature window.



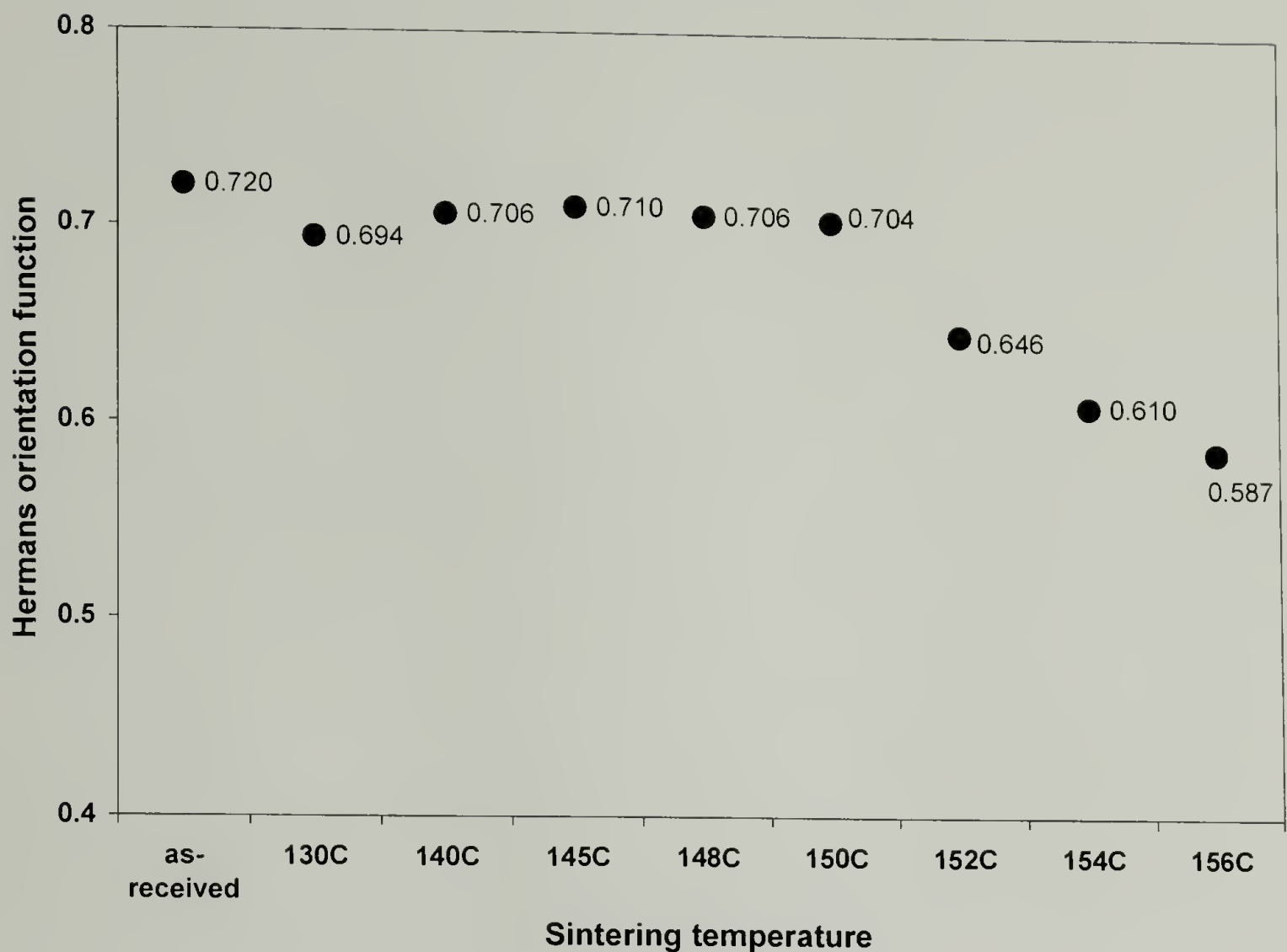


Figure 6.8 Hermans orientation function of the as-received Spectra Shield<sup>®</sup> Plus PCR and single layer Spectra Shield<sup>®</sup> Plus PCR consolidated under 7.6MPa for 30 minutes at different processing temperatures

#### 6.3.2.2 Impact properties

The impact resistance of consolidated single layer of Spectra Shield<sup>®</sup> Plus PCR prepregs was measured, normalized, and the NTT total energy of impact is compared to that of the as-received prepreg (Figure 6.9). Spectra Shield<sup>®</sup> Plus PCR consolidated at 140°C exhibits maximum impact energy, nearly four-fold increase over the original material due to the partial melting of the fiber surface allowing the polymer chains to penetrate into the surrounding polymeric matrix and form interlocking network with the matrix on recrystallization. The enhanced interphase adhesion is responsible for the better impact properties. At sintering temperatures below 140°C, impact resistance is

gradually improved. At sintering temperatures above 140°C, impact properties decreases gradually due to increased fiber melting. If the sintering temperature is lower than 150°C, the test specimen failed as fibers were pulled out of the prepreg without visible fiber breakage. If the sintering temperature is greater than 150°C, the specimen fractured and the fibers were broken. At 154°C the sintering process destroyed the fiber content and the specimen has no impact resistance.

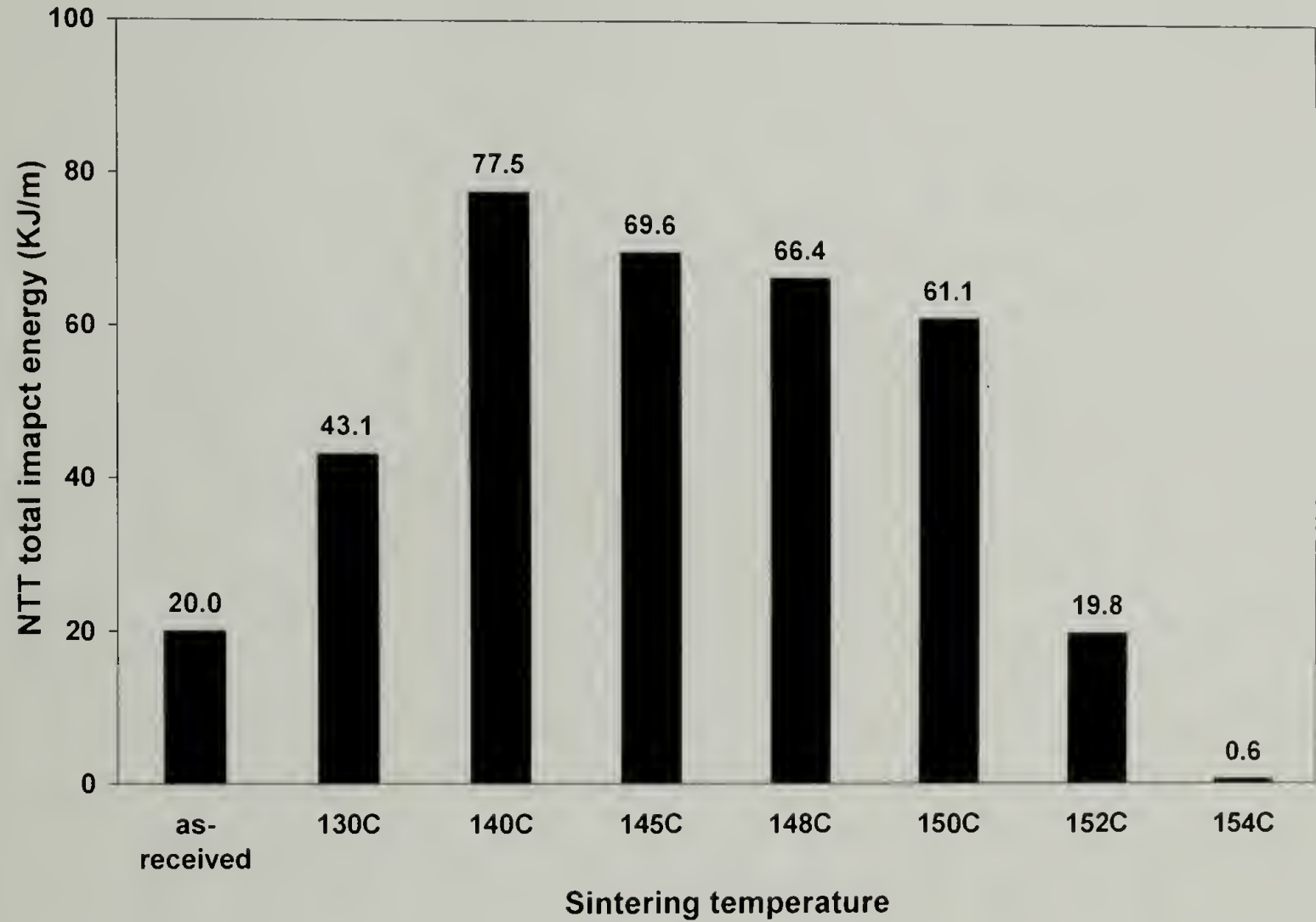


Figure 6.9 NTT total impact energy (KJ/m) of the as-received Spectra Shield<sup>®</sup> Plus PCR and single layer Spectra Shield<sup>®</sup> Plus PCR consolidated under 7.6MPa for 30 minutes at different processing temperatures

6.3.2.3 Interlayer adhesion

Interlayer adhesion for Spectra Shield<sup>®</sup> Plus PCR was measured as the peel load needed to separate the bonded bilayers (Figure 6.10). Interlayer adhesion increases steadily with increasing sintering temperature. At sintering temperatures between 130°C and 140°C, the interlayer adhesion does not improve significantly. Above 140°C, the interlayer adhesion increases at a faster rate due to partial melting and recrystallization of the Spectra<sup>®</sup> fibers, which adds to the adhesive strength in addition to that generated by the matrix.

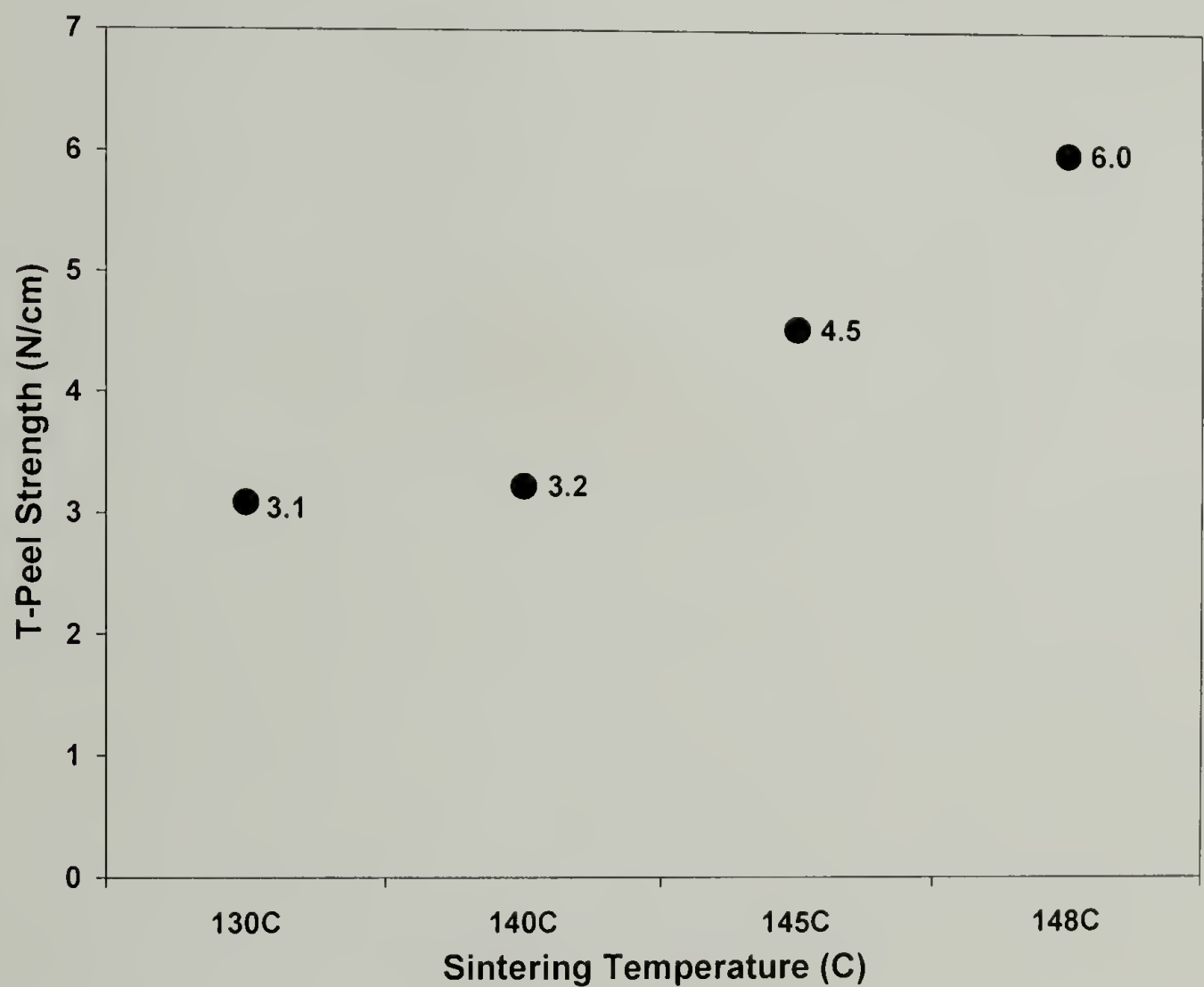


Figure 6.10 T-peel strength for Spectra Shield<sup>®</sup> Plus PCR bilayers sintered under 7.6MPa for 30 minutes at different processing temperatures

#### 6.3.2.4 Flexural properties

The flexural modulus and strength of 32 layer Spectra Shield<sup>®</sup> Plus PCR flat panels sintered at different processing temperatures for 30 minutes under a pressure of 17.2MPa were determined (Figure 6.11). The Spectra Shield<sup>®</sup> Plus PCR panels are more flexible than those made from Spectra<sup>®</sup> cloth 903 or Dyneema<sup>®</sup> felt. Low determined flexural modulus results from the use of a soft matrix and lower modulus fibers.

Although the prepreg possesses straight and unidirectional fibers, the flexural properties of the consolidated panels are offset by the use of a soft matrix. All test specimens exhibited a yielding point within the 5% strain and flexural strength is reported. At higher strains all test specimens developed delamination between the layers, indicating relatively low interlayer adhesion. The flexural modulus reaches a maximum value at a sintering temperature of 140°C and flexural strength remains predominantly constant over the entire processing temperature range.



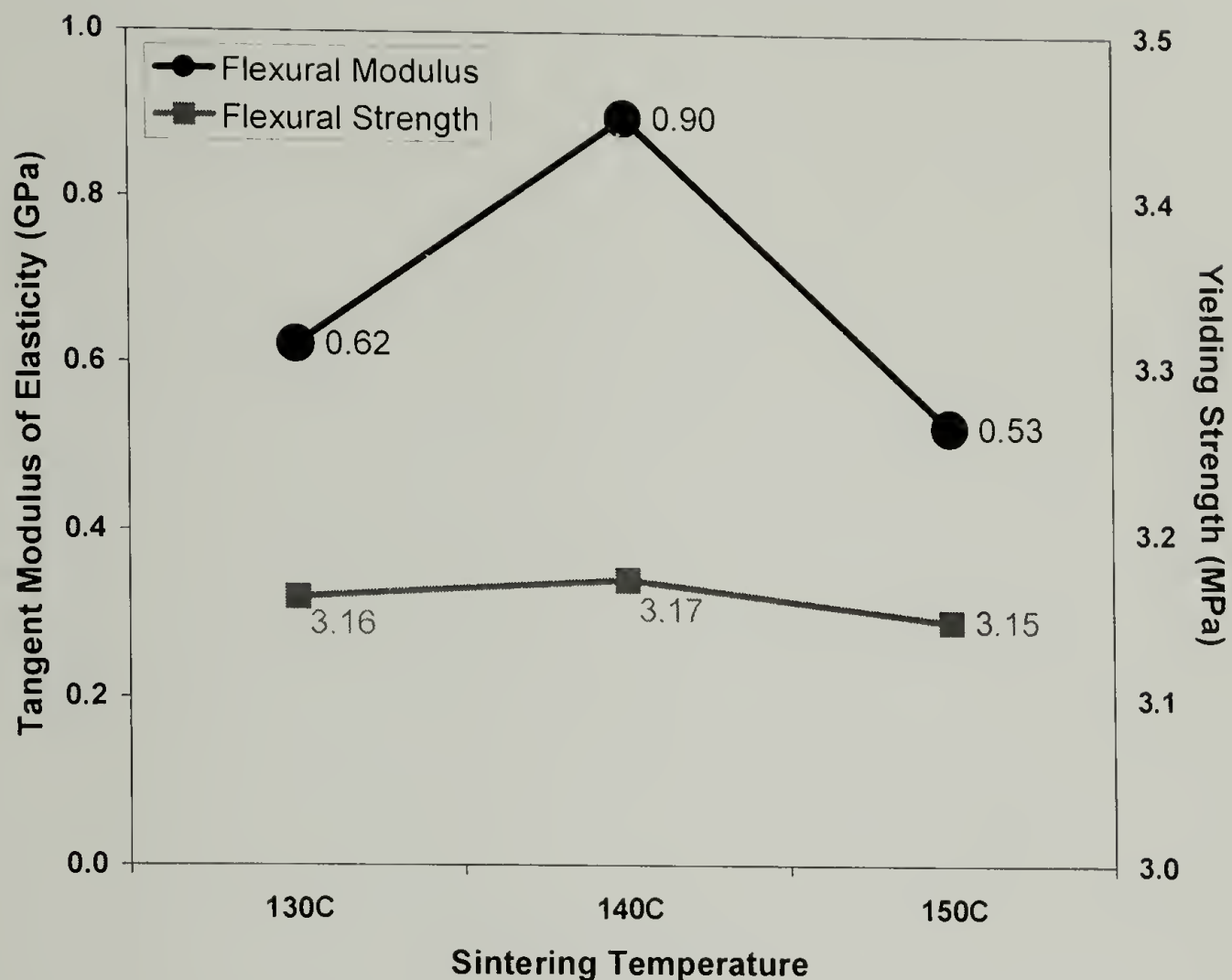


Figure 6.11 Flexural properties of 32 layers Spectra Shield<sup>®</sup> Plus PCR panels consolidated under 17.2MPa for 30 minutes at different processing temperatures

#### 6.3.2.5 Thermoformability

Multilayer Spectra Shield<sup>®</sup> Plus PCR was molded into a hemispherical dome using 50 layers of prepreg to produce a dome with similar dimensions to that of the 25 layer Spectra<sup>®</sup> cloth dome. Since adhesion between the Spectra<sup>®</sup> fibers and the matrix is low, the fibers easily slipped from the surrounding matrix when the load was applied to form the shape. At high molding temperatures the viscosity of the matrix lowers and the matrix tended to squeeze out as a result of pressure; the constraint exerted by the blank holder was questionable. The fibers were inclined to slip inside the prepreg when molding pressure was applied and fiber stretching was not as prominent as with Spectra<sup>®</sup>

cloth. Spectra Shield<sup>®</sup> Plus PCR is not a good material for direct shaping and would be better processed using the conventional method of cutting patterns and laying-up.

### 6.3.3 Comparison of consolidated Spectra<sup>®</sup> cloth, Dyneema Fraglight<sup>®</sup> and Spectra Shield<sup>®</sup> Plus PCR

Spectra<sup>®</sup> cloth, Dyneema Fraglight<sup>®</sup> and Spectra Shield<sup>®</sup> Plus PCR are all extended chain UHMWPE fiber products of different forms: woven fabric, nonwoven felt, and nonwoven prepreg, respectively. Spectra<sup>®</sup> cloth and Dyneema Fraglight<sup>®</sup> are single component materials containing only fibers and Spectra Shield<sup>®</sup> Plus PCR is a two component material containing fibers and matrix. Studies of high-temperature high-pressure sintering on each material and their physical, thermo-mechanical, structural properties of the resulting products have been discussed. The load bearing component in all three materials is highly oriented UHMWPE fibers. Spectra<sup>®</sup> fiber and Dyneema<sup>®</sup> fiber have similar properties. The properties of the consolidated structures are dependent on the structural and morphological properties of the load bearing fibers, although fiber alignment and the introduction of the matrix influence the final properties of the composite.

#### 6.3.3.1 Crystallinity

Extended chain UHMWPE fibers have high crystallinity, which is essential to obtain their outstanding properties. High-temperature high-pressure sintering process involves a series of structural changes including: partial melting of the fibers, molecular reorientation due to increasing molecular relaxation at high temperatures, orthorhombic

to hexagonal crystalline transformation, and pressure induced crystallization. The consolidated structures change crystallinity depending on the different processing conditions (Table 6.4 and Figure 6.12). For the as-received materials, Spectra<sup>®</sup> cloth 903 has the highest crystallinity since Spectra<sup>®</sup> fiber has an inherently higher crystallinity than Dyneema<sup>®</sup> fiber and the crystallinity of Spectra Shield<sup>®</sup> Plus PCR was partially destroyed during manufacturing. For the consolidated materials, Spectra<sup>®</sup> cloth 903 maintains the highest crystallinity over the processing temperature range due predominantly to the fact that it has the highest initial crystallinity, in addition to pressure induced crystallization. The crystallinity of consolidated Spectra<sup>®</sup> cloth is extremely sensitive to the processing temperature; a two degree change in temperature results in a great difference in crystallinity. Dyneema Fraglight<sup>®</sup> and Spectra Shield<sup>®</sup> Plus PCR exhibit a plateau in crystallinity over a large processing temperature range, implying a broader processing temperature window for these two materials.

Table 6.4 Overall crystallinity of the as-received and consolidated single layer Spectra<sup>®</sup> cloth, Dyneema Fraglight<sup>®</sup>, and Spectra Shield<sup>®</sup> Plus PCR sintered under 7.6MPa for 30 minutes at different processing temperatures

Specimen	as-received	130°C	140°C	145°C	148°C	150°C	152°C	154°C
Spectra <sup>®</sup> cloth	95.2%	-	-	-	97.5%	94.8%	90.6%	84.1%
Dyneema Fraglight <sup>®</sup>	92.4%	-	93.3%	93.7%	92.7%	90.6%	82.1%	75.1%
Spectra Shield <sup>®</sup>	90.3%	93.9%	92.8%	92.0%	90.7%	85.9%	80.8%	70.0%

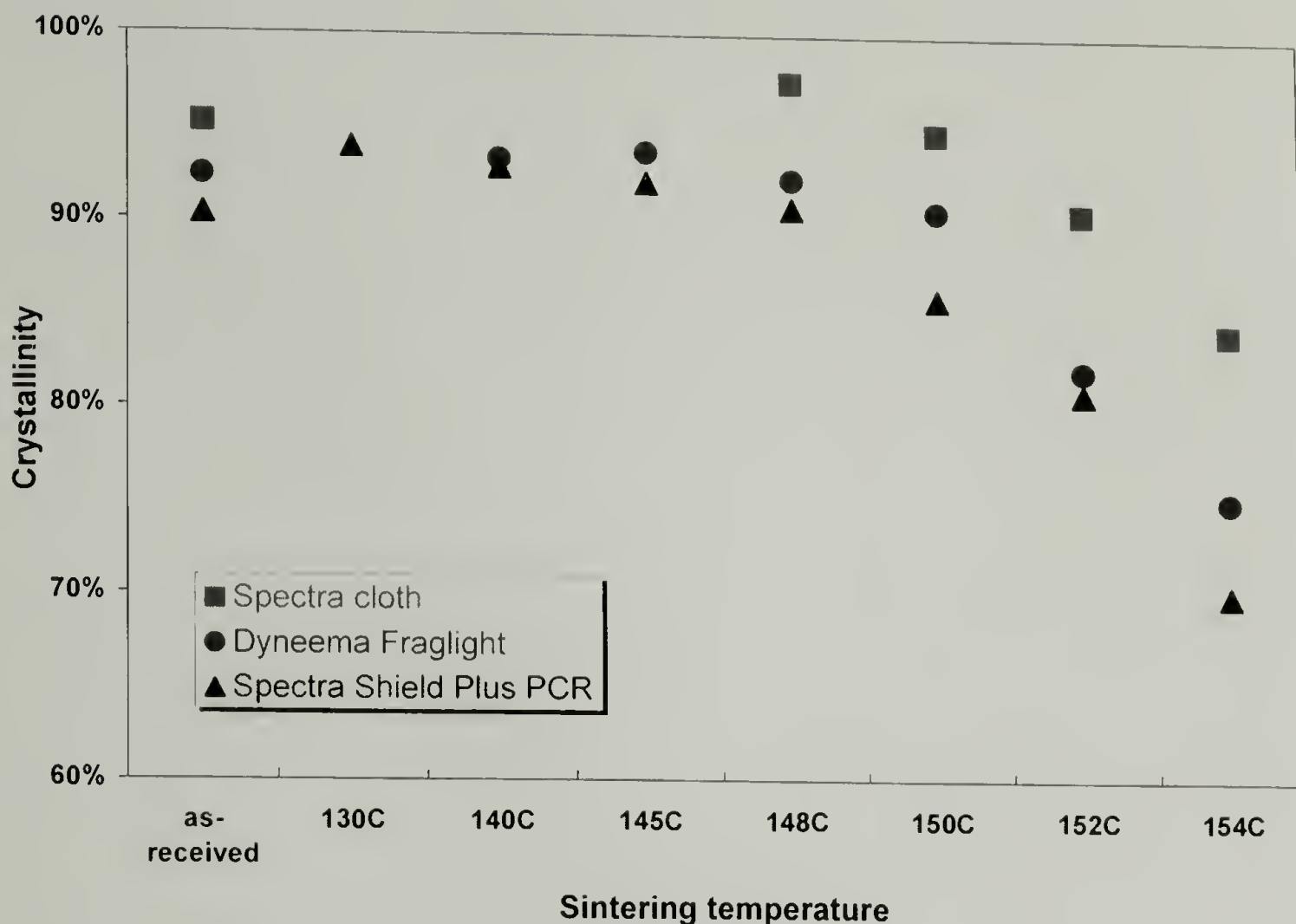


Figure 6.12 Overall crystallinity of the as-received and consolidated single layer Spectra<sup>®</sup> cloth, Dyneema Fraglight<sup>®</sup>, and Spectra Shield<sup>®</sup> Plus PCR sintered under 7.6MPa for 30 minutes at different processing temperatures

### 6.3.3.2 Molecular orientation

Extended chain UHMWPE fibers have high molecular orientation due to the ultra drawing process experienced during manufacturing, high orientation is a crucial factor to their outstanding properties. During high-temperature high-pressure sintering process, the melted phase recrystallizes upon cooling to form a less oriented phase. Increasing molecular mobility at high temperatures resulting in the rearrangement of the molecules and pressure induced crystallization forcing the molecules to adopt more ordered conformations plays a role in determining final orientation. Macroscopic alignment of the fibers within each material also influences Hermans orientation function as measured



by WAXD. Lateral movement of the fibers during sintering results in the misalignment of fibers and affects the measured orientation. In Dyneema<sup>®</sup> felt the fibers are randomly distributed and the material is inplane isotropic. The molecular orientation changes of Spectra<sup>®</sup> cloth and Spectra Shield<sup>®</sup> Plus PCR after processing are measurable by WAXD (Table 6.5 and Figure 6.13). Both Spectra<sup>®</sup> cloth and Spectra Shield<sup>®</sup> Plus PCR preserve relatively high orientation up to the processing temperature range of 150°C – 152°C range, followed by a rapid decrease in orientation due to the excessive melting of the fibers at higher temperatures. Consolidated Spectra<sup>®</sup> cloth shows a higher orientation than the original cloth at 148°C due to pressure induced crystallization. Consolidated Spectra Shield<sup>®</sup> Plus PCR does not show this behavior, but rather a plateau that covers nearly 20 degrees in processing temperature range at which Hermans orientation function remains unchanged, indicating a broader processing temperature window.

Table 6.5 Hermans orientation function of the as-received and consolidated single layer Spectra<sup>®</sup> cloth and Spectra Shield<sup>®</sup> Plus PCR sintered under 7.6MPa for 30 minutes at different processing temperatures

Specimen	as- received	130°C	140°C	145°C	148°C	150°C	152°C	154°C	156°C
Spectra <sup>®</sup> cloth	0.887	-	-	-	0.911	0.873	0.857	0.760	0.651
Spectra Shield <sup>®</sup>	0.720	0.694	0.706	0.710	0.706	0.704	0.646	0.610	0.587

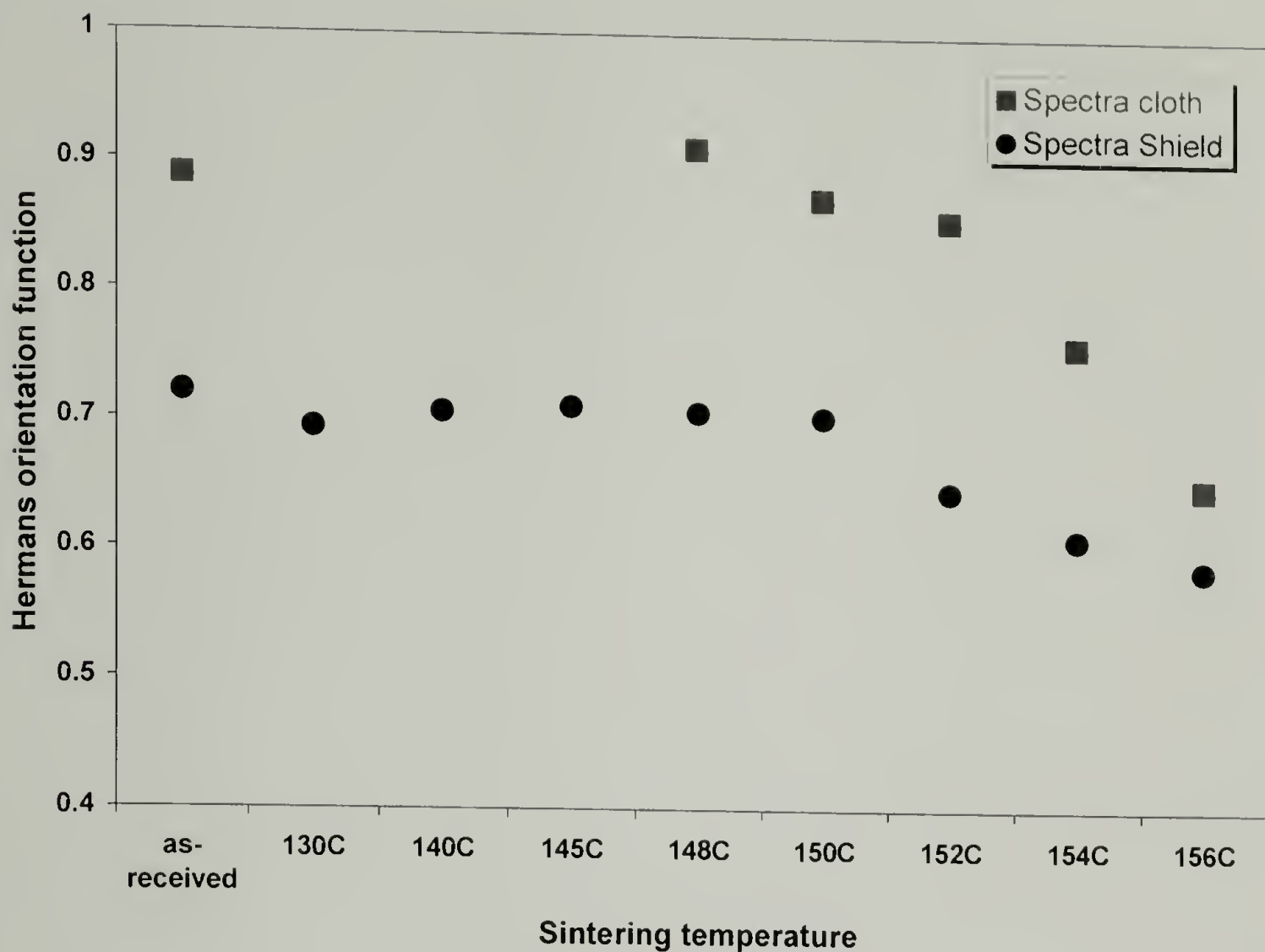


Figure 6.13 Hermans orientation function of the as-received and consolidated single layer Spectra<sup>®</sup> cloth and Spectra Shield<sup>®</sup> Plus PCR sintered under 7.6MPa for 30 minutes at different processing temperatures

### 6.3.3.3 Impact properties

NTT total impact energies are compared for the as-received and consolidated single layer Spectra<sup>®</sup> cloth, Dyneema Fraglight<sup>®</sup>, and Spectra Shield<sup>®</sup> Plus PCR sintered at various processing temperatures (Table 6.6 and Figure 6.14). For the as-received materials, Dyneema<sup>®</sup> felt has the best impact resistance due to the fiber entanglements. Consolidated Spectra<sup>®</sup> cloth 903 has a peak NTT impact energy of 92.0KJ/m if processed at 150°C and Dyneema<sup>®</sup> felt at 76.2KJ/m if processed at 148°C due to the random alignment of Dyneema<sup>®</sup> fibers which can not be constrained as effectively as the aligned fibers in Spectra<sup>®</sup> cloth. Dyneema<sup>®</sup> fibers begin to melt earlier than Spectra<sup>®</sup> fibers,

therefore, their maximum impact properties occur at a lower temperature. For Spectra Shield<sup>®</sup> Plus PCR, the optimal processing temperature, in terms of the highest attained impact resistance 77.5KJ/m, is 140°C which is considerably lower than the other two materials. The matrix of Spectra Shield<sup>®</sup> Plus PCR has a relatively low viscosity at high temperatures and when under a large pressure tends to flow; so the pressure can not to be effectively exerted onto the fibers. The fibers in Spectra Shield<sup>®</sup> Plus PCR are not as sufficiently constrained as those in Spectra<sup>®</sup> cloth and Dyneema<sup>®</sup> felt and consequently lose crystallinity and orientation during sintering, resulting in lower impact properties. Consolidated Spectra<sup>®</sup> cloth has the best maximum impact resistance among the three materials and proves to be the best candidate for making high strength, high impact resistant composites. The impact properties of Dyneema<sup>®</sup> felt and Spectra Shield<sup>®</sup> Plus PCR sintered at a temperature slightly below or above their respective optimal temperatures do not drop greatly when compared to Spectra<sup>®</sup> cloth and these materials have somewhat broader processing temperature window.

Table 6.6 NTT total impact energy (KJ/m) of the as-received and consolidated single layer Spectra<sup>®</sup> cloth, Dyneema Fraglight<sup>®</sup>, and Spectra Shield<sup>®</sup> Plus PCR sintered under 7.6MPa for 30 minutes at different processing temperatures

Specimen	as-received	140°C	145°C	148°C	150°C	152°C	154°C	156°C
Spectra <sup>®</sup> cloth	16.6	-	-	78.1	92.0	13.7	3.2	2.3
Dyneema Fraglight <sup>®</sup>	64.5	65.8	66.7	76.2	63.0	20.0	1.8	0.5
Spectra Shield <sup>®</sup>	20.0	77.5	69.6	66.4	61.1	19.8	0.6	-

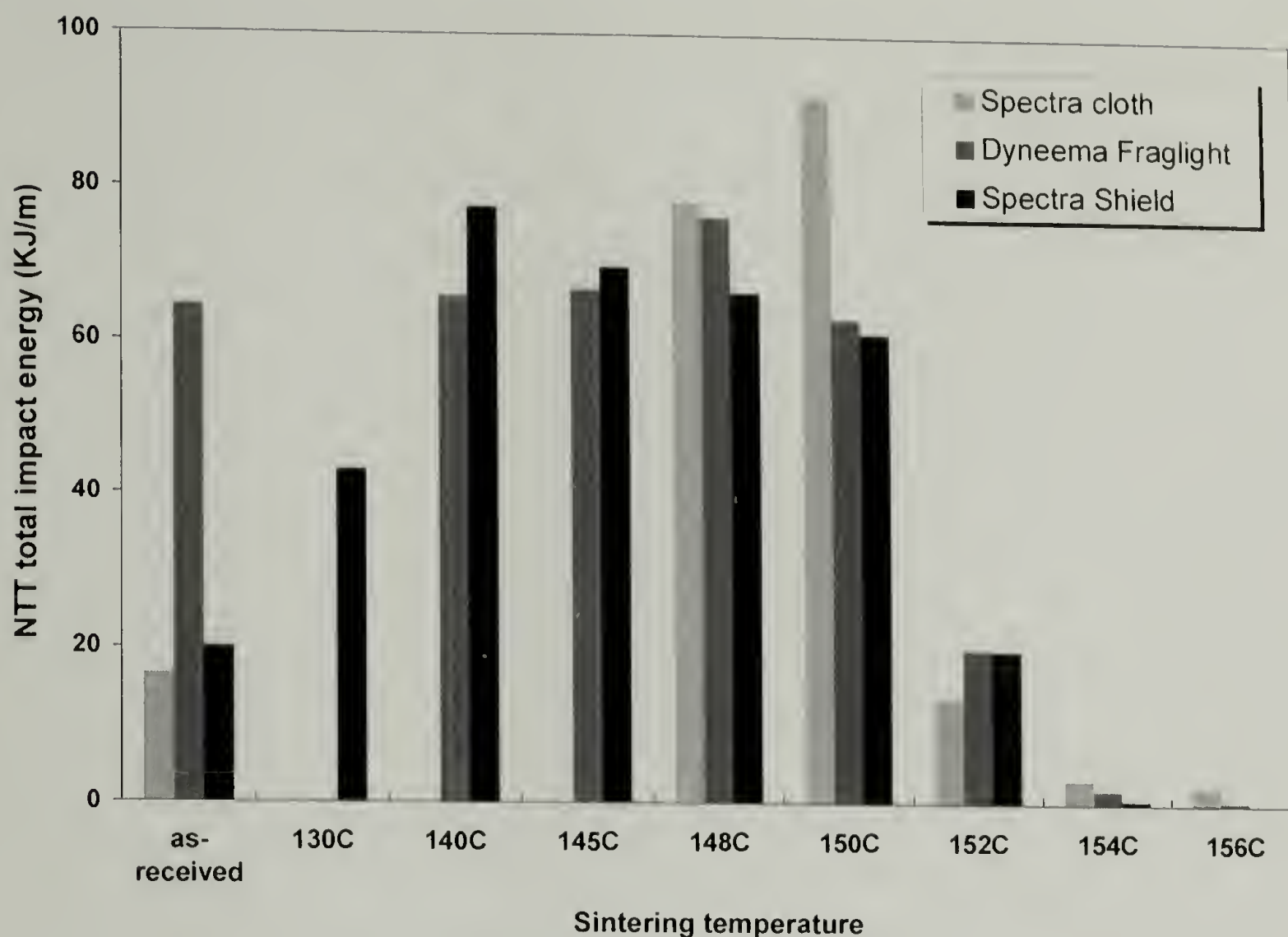


Figure 6.14 NTT total impact energy (KJ/m) of the as-received and consolidated single layer Spectra<sup>®</sup> cloth, Dyneema Fraglight<sup>®</sup>, and Spectra Shield<sup>®</sup> Plus PCR sintered under 7.6MPa for 30 minutes at different processing temperatures

### 6.3.2.3 Interlayer adhesion

Interlayer adhesion for bilayers of Spectra<sup>®</sup> cloth 903, Dyneema Fraglight<sup>®</sup> and Spectra Shield<sup>®</sup> Plus PCR bonded at various temperatures are shown in Table 6.7 and Figure 6.15. The T-peel strength for each material increases monotonically with increasing bonding temperature due to increased melting and recrystallization. Interlayer adhesion is developed at the expense of longitudinal strength. At a given bonding temperature, Spectra Shield<sup>®</sup> Plus PCR has the greatest interlayer adhesion of all the materials due to its adhesive matrix. Dyneema<sup>®</sup> felt has better adhesion than Spectra<sup>®</sup>



cloth due to its flat surface which enables better contact. Also, physical entanglements of the fibers in Dyneema<sup>®</sup> felt hinder the separation of the bonded layers.

Table 6.7 T-peel strength (N/cm) of bilayer Spectra<sup>®</sup> cloth, Dyneema Fraglight<sup>®</sup>, and Spectra Shield<sup>®</sup> Plus PCR bonded under 7.6MPa for 30 minutes at different temperatures

Specimen	140°C	145°C	148°C	150°C	152°C	154°C	156°C
Spectra <sup>®</sup> cloth	-	-	1.7	2.0	3.5	11.4	13.3
Dyneema <sup>®</sup> Fraglight <sup>®</sup>	-	-	2.3	3.4	17.3	38.0	-
Spectra Shield <sup>®</sup>	3.2	4.5	6.0	-	-	-	-

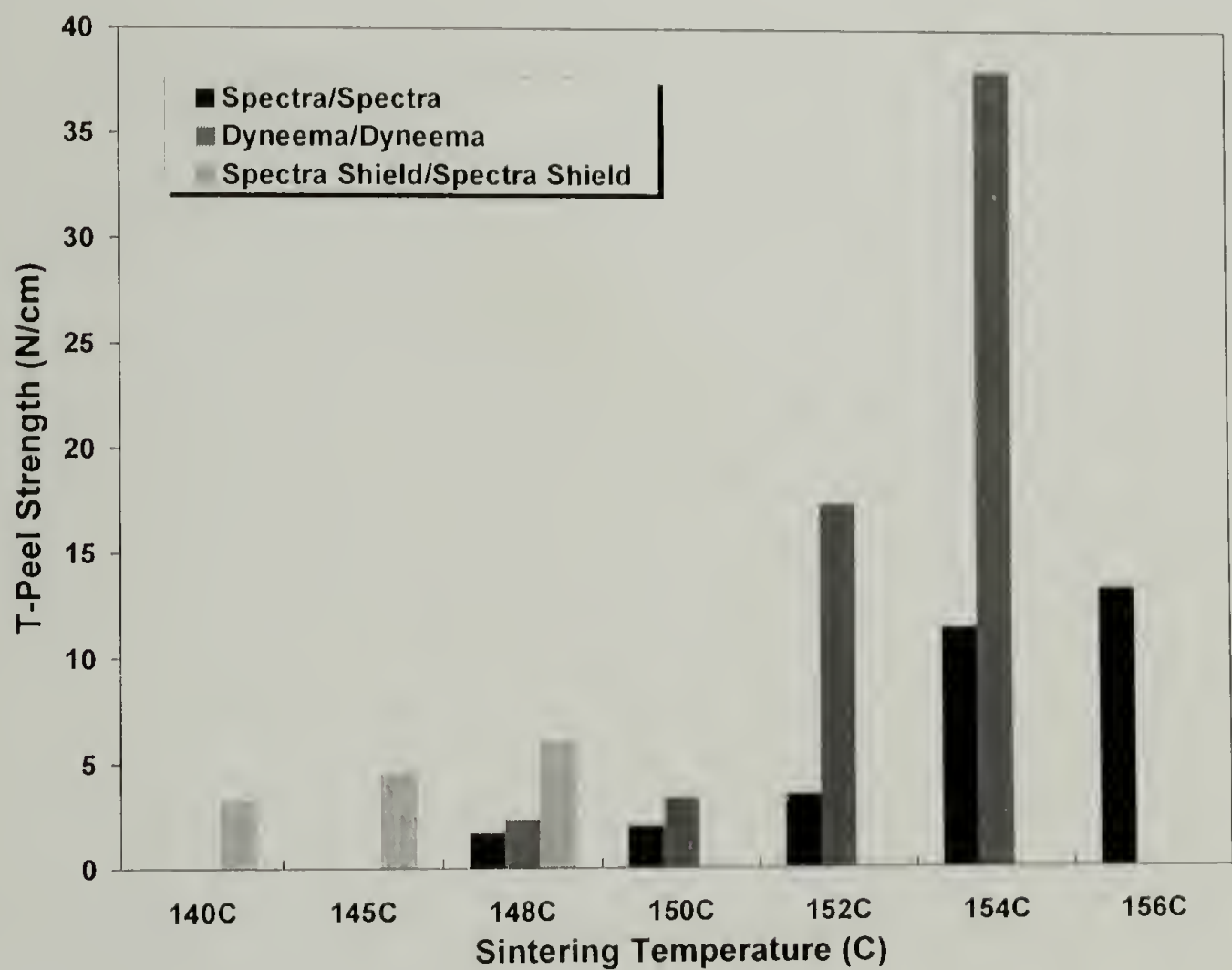


Figure 6.15 T-peel strength of bilayer Spectra<sup>®</sup> cloth, Dyneema Fraglight<sup>®</sup>, and Spectra Shield<sup>®</sup> Plus PCR bonded under 7.6MPa for 30 minutes at different temperatures

If Spectra<sup>®</sup> cloth is bonded with Dyneema<sup>®</sup> felt, it is anticipated that the interlayer adhesion would fall between the values of the Spectra<sup>®</sup> bilayers and the Dyneema<sup>®</sup> bilayers as found in Table 6.8 and Figure 6.16. By sintering alternating layers of Spectra<sup>®</sup> cloth and Dyneema<sup>®</sup> felt an excellent method to prepare a composite with a balanced interlayer adhesion and longitudinal strength is offered which utilizes the different advantages of two materials.

Table 6.8 T-peel strength (N/cm) of Spectra<sup>®</sup> cloth bilayer, Dyneema Fraglight<sup>®</sup>, bilayer and Spectra<sup>®</sup> cloth- Dyneema Fraglight<sup>®</sup> bilayer bonded under 7.6MPa for 30 minutes at different temperatures

Specimen	148°C	150°C	152°C	154°C	156°C
Spectra <sup>®</sup> /Spectra <sup>®</sup>	1.7	2.0	3.5	11.4	13.3
Spectra <sup>®</sup> /Dyneema <sup>®</sup>	2.2	3.8	5.5	23.5	47.7
Dyneema <sup>®</sup> /Dyneema <sup>®</sup>	2.3	3.4	17.3	38.0	-

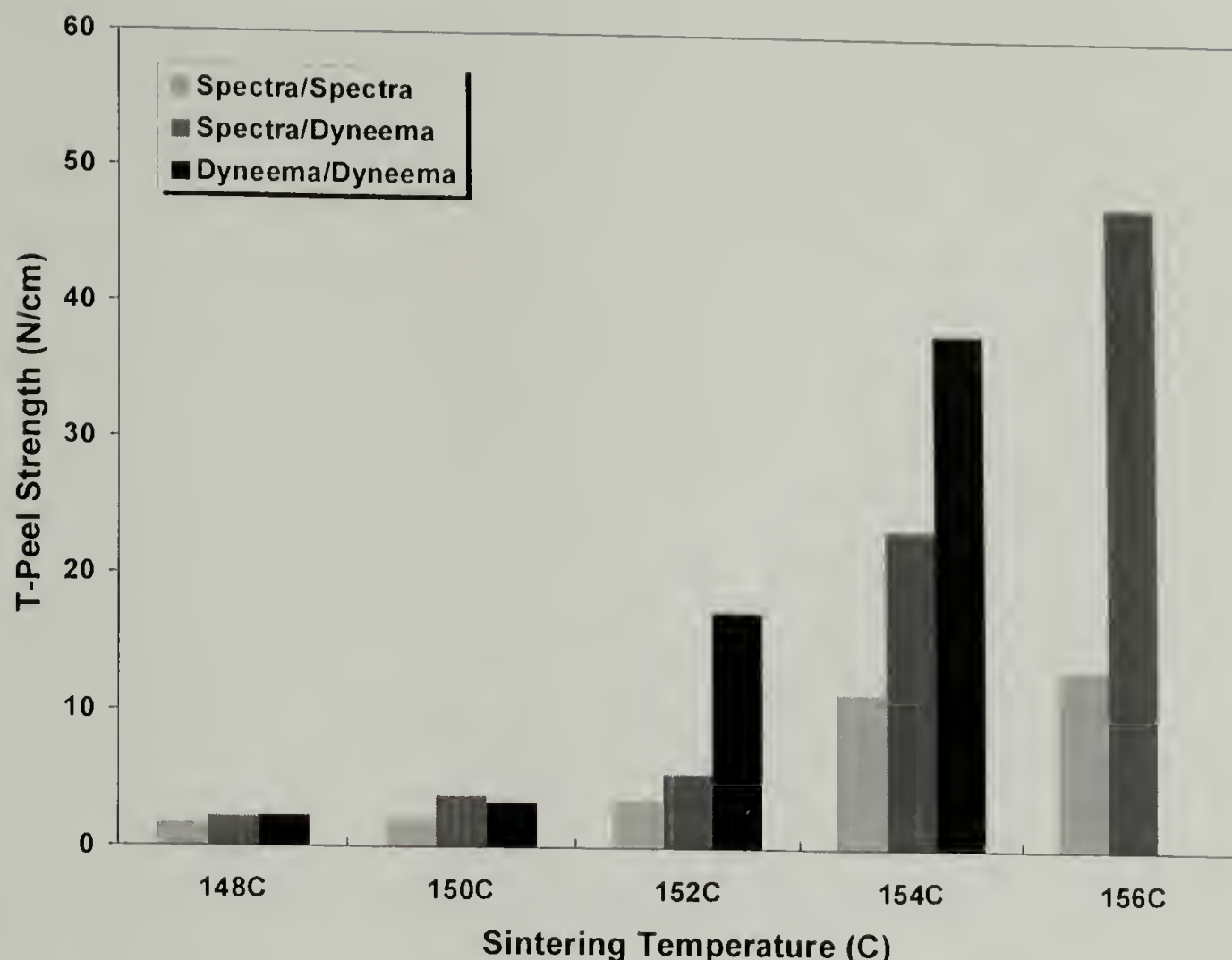


Figure 6.16 T-peel strength of Spectra<sup>®</sup> cloth bilayer, Dyneema Fraglight<sup>®</sup> bilayer, and Spectra<sup>®</sup> cloth- Dyneema Fraglight<sup>®</sup> bilayer bonded under 7.6MPa for 30 minutes at different temperatures

#### 6.3.2.4 Flexural properties

Flexural modulus for multilayer consolidated Spectra<sup>®</sup> cloth 903, Dyneema Fraglight<sup>®</sup>, Spectra Shield<sup>®</sup> Plus PCR, and unoriented UHMWPE sintered at various temperatures is shown in Figure 6.17. Consolidated Spectra<sup>®</sup> cloth panels have much higher flexural moduli than the other two UHMWPE fiber materials. Consolidated Dyneema<sup>®</sup> felt has about half the rigidity of Spectra<sup>®</sup> cloth 903, if their achieved maxima are compared. Consolidated Spectra Shield<sup>®</sup> Plus PCR has rigidity comparable to unoriented UHMWPE panel due to its soft matrix, despite its better fiber alignment which illustrates one of the advantages of eliminating the use of matrix by making matrix

free Spectra<sup>®</sup> fiber reinforced composite from plain woven Spectra<sup>®</sup> cloth. Matrix free Spectra<sup>®</sup> composite has higher fiber volume fraction which translates to better properties, therefore, is the best candidate among three materials to make rigid hard armor such as helmets and breast plates.

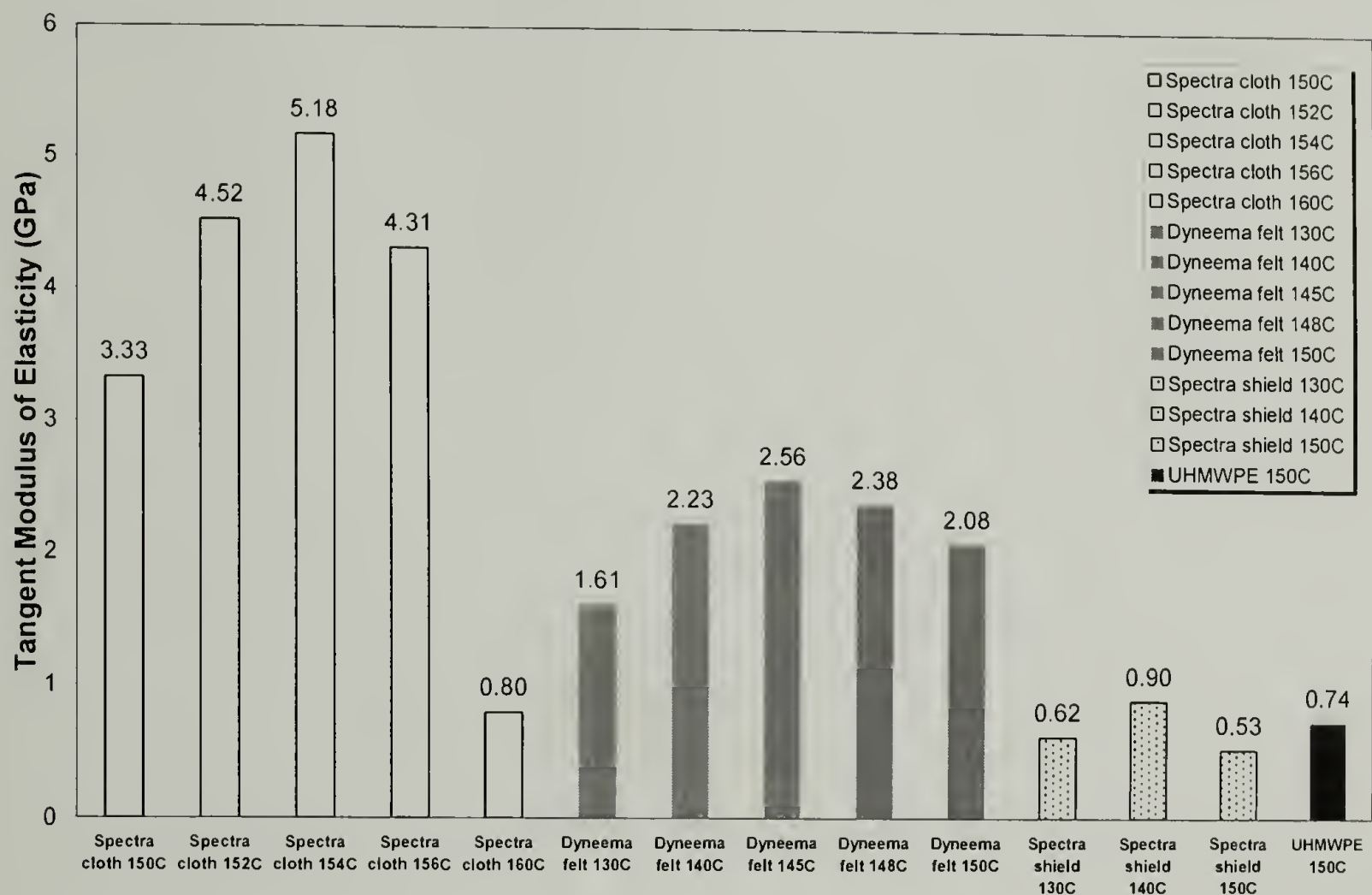


Figure 6.17 Flexural modulus of multilayer consolidated Spectra<sup>®</sup> cloth, Dyneema Fraglight<sup>®</sup>, Spectra Shield<sup>®</sup> Plus PCR, and UHMWPE panels sintered under 17.2MPa for 30 minutes at different processing temperatures

## 6.4 Conclusion

Two other materials Dyneema Fraglight<sup>®</sup>, a nonwoven felt, and Spectra Shield<sup>®</sup> Plus PCR, a prepreg, containing the extended chain UHMWPE fibers were subject to the similar high-temperature high-pressure sintering process used on Spectra<sup>®</sup> cloth. The physical, thermo-mechanical, microstructural and morphological properties of the



consolidated products were comprehensively investigated and compared to Spectra<sup>®</sup> cloth. Differences in the materials and their structures are reflected in the properties of the final products. Also, the influence of processing conditions on the properties of the consolidated products is different.

Consolidated Spectra<sup>®</sup> cloth 903 achieves the highest crystallinity and better molecular orientation than consolidated Spectra Shield<sup>®</sup> Plus PCR. Consolidated Spectra<sup>®</sup> cloth 903 also shows the best impact resistance and the highest flexural modulus since fibers were effectively constrained during sintering and the possibility of excessive fiber melting and orientation loss was reduced. Consolidated Dyneema Fraglight<sup>®</sup> is not as rigid as consolidated Spectra<sup>®</sup> cloth and consolidated Spectra Shield<sup>®</sup> Plus PCR suffers the lowest stiffness. In terms of interlayer adhesion, Dyneema Fraglight<sup>®</sup> has an advantage which prompts the use of alternative layers of Spectra<sup>®</sup> cloth and Dyneema<sup>®</sup> felt to make composites having both high longitudinal and lateral strengths. The properties of consolidated Spectra<sup>®</sup> cloth are very sensitive to the processing temperature which is not the case for Dyneema Fraglight<sup>®</sup> and Spectra Shield<sup>®</sup> Plus PCR. All the studied materials are thermoformable; Dyneema Fraglight<sup>®</sup> is the easiest to shape while Spectra Shield<sup>®</sup> Plus PCR has difficulty in molding because the flow of the matrix at high temperatures.

Matrix free Spectra<sup>®</sup> fiber reinforced composite made of Spectra<sup>®</sup> cloth is proven to be the best material to make body armor and helmets. It has the lowest density and extraordinary impact resistance and ballistic performance, and the simplest manufacturing processing by eliminating the need to cut patterns and add matrix.

## CHAPTER 7

### CONCLUSIONS AND FUTURE WORK

#### 7.1 Matrix free Spectra<sup>®</sup> fiber reinforced composites

Spectra<sup>®</sup> cloth 903 can be consolidated using high-temperature high-pressure sintering and resulting in a one-polymer composite. The partially melted fibers recrystallize on cooling and form the matrix phase. Since no additional matrix is used in the process, the product is dubbed as a “matrix free” composite. Three important processing parameters are temperature, time, and pressure. Too low a sintering temperature does not induce sufficient surface melting to provide adhesion to consolidate the cloth. Too high a temperature results in excessive melting that leads to a decrease in crystallinity and orientation. Time is critical to heat transfer to allow fiber lateral deformation and achieve adequate adhesion between the layers and fibers with minimum loss of the original fiber strength. High pressure is required to constrain the fibers from shrinking, losing orientation, and to consolidate the material. Among these three parameters, temperature and time are the most important to determine the properties of the final structures because they influence the degree of crystallinity and orientation of the consolidated material. Higher temperature and shorter time may achieve the same effect on the consolidated material as a lower temperature and longer time, which may be considered as a time-temperature superposition. The properties of the sintered structure are very sensitive to the processing conditions; two degree difference in sintering temperature results in a large difference in material properties. Process-structure-property relationship was carefully studied using various analysis and characterization methods including: thermal analysis, microscopic investigation and mechanical testing.

The optimal processing window was determined to maximize impact resistance and balance other properties of the consolidated structure.

Spectra<sup>®</sup> fiber has a high degree of crystallinity and consolidation at high temperatures destroys the crystals to some extent even with constraint, although pressure induced crystallization makes up for some loss in crystallinity. High crystallinity can be preserved if Spectra<sup>®</sup> cloth is sintered in the optimal processing window.

Spectra<sup>®</sup> fiber has very high crystalline orientation and molecular orientation. At high processing temperatures, polymer chains tend to recoil as driven by an entropy gain and orientation loss is inevitable. High orientation can be preserved if Spectra<sup>®</sup> cloth is sintered in the optimal processing window. Pressure induced crystallization manifests itself again in the unusual increase of orientation for some sintered cloths by forcing the molecules to reorient and participate in forming ordered crystalline lattices. The highest crystallinity and orientation are obtained for the cloth consolidated at 148°C. In fact there is a linear relationship between the crystallinity and orientation for cloths sintered at different temperatures.

The ability to maintain high crystallinity and orientation of the cloth after processing enables the composites to have outstanding mechanical properties. Sintered Spectra<sup>®</sup> cloth has exceptional impact resistance. The processing temperature at which the best impact property is obtained is just two degrees higher than the temperature at which the highest crystallinity and orientation are obtained, indicating that the preservation of the longitudinal strength and development of the lateral adhesion are the reasons behind their high impact resistance. Multilayer consolidated Spectra<sup>®</sup> cloth is very rigid and the flat panels have a high flexural modulus. High modulus and low



density of the cloth are beneficial for fast strain wave propagation and impact energy transportation<sup>67</sup>, especially for the anisotropic composite in which the in-plane modulus is an order of magnitude larger than the modulus through the thickness. Superior impact and flexural properties make Spectra<sup>®</sup> cloth a very promising candidate for light weight high performance ballistic shields.

Interlayer adhesion between sintered Spectra<sup>®</sup> cloth is sufficient but not high. Inferior adhesion is actually good for ballistic performance by offering an energy dissipation mechanism through delamination. Interlayer adhesion is developed at the cost of fiber melting, and the loss of longitudinal properties. If interlayer adhesion is desired in applications other than ballistic shields, consolidating alternative layers of Spectra<sup>®</sup> cloth and Dyneema<sup>®</sup> felt would be a good approach. Surface treatment of Spectra<sup>®</sup> fiber, such as by chemical etching or plasma treatment, used together with an adhesive matrix is another way to promote interlayer adhesion.

The evaluation of ballistic performance of matrix free Spectra<sup>®</sup> fiber composites was conducted and the  $V_{50}$  results show that multilayer sintered Spectra<sup>®</sup> cloth has superb ballistic resistance. Matrix free Spectra<sup>®</sup> fiber composites perform better than Spectra<sup>®</sup> fiber containing a matrix and Kevlar<sup>®</sup> composites at the same areal density level. Also, matrix free Spectra<sup>®</sup> fiber composites are lighter and easier to manufacture. Spectra<sup>®</sup> cloth can be thermoformed into complex shaped objects with double curvatures providing that a proper mold and appropriate molding sequences are used. There is no need to cut complex patterns and the cloth can sustain large deformation to conform to the shape. Different shaping schemes were used to make hemispherical domes, analog to actual helmets and manufacturing versatility was demonstrated. It is clear that matrix



free Spectra<sup>®</sup> fiber reinforced composites produced by high-temperature high-pressure sintering has high potential in ballistic application.

Microscopic examination of the multilayer sintered Spectra<sup>®</sup> cloth shows that consolidation was excellent. During the sintering process, the fibers deform laterally and fill the void space. Selectively melted fiber surface recrystallizes upon cooling and welds the fibers together; there is molecular continuity through the fibers and the recrystallized phase. It is also expected, based on other researchers' work, that transcrystallinity<sup>28,29,75</sup> developing in the region near the fiber surface would promote interfiber and interlayer adhesion. The adhesive strength is good for polyethylene which is notoriously self-lubricating. Spectra<sup>®</sup> fibers are not circular but rather polygonal, the structure is not uniform across the fiber diameter, and there are density deficient regions which grow and eventually populate the entire volume if the fibers are treated at high temperatures.

The surface and center layers of the consolidated multilayer Spectra<sup>®</sup> cloth have essentially the same crystallinity and orientation when sintered under optimal processing conditions, suggesting homogenous consolidation and uniform properties throughout the entire structure.

Dyneema Fraglight<sup>®</sup> and Spectra Shield<sup>®</sup> Plus PCR can also be consolidated by high-temperature high-pressure sintering. Interlayer adhesion between sintered Dyneema<sup>®</sup> felt is great. Impact resistance of consolidated felt and prepreg is not as good as consolidated Spectra<sup>®</sup> cloth, mainly due to their lower degree of crystallinity and molecular orientation. Flat panels made by multilayer felts or prepregs show lower flexural properties than that of Spectra<sup>®</sup> cloth, which is due to the random fiber orientation in Dyneema<sup>®</sup> felt and the incorporation of a soft matrix in Spectra Shield<sup>®</sup>

Plus PCR. Dyneema Fraglight<sup>®</sup> and Spectra Shield<sup>®</sup> Plus PCR are not as good candidates as Spectra<sup>®</sup> cloth to make high strength and high impact resistance composites, although they exhibit a broader processing window to obtain relatively constant properties.

## 7.2 Potential Applications

Besides the potential for ballistic protective shields, there are many other prospective applications for matrix free Spectra<sup>®</sup> fiber reinforced composites such as: orthopedic implants such as artificial joints, pressure vessels, high strength tubes, automobile parts, sporting goods such as kayaks, tennis racquets, tear and cut resistant protective coatings similar to Tyvek<sup>®</sup>, sailcloth, and radomes.

Orthopedic implants are used to replace fractured bones as well as to reconstruct various degenerated joints in the human body. The most commonly used implant today is the artificial hip joint. Fiber reinforced polymer composites have already demonstrated great advantages over traditional metal implants since they are chemically and biologically more compatible to bones than metals. There is less of a possibility of developing hypersensitivity and allergic reactions to polymeric composites and in addition polymeric composites distribute the load and stress more evenly than metals. Currently, people are using powder sintering of UHMWPE to make joints and there are problems associated with wear, fatigue and creep, etc. Using carefully designed molds and processing techniques, it should be possible to make better bone replacement by consolidating Spectra<sup>®</sup> cloth.

Radomes safeguard the inside equipment against environmental concern, such as wind, blowing sand, snow, ice, rain, ultra violet sun light, temperature, fungus and corrosion. Matrix free Spectra<sup>®</sup> fiber composite is an excellent candidate for the construction of radomes due to its high impact resistance, high abrasion tolerance, low dielectric constant, radar transparency, good UV resistance, low moisture absorption, and hydrophobicity. Light weight is another attribute superior to the currently used glass fiber or aramid fiber composites. The manufacturing of consolidated Spectra<sup>®</sup> cloth is simpler compared to the wet/dry lay-up or prepreg routes and the product is ballistic resistant. To make small radomes, direct molding can be used to manufacture them to precise specifications. For large radomes, individual panels can be molded to doubly curved shapes and then welded together by thermal or laser welding to yield a faceted geodesic or spherical smooth appearance.

In conclusion, matrix free Spectra<sup>®</sup> fiber reinforced composites made by high-temperature high-pressure sintering process offer a novel and promising approach to make products with light weight and extraordinary performance.

### 7.3 Processable Polymers

Apart from Spectra<sup>®</sup> fibers and Dyneema<sup>®</sup> fibers, other materials may be also consolidated by this high-temperature high-pressure sintering technique such as: PET fibers, PP fibers, Vectran<sup>®</sup> LCP fibers, Nomex<sup>®</sup> papers, Lycra<sup>®</sup> fibers, Nylon fibers and fabrics, etc. Theoretically, any thermoplastic fibrous material should work, especially high molecular weight materials. Mixed compatible materials can also be sintered to prepare products with combined properties and multiple functions.



## BIBLIOGRAPHY

1. Spectra<sup>®</sup> is a trademark of Honeywell.
2. Dyneema<sup>®</sup> is a trademark of DSM.
3. Dyneema Fraglight<sup>®</sup> is a trademark of DSM.
4. Spectra Shield<sup>®</sup> Plus PCR is a trademark of Honeywell.
5. Mallick P K, *Composites Engineering Handbook*, Marcel Dekker, **1997**
6. Mallick P K, *Fiber-reinforced Composites: Materials, Manufacturing and Design*, Marcel Dekker, **1998**
7. Kevlar<sup>®</sup> is a trademark of DuPont.
8. Weedon G C, Tam T Y, *Modern Plastics*, March, 64-68, **1986**
9. Southern J H, Porter R S, *J. Appl. Polym. Sci.*, 14, 2305-2317, **1970**
10. Capaccio G, Ward I M, *Polym. Eng. Sci.*, 15(3), 219-224, **1975**
11. Smith P, Lemstra P J, Kalb B, Pennings A J, *Polym. Bull.*, 1(11), 733-736, **1979**
12. Tekmilon<sup>®</sup> is a trademark of Mitsui.
13. Schaper A, Zenke D, Schultz E, Hirte A, Taege M, *Phys. Status Solidi. A: Appl. Res.*, 116(1), 179-195, **1989**
14. Grubb D T, Prasad K, *Macromolecules*, 25(18), 4575-4582, **1992**
15. Kavesh S, Prevorsek D C, *Int. J. Polym. Mater.*, 30, 15-56, **1995**
16. Fu Y G, Chen W, Pyda M, Londono D, Annis B, Boller A, Habenschuss A, Cheng J L, Wunderlich B, *J. Macromol. Sci. Phys.*, B35(1), 37-87, **1996**
17. Tam T Y, Boone M B, Weedon G C, *Polym. Eng. Sci.*, 28(13), 871-874, **1988**
18. Snia<sup>®</sup> is a trademark of Snia BVP.
19. Silverstein M S, Breuer O, Dodiuk H, *J. Appl. Polym. Sci.*, 52(12), 1785-1795, **1994**



20. Chiu H-T, Wang J-H, *J. Appl. Polym. Sci.*, 68, 1387-1395, **1998**
21. Kaplan S L, Rose P W, Nguyen H X, Chang H-W, *SAMPE, Quarterly*, 19(4), 55-59, **1988**
22. Tissington B, Pollard G, Ward I M, *J. Mater. Sci.*, 26, 82-92, **1991**
23. Cohen Y, Rein D M, Vaykhansky L, *Compos. Sci. Technol.*, 57, 1149-1154, **1997**
24. Cohen Y, Rein D M, Vaykhansky L, Porter R S, *Composites, Part A*, 30, 19-25, **1999**
25. Sloan F, Nguyen H, *J. Compos. Mater.*, 29(16), 2092-2107, **1995**
26. Lin L C, Bhatnagar A, Chang H W, *Proc. 22nd Int. SAMPE Tech. Conf.*, 1-13, **1990**
27. Vigo T L, Turbak A F, *High-Tech Fibrous Materials: Composites, Biomedical Materials, Protective Clothing, and Geotextiles*, ACS Symposium Series 457, **1991**
28. Capiati N J, Porter R S, *J. Mater. Sci.*, 10, 1671-1677, **1975**
29. Teishev A, Incardona S, Migliaresi C, Marom G, *J. Appl. Polym. Sci.*, 50, 503-512, **1993**
30. Marais C, Feillard P, *Compos. Sci. Technol.*, 45, 247-255, **1992**
31. Hinrichsen G, Kreuzberger S, Pan Q, Rath M, *Proceedings of the Ninth International Conference on the Mechanics of Composite Materials*, Riga, 719-728, **1996**
32. Lacroix F V, Werwer M, Schulte K, *Composites, Part A*, 29A, 371-376, **1998**
33. Morye S S, Hine P J, Duckett, R A, Carr D J, Ward I M, *Composites, Part A*, 30, 649-660, **1999**
34. Yan R J, Hine P J, Ward I M, Olley R H, Bassett D C, *J. Mater. Sci.*, 32, 4821-4831, **1997**
35. Hine P J, Ward I M, Abo El Maaty M I, Olley R H, Bassett D C, *J. Mater. Sci.*, 35, 5091-5099, **2000**
36. Hine P J, Ward I M, Olley R H, Bassett D C, *J. Mater. Sci.*, 28, 316-324, **1993**
37. Ward I M, Hine P J, *Polym. Eng. Sci.*, 37(11), 1809-1814, **1997**

38. Kabeel M A, Bassett D C, Olley R H, Hine P J, Ward I M, *J. Mater. Sci.*, 29, 4694-4699, **1994**
39. Bonner M J, Hine P J, Ward I M, *Plast. Rubber Compos. Process. Appl.*, 27(2), 59-64, **1998**
40. Hine P J; Ward I M; Jordan N D; Olley R H; Bassett D C, *J. Macromol. Sci. Phys.*, B40(5), 959-989, **2001**
41. Rasburn J, Hine P J, Ward I M, Olley R H, Bassett D C, Kabeel M A, *J. Mater. Sci.*, 30, 615-622, **1995**
42. El-Maaty M I A, Bassett D C, Olley R H, Hine P J, Ward I M, , *J. Mater. Sci.*, 31, 1157-1163, **1996**
43. Klocek P.; MacKnight W. J.; Farris R. J.; Lietzau C. (Texas Instruments; University of Massachusetts) U.S. Patent 5,573,824, November 12, **1996**
44. Klocek P.; MacKnight W. J.; Farris R. J.; Lietzau C. (Raytheon TI Systems; University of Massachusetts) U.S. Patent 5,879,607, March 9, **1999**
45. Klocek P.; MacKnight W. J.; Farris R. J.; Lietzau C. (Raytheon TI Systems; University of Massachusetts) U.S. Patent 5,935,651, August 10, **1999**
46. Klocek P.; MacKnight W. J.; Farris R. J.; Lietzau C. (Raytheon Company) U.S. Patent 6,077,381, June 20, **2000**
47. Klocek P.; MacKnight W. J.; Farris R. J.; Lietzau C. (Raytheon Company; University of Massachusetts) U.S. Patent 6,083,583, July 04, **2000**
48. Xu T, Farris R J, *Plastics Country USA*, Proceedings of the Society of Plastic Engineers Annual Technical Conference ANTEC 2003, Nashville, Tennessee, May 4-8, **2003**
49. Fischer L, Haschberger A, Ziegeldorf A, Ruland W, *Colloid Polym. Sci.*, 260, 174-181, **1982**
50. Sajkiewicz P, Wasiak A, *Colloid Polym. Sci.*, 277, 646-657, **1999**
51. Boller A, Wunderlich B, *J. Therm. Anal.*, 49, 343-349, **1997**
52. Capaccio G, Ward I M, *Colloid Polym. Sci.*, 260, 46-55, **1982**
53. Amornsakchai T, Unwin A P, Ward I M, Batchelder D N, *Macromolecules*, 30, 5034-5044, **1997**

54. Flores A, Calleja F J B, Bassett D C, *J. Polym. Sci. Pol. Phys.*, 37(21), 3151-3158, **1999**
55. Calleja F J B, Flores A, Ania F, Bassett D C, *J. Mater. Sci.*, 35(6), 1315-1319, **2000**
56. Flores A, Calleja F J B, Attenburrow G E, Bassett D C, *Polymer*, 41(14), 5431-5435, **2000**
57. [http://www.spectrafiber.com/products/spectra\\_900.html](http://www.spectrafiber.com/products/spectra_900.html)
58. Wunderlich B, *Macromolecular Physics, Vol. 3, Crystal Melting*, Academic Press, New York, **1980**
59. Peacock A J, *Handbook of Polyethylene: Structures, Properties and Applications*, Marcel Dekker, New York, 2000
60. van Aerle N A J M, Lemstra P J, *Polym. J.*, 20, 131-141, **1988**
61. Flory P J, Vrij A, *J. Amer. Chem. Soc.*, 85, 3548-3553, **1963**
62. Nakajima A, Hamada F, *Koll. Z. Z. Polymere*, 205, 55, **1965**
63. Department of Defense Test Method Standard, *MIL-STD-662F*, December 18, **1997**
64. Cunniff, P M, *Proceeding of the 18th International Symposium on Ballistics*, San Antonio, Texas, Nov, **1999**
65. Olley R H, Bassett D C, *Polymer*, 23, 1707-1710, **1982**
66. Morye S S, Hine P J, Duckett R A, Carr D J, Ward I M, *Compos. Sci. Technol.*, 60, 2631-2642, **2000**
67. Prevorsek D C, Kwon Y D, Chin H B, *Polym. Eng. Sci.*, 34(2), 141-152, **1994**
68. Pennings A J, Zwijnenburg A, *J. Polym. Phys.*, 17(6), 1011-1032, **1979**
69. van Aerle N A J M, Lemstra P J, Braam A W M, *Polym. Commun.*, 30(1), 7-10, **1989**
70. Kurelec L, Rastogi S, Meier R J, Lemstra P J, *Macromolecules*, 33, 5593-5601, **2000**
71. Rastogi S, Kurelec L, Lemstra P J, *Macromolecules*, 31, 5022-5031, **1998**
72. Tsubakihara S, Nakamura A, Yasuniwa M, *Polym. J.*, 23(11), 1317-1324, **1991**

73. Garcia-Leiner M, Song J, Lesser A J, *J. Polym. Sci. Part B*, 41, 1375-1386, **2003**
74. [http://www.spectrafiber.com/products/ssplus\\_pcr.html](http://www.spectrafiber.com/products/ssplus_pcr.html)
75. Ishida H, Bussi P, *Macromolecules*, 24, 3569-3577, **1991**



